

**Characterization of altered inflorescence architecture
in *Arabidopsis thaliana*
BG-5 x Kro-0 hybrid**

**Dissertation
zur Erlangung des akademischen Grades
"doctor rerum naturalium"
(Dr. rer. nat.)
in der Wissenschaftsdisziplin "Molekulare Pflanzenphysiologie"**

**eingereicht an der
Mathematisch-Naturwissenschaftlichen Fakultät
der Universität Potsdam**

**von
Dema Alhajturki**

Potsdam im August, 2018

This work is licensed under a Creative Commons License:
Attribution 4.0 International
To view a copy of this license visit
<https://creativecommons.org/licenses/by/4.0/>

The dissertation was accomplished from October 2014 until August 2018 in the group of Dr Roosa Laitinen at the Max Planck Institute of Molecular Plant Physiology in Potsdam-Golm.

Reviewer 1: Dr. Roosa Laitinen
Reviewer 2: Prof. Dr. Michael Lenhard
Reviewer 3: Dr. Joost Keurentjees

Published online at the
Institutional Repository of the University of Potsdam:
URN urn:nbn:de:kobv:517-opus4-420934
<http://nbn-resolving.de/urn:nbn:de:kobv:517-opus4-420934>

To my Father...

أبي الحبيب

You were and will always be all my reasons..

كنت وستبقى كل أسبابي

CONTENTS

1. Introduction	11
1.1 Hybrid incompatibility	11
1.1.1 Pre- and post-zygotic hybrid incompatibility.....	11
1.1.2 BDM-model of post-zygotic hybrid incompatibility.....	11
1.2 Mechanisms of post-zygotic hybrid incompatibility in plants	13
1.2.1 Hybrid sterility.....	14
1.2.2 Hybrid necrosis.....	15
1.2.3 Embryo lethality.....	17
1.3 Control of shoot architecture in plants	18
1.3.1 Genetic control of shoot architecture	19
1.3.2 Hormonal control of shoot architecture	21
1.3.3 Sugars as regulators of shoot architecture	24
1.3.4 Role of flavonoids in shoot architecture	25
1.3.5 Environmental factors and shoot architecture	25
1.4 <i>Arabidopsis thaliana</i> as model to study hybrid incompatibilities	26
1.5 Altered shoot branching in BG-5 x Kro-0 F₁ hybrids	27
1.6 Aims of this study	27
2. Material and Methods	29
2.1 Plant growth conditions	29
2.2 Accessions used in this study	29
2.3 Phenotyping	30
2.4 Confocal laser Scanning microscopy	30
2.5 Metabolite measurements	30
2.5.1 Measurement of Tre6P, phosphorylated intermediates and organic acids.....	30
2.5.2 Secondary metabolites.....	31
2.6 Hormone measurements	31
2.7 Genotyping	31
2.8 Construction of artificial microRNA constructs	33
2.9 Analysis of amiRNA hybrids	35
2.10 Gene expression assay	36
2.11 Cloning of genomic constructs	36
2.12 GUS staining assay	37
2.13 Segregation analysis in successive hybrid generations and backcrosses	38
2.14 Statistical analysis	38
2.15 Boxplot diagrams	38
3. Results	40
3.1 Temperature-dependent BG-5x Kro-0 F₁ phenotype	40
3.1.1 Quantification of F ₁ and parental phenotypes at 17°C.....	41

3.1.2 Response of shoot architecture related traits to temperature in F ₁ hybrids and parents.....	43
3.1.3 Developmental control of temperature induced F ₁ phenotype.....	45
3.2 Analysis of compounds associated with the F₁ phenotype.....	46
3.2.1 Sugar and secondary metabolites analysis.....	46
3.2.2. Hormone analysis.....	49
3.3 Genetic analysis of genes underlie the F₁ phenotype.....	51
3.3.1 Artificial microRNAs approach (amiRNAs) to identify candidate genes.....	51
3.3.2 Genetic complementation of parental accessions	53
3.3.3 Polymorphisms among parental accessions in candidate genes	55
3.3.4 Characterization of crosses among parental-like accessions	56
3.4 Characterization of F₂ phenotypes.....	58
3.4.1 Classification of F ₂ phenotypes.....	59
3.4.2 Testing the two-locus model for F ₂ segregations	61
3.5 Analysis of backcrosses.....	64
3.5.1 Phenotypic characterization of backcrosses.....	64
3.5.2 Analysis of phenotypic ratios in backcrosses.....	67
3.5.3 Crosses between backcross recombinant lines.....	68
4. Discussion.....	70
4.1 F₁ phenotype depends on temperature and developmental stage.....	70
4.2 Metabolic and hormonal changes associated with F₁ phenotype.....	71
4.2.1 Flavonoids are increased by temperature in hybrids.....	71
4.2.2 Hormonal changes are associated with the altered stem growth.....	71
4.3 Four genes are necessary for F₁ phenotype.....	72
4.4 The two-locus interaction is dose-dependent	75
4.5 F₁ phenotype depends on the parental background	76
4.6 Proposed model for the mechanism of BG-5xKro-0 hybrid incompatibility	77
5. Conclusion and future perspectives.....	79
6. Acknowledgements.....	80
7. Bibliography	82
8. Supplemental data.....	91
9. Curriculum vitae.....	102

LIST OF FIGURES

Figure 1.1	BDM-model showing evolution of hybrid incompatibility	13
Figure 1.2	Schematic representations for different types of meristematic tissues on plant stem	18
Figure 1.3	Schematic representation for shoot meristem maintenance by <i>WUS-CLV3</i> and <i>DELLA</i>	19
Figure 1.4	Schematic representation of the central coordinating role of <i>BRC1</i> in lateral bud outgrowth.....	21
Figure 1.5	<i>A.thaliana</i> BG-5 × Kro-0 hybrid phenotypes and genetic mapping	28
Figure 2.1	Scheme illustrating the followed segregating generations and their phenotypic classes.....	39
Figure 3.1	Phenotypic analysis of the temperature-dependent F ₁ phenotype.....	40
Figure 3.2	Characterization of shoot architecture in F ₁ hybrids at 17°C.....	42
Figure 3.3	Shoot apical meristem (SAM) at bolting and root apical meristem (RAM) two-weeks after germination of F ₁ and parents at 17°C	43
Figure 3.4	Response of shoot architecture related traits to temperature in F ₁ and parents	44
Figure 3.5	Developmental-dependent F ₁ phenotype.....	46
Figure 3.6	The role of Tre6P in F ₁ phenotype at 17°C.	47
Figure 3.7	Analysis of metabolites in F ₁ and BG-5 and Kro-0	48
Figure 3.8	Analysis of hormones in leaves, the first internode and the second internode at 17 °C and 21 °C of F ₁ hybrids, BG-5, and Kro-0.....	50
Figure 3.9	Characterization of amiRNA- <i>gene</i> -F ₁ in comparison to parents and the F ₁ phenotype at 17°C.....	52
Figure 3.10	Relative expressions of the targeted genes in amiRNA-lines and parental accessions	53
Figure 3.11	<i>GUS</i> staining showing the expression of cloned candidate genes by native promoters.....	54
Figure 3.12	Phenotypes of T ₁ p <i>Gene::Gene</i> transformants with parental alleles at 17°C.....	55
Figure 3.13	Additional crosses with BG-5- and Kro-like accessions that show F ₁ -like phenotype at 17°C.....	58
Figure 3.14	Phenotypic characterizations of F ₂ hybrids at 17°C.....	60
Figure 3.15	Correlation analyses between root and shoot phenotypes in F ₂ and F ₃ grown at 17°C.....	61
Figure 3.16	Phenotypic segregation of F ₃ plants of F ₂ class-III plant and plant class-IV grown at 17°C.....	62
Figure 3.17	Phenotypic characteristics of backcrosses grown at 17°C.....	66
Figure 3.18	Comparison of different segregating phenotypic classes with F ₁ and parental grown at 17°C.....	67
Figure 4.1	Schematic diagrams presenting peroxisome functions (A) and peroxisome proliferation and replication in Arabidopsis (B).....	79

LIST OF SUPPLEMENTAL FIGURES

Figure S 1	Phenotypic characterization of F ₁ and parents at 17°C.....	93
Figure S 2	Phenotypic characterization of F ₁ and parents at 21°C.....	94
Figure S 3	F ₁ hybrids grown at 17°C targeted with amiRNAs against Chr2 candidate genes.....	95
Figure S 4	F ₁ hybrids grown at 17°C targeted with amiRNA against Chr3 candidate genes.....	96
Figure S 5	Phenotypic characterization of F ₂₋₂ generation grown at 17°C.....	97
Figure S 6	Phenotypic characterization of F ₂₋₃ generation grown at 17°C.....	98
Figure S 7	Root phenotypes in F ₁ , parents, F _{2s} and backcross segregants grown at 17 °C.....	99
Figure S 8	Developmental map of the expression of <i>AT2G14120 (DRP3B)</i> indicated by eFPbrowser.....	100
Figure S 9	Developmental map of the expression of <i>AT2G14100 (CYP705A13)</i> indicated by eFPbrowser.....	101
Figure S 10	Developmental map of the expression of <i>AT3G60840 (MAP65-4)</i> indicated by eFPbrowser.....	102

LIST OF TABLES

Table 2.1	Accessions that were used in this study.....	29
Table 2.2	Marker type, name, sequence for the forward (F) and reverse (R) primers and position for the markers that were used for genotyping in this study	33
Table 2.3	Chr2/Chr3 candidate genes and their amiRNA target sequence.....	34
Table 2.4	List of primers used for quantitative RT-PCR.....	36
Table 2.5	Forward (F) and reverse (R) primers designed for the genomic constructs of the candidate genes	37
Table 3.1	The selected accessions and the genes they shared SNPs with and the phenotype of their F ₁ hybrid.....	57
Table 3.2	Phenotypic classification of F ₂ progeny and their expected numbers.....	63
Table 3.3	χ^2 test of a two-gene model for observed phenotypes of three F ₂ s populations	63
Table 3.4	Expected and observed phenotypes of amiR- <i>DRP3B</i> F ₂ s based on their genotype.....	64
Table 3.5	Table 3.5 χ^2 test of two-gene model for BC ₁ F ₁ ^{BG-5} observed phenotypes.....	67
Table 3.6	Table 3.6 χ^2 test of two-gene model for BC ₁ F ₁ ^{Kro-0} observed phenotypes.....	68
Table 3.7	Genotypes of BC ₁ F ₁ ^{Kro-0} C-I lines and the lines they were crossed with and their hybrid phenotypes.....	69
Table 3.8	Genotypes of BC ₁ F ₁ ^{BG-5} C-I lines and the lines they were crossed with and their hybrid phenotypes.....	69

ABBREVIATIONS

μE	Micro Einstein = $1 \mu\text{mol}\cdot\text{m}^2\cdot\text{s}^{-1}$
16h	16 hours
<i>A.thaliana</i>	<i>Arabidopsis thaliana</i>
ABA	Abscisic acid
amiR- <i>Gene</i> -BG-5	BG-5 with artificial microRNA against specific gene
amiR- <i>Gene</i> -F ₁	F ₁ with artificial microRNA against specific gene
amiR- <i>Gene</i> -Kro-0	Kro-0 with artificial microRNA against specific gene
amiRNA	Artificial microRNA
B	BG-5 allele on Chr3
BASTA	Glufosinate-ammonium
BC	Backcross
BC ₁ -B-CI	Class-I in first generation of backcross with BG-5
BC ₁ F ₁	First generation of backcrosses
BC ₁ F ₁ ^{BG-5}	First generation of backcross with BG-5
BC ₁ F ₁ ^{Kro-0}	First generation of backcross with Kro-0
BC ₁ -K-CI	Class-I in first generation of backcross with Kro-0
BDM-model	Bateson-Dobzhansky-Muller Model
BG-5	<i>A.thaliana</i> accession BG-5 (Seattle, USA)
CaMV	Cauliflower mosaic virus
CAPS	Cleaved Amplified Polymorphic Sequences
Chr	Chromosome
C-I	Class-I phenotype of F ₂ progeny
C-II	Class-II phenotype of F ₂ progeny
C-III	Class-III phenotype of F ₂ progeny
C-IV	Class-IV phenotype of F ₂ progeny
CTAB	Cetyltrimethylammoniumbromide
C-V	Class-V phenotype of F ₂ progeny
<i>CYP705A13</i>	Gene encodes for a cytochrome p450, family 705, subfamily a, polypeptide 13 protein
<i>CYP76C8P</i>	Pseudogene encodes for cytochrome P450 superfamily protein
DNA	Deoxyribonucleic acid
<i>DRP3B</i>	A gene encodes for DYNAMIN-RELATED PROTEIN 3B
<i>E.coli</i>	<i>Escherichia coli</i>
EDTA	Ethylenediaminetetraacetic acid
EtOH	Ethanol
F ₁	First generation after crossing two parents
F ₁ phenotype	Dwarf-bushy phenotype
F ₁ -like phenotype	Similar phenotype to dwarf-bushy phenotype
F ₂	Second generation after crossing two parents

F ₃	Third generation after crossing two parents
GUS	<i>beta-glucuronidase</i> gene
H	Heterozygous
HB	Hybrid breakdown
IAA	Indole-3-acetic acid
JA	Jasmonic acid
K	Kro-0 allele on Chr2
Kro-0	<i>A.thaliana</i> accession Krotzenburg-0 (Krotzenburg Germany)
LD	Long day
MAP65-4	A gene encoding for a MICROTUBULE-ASSOCIATED PROTEIN 65-4
NI	Number of internodes
PCR	Polymerase chain reaction
QTL	Quantitative trait locus
RAM	Root apical meristem
RNA	Ribonucleic acid
qRT-PCR	Quantitative real timer polymerase chain reaction
SA	Salicylic acid
SAM	Shoot apical meristem
SL	Strigolactones
SSLP	Simple sequence length polymorphism
stage I	Stage when plants have 8 leaves
stage II	Stage when plants are bolting
stage III	Stage when plant have formed the 1 st internode of the stem
stage IV	Stage when plants have formed 2 nd internode of the stem
TFs	Transcription factors
Ti-plasmid	Tumor inducing plasmid
Tre6P	Trehalose 6-phosphate
Tre6P:sucrose	The sucrose-trehalose 6-phosphate (Tre6P) nexus
Tris-HCl	Tris (hydroxymethyl) aminomethane hydrochloride
WT-like	Wild type (parental accessions)- like phenotype
χ ²	Chi-square test

SUMMARY

A reciprocal cross between two *A. thaliana* accessions, Kro-0 (Krotzenburg, Germany) and BG-5 (Seattle, USA), displays purple rosette leaves and dwarf bushy phenotype in F₁ hybrids when grown at 17 °C and a parental-like phenotype when grown at 21 °C. This F₁ temperature-dependent-dwarf-bushy phenotype is characterized by reduced growth of the primary stem together with an increased number of branches. The reduced stem growth was the strongest at the first internode. In addition, we found that a temperature switch from 21 °C to 17 °C induced the phenotype only before the formation of the first internode of the stem. Similarly, the F₁ dwarf-bushy phenotype could not be reversed when plants were shifted from 17 °C to 21 °C after the first internode was formed. Metabolic analysis showed that the F₁ phenotype was associated with a significant upregulation of anthocyanin(s), kaempferol(s), salicylic acid, jasmonic acid and abscisic acid. As it has been previously shown that the dwarf-bushy phenotype is linked to two loci, one on chromosome 2 from Kro-0 and one on chromosome 3 from BG-5, an artificial micro-RNA approach was used to investigate the necessary genes on these intervals. From the results obtained, it was found that two genes, *AT2G14120* that encodes for a DYNAMIN RELATED PROTEIN3B and *AT2G14100* that encodes a member of the Cytochrome P450 family protein CYP705A13, were necessary for the appearance of the F₁ phenotype on chromosome 2. It was also discovered that *AT3G61035* that encodes for another cytochrome P450 family protein CYP705A13 and *AT3G60840* that encodes for a MICROTUBULE-ASSOCIATED PROTEIN65-4 on chromosome 3 were both necessary for the induction of the F₁ phenotype. To prove the causality of these genes, genomic constructs of the Kro-0 candidate genes on chromosome 2 were transferred to BG-5 and genomic constructs of the chromosome 3 candidate genes from BG-5 were transferred to Kro-0. The T₁ lines showed that these genes are not sufficient alone to induce the phenotype. In addition to the F₁ phenotype, more severe phenotypes were observed in the F₂ generations that were grouped into five different phenotypic classes. Whilst seed yield was comparable between F₁ hybrids and parental lines, three phenotypic classes in the F₂ generation exhibited hybrid breakdown in the form of reproductive failure. This F₂ hybrid breakdown was less sensitive to temperature and showed a dose-dependent effect of the loci involved in F₁ phenotype. The severest class of hybrid breakdown phenotypes was observed only in the population of backcross with the parent Kro-0, which indicates a stronger contribution of the BG-5 allele when compared to the Kro-0 allele on the hybrid breakdown phenotypes. Overall, the findings of my thesis provide a further understanding of the genetic and metabolic factors underlying altered shoot architecture in hybrid dysfunction.

ZUSAMMENFASSUNG

Die reziproke Kreuzung der zwei *A. thaliana*-Akzessionen Kro-0 aus Krotzenburg (Deutschland) sowie BG-5 aus Seattle (USA) manifestiert sich in einem Zwergbusch-Phänotyp in den F₁ Hybriden bei 17 °C. Dagegen zeigen die Nachkommen bei 21 °C einen Phänotyp, der den Eltern ähnelt. Somit handelt es sich bei dieser Kreuzung um einen temperaturabhängigen Phänotyp. Dieser ist gekennzeichnet durch einen gestörten Wuchs des Primärstammes sowie einer vermehrten Anzahl an gebildeten Seitenzweigen. Das gestörte Wachstum des Hauptsprosses ist am gravierendsten rund um das 1. Internodium der Pflanzen. Es konnte gezeigt werden, dass durch einen Temperaturwechsel von 21 °C auf 17 °C der Phänotyp nur induziert werden kann vor der Bildung des 1. Internodiums. Im Gegenzug dazu ist ebenfalls die Rettung des parental Phänotyps nur möglich vor der Bildung des 1. Internodiums am Hauptspross. Des Weiteren zeigten metabolische und hormonelle Analysen der F₁ Hybriden eine signifikante Erhöhung von Anthozyanen, Kaempferol, Salizylsäure, Jasmonsäure sowie Abscisinsäure. In Vorarbeiten wurde der Phänotyp bereits mit zwei verschiedenen Loci verknüpft, einer befindet sich auf Chromosom 2 der Elternlinie Kro-0, der andere auf Chromosom 3 von BG-5. Mittels eines micro-RNA Versuches konnte ich zeigen, dass die zwei Gene *AT2G14120 DYNAMIN RELATED PROTEIN3B* und *CYP705A13*, welches zur Familie des Zytochrom P450 gehört, auf dem Chromosom 2 von Kro-0 involviert sind. Auf Chromosom 3 von BG-5 gehören die Gene *CYP76C8P (AT3G61035)* sowie *MICROTUBULE-ASSOCIATED65-4 (AT3G60840)* zu den verantwortlichen Genen. Es wurden genomische Konstrukte der Kro-0-Kandidatengene auf BG-5 übertragen sowie ebenfalls genomische Konstrukte der Chr3-Kandidatengene auf Kro-0 übertragen. Die T1-Linien bewiesen keines dieser Gene als allein ausreichend. Zusätzlich zu dem F₁-Phänotyp wurden in den F₂-Generationen, die in fünf verschiedene phänotypische Klassen eingeteilt waren, schwerwiegendere Phänotypen beobachtet. Während die Samenausbeute zwischen F₁-Hybriden und Elternlinien vergleichbar war, zeigten drei phänotypische Klassen in der F₂-Generationen einen Hybridabbau in Form von Fortpflanzungsversagen. Dieser F₂-Hybridabbau war weniger temperaturempfindlich und zeigte einen dosisabhängigen Effekt, basierend auf der genetischen Architektur der am F₁-Phänotyp beteiligten Loci. Die schwerste Klasse von hybriden Abbauphänotypen wurde nur in der Population von Rückkreuzungen mit dem Elternteil Kro-0 beobachtet, was einen stärkeren Beitrag des BG-5-Allels im Vergleich zu dem Kro-0-Allel auf den hybriden Abbauphänotypen anzeigt. Insgesamt liefern die Ergebnisse meiner Dissertation ein weiteres Verständnis der genetischen und metabolischen Faktoren, die der veränderten Sprossarchitektur bei hybrider Dysfunktion zugrunde liegen.

1. Introduction

1.1 Hybrid incompatibility

Hybridization is a process that takes place across taxa in nature and is the process by which different alleles or genomes are combined in one individual called a hybrid (Anderson, 1953; Arnold and Martin, 2009). It is well-known that consequences of hybridization can lead to hybrid vigor (heterosis), but they may also lead to hybrid failure; a phenomenon known as hybrid incompatibility. Hybrid incompatibilities are found across inter- and intraspecific hybrids and have always mystified scientists (Anderson, 1953; Arnold and Martin, 2009; Bomblies and Weigel, 2007; Rieseberg and Willis, 2007; Smith *et al.*, 2011; Maheshwari and Barbash, 2011). In 1859, Charles Darwin in his book “The Origin of Species” stated that species diverge from a common ancestor by accumulating adaptive changes refined by natural selection in favor of fitness (Darwin, 1859). Thus, Darwin concluded that sterility is not a trait selected by means of natural selection but is rather a by-product of selective pressure on other beneficial traits.

“In as much the **sterility of hybrids** could **not** possibly be of **any advantage** to them, and therefore could not have been acquired by the continued preservation of successive profitable degrees of sterility. I hope, however, to be able to show that sterility is not a specially acquired or endowed quality, but **is incidental on other acquired differences**” Darwin, 1859 (p. 245 the origin of species)

Since Darwin, scientists have been investigating the mechanisms that underlie hybrid incompatibilities to understand how they evolve in populations.

1.1.1 Pre- and post-zygotic hybrid incompatibility

Reproductive barriers can be formed before (pre-zygotic) or after (post-zygotic) fertilization. Pre-zygotic barriers include behavioural, mechanical, spatial or temporal and gametic isolations (Seehausen *et al.*, 2014). While pre-zygotic reproduction barriers prevent the formation of a hybrid, post-zygotic reproductive barriers prevent the development of the formed hybrid and its ability to produce successive generations (Coyne and Orr, 2004; Coyne, 2016). Post-zygotic reproductive barriers evolve as a by-product of cumulated adaptive or non-adaptive changes between lineages and can be driven by ecological factors. These barriers can result in many phenotypic defects in hybrids that drastically reduce their fitness (Rieseberg and Blackman, 2010).

1.1.2 BDM-model of post-zygotic hybrid incompatibility

The first genetic model for hybrid incompatibility was proposed by William Bateson, Theodosius Dobzhansky and Hermann Muller. William Bateson was the first geneticist who introduced the terms “epistasis” and “genetics” in his publication “Mendel's Principles of

Heredity” (Bateson, 1909). In his publication “Heredity and variation in modern lights” (Bateson, 1909), he speculated on the cause of hybrid sterility and its role in speciation. Bateson proposed that hybrid sterility is due to epistatic interaction between two complementary factors that acquired variation in parents through divergence (Bateson, 1909).

“When **two species**, both perfectly **fertile** severally, produce on crossing a **sterile progeny**, there is a presumption that the sterility is due to the development in the hybrid of some substance which can only be **formed by meeting of two complementary factors**... we see that the phenomenon could only be produced among the **divergent offspring of one species** by the acquisition of **at least two new factors**”-Bateson, 1909 (p43 Heredity and variation in modern lights)

In 1936, Theodosius Dobzhansky published a study that investigated hybrid male sterility between two subgenera of *Drosophila* *D. pseudoobscura* and *D. persimilis*. He showed that hybrid sterility is a consequence of the interaction between complementary genetic factors that acquired different variants in parents (Dobzhansky 1936; Dobzhansky and Beadle, 1936).

In 1940 and 1942, Hermann Muller proposed multiple models explaining reproductive failure in hybrids as a consequence of lethal interactions between genetic variations evolved in the nascent species by adaptive or non-adaptive changes i.e. selection or genetic drift (Muller, 1940; Muller, 1942). Thus, he proposed that mechanisms of hybrid incompatibility are concomitant with speciation through preventing nascent species from having shared offspring (Muller, 1940; Muller, 1942). Combining the work of Bateson, Dobzhansky and Muller, a BDM-model was proposed to explain the genetic basis for how hybrid incompatibilities could evolve in one population (Bateson, 1909; Dobzhansky, 1936; Muller, 1940).

According to the BDM model (Figure 1.1), independent mutations in at least two interacting genes in one ancestral population ‘aabb’ cause a change from ‘a’ into ‘A’ in one population and ‘b’ into ‘B’ in the second population. These changes could become fixed by adaptive or non-adaptive mechanisms. When a new gene variant A is combined with other new gene variant B in a hybrid, the hybrid between these diverged lineages ‘AaBb’ exhibits reduced fitness or even reproductive failure (Bateson, 1909; Dobzhansky, 1936; Muller, 1940, 1942).

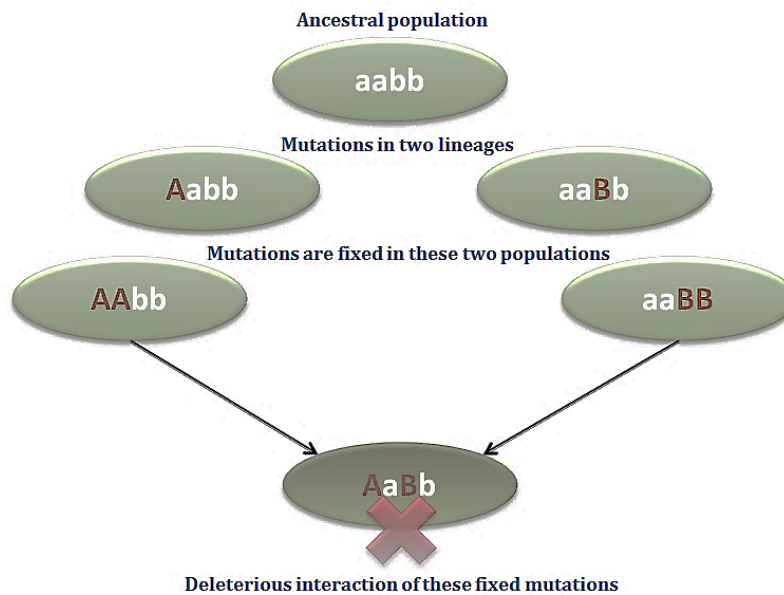


Figure 1.1 BDM-model showing evolution of hybrid incompatibility. According to this model, there are at least two interacting genes in the ancestral population *aabb* that acquire mutations changes ‘a’ to ‘A’ in one population and ‘b’ into ‘B’ in the second population. If these mutations became fixed by adaptive or non-adaptive mechanisms, the population ‘Aabb’ would become ‘AAbb’ and the ‘aaBb’ would become ‘aaBB’. When the new gene variant A is combined with the other new gene variant B in a hybrid, the hybrid between these diverged lineages ‘AaBb’ exhibits a reduced fitness or even reproductive failure.

1.2 Mechanisms of post-zygotic hybrid incompatibility in plants

BDM-incompatibilities have been reported across inter- and intraspecific hybrids in different plant species including crops such as *Oryza* as well as model species such as *Nicotiana*, *Arabidopsis*, *Gossypium*, *Capsella* and *Oenothera* (Seehausen *et al.*, 2014; Fishman and Sweigart, 2018). So far, the most studied cases of post-zygotic hybrid incompatibilities (HIs) in plants are hybrid sterility, hybrid necrosis or weakness and embryo lethality (Presgraves, 2010; Seehausen *et al.*, 2014). Many of the reported HI cases in the F_1 generation were linked to simple genetic basis of two interacting loci or an allelic interaction at one locus. The deleterious combination of complementary factors in hybrid incompatibility that do not affect the fitness in F_1 would also segregate hybrid breakdown in F_2 or backcrosses (Seehausen *et al.*, 2014; Fishman and Sweigart, 2018). Often, in hybrid breakdown cases, the genetic base is either a recessive interaction of two genes, more than two genes, or it is an interaction between cytonuclear and nuclear genes (Burton *et al.*, 2013).

1.2.1 Hybrid sterility

In plants, hybrid sterility is the most common mechanism of BDM-type post-zygotic hybrid incompatibility within and between species (Rieseberg and Blackman, 2010; Maheshwari and Barbash, 2011). Hybrid sterility is often due to the incompatible interaction between nuclei or the incompatible interaction between nuclei and mitochondria leading to cytoplasmic male sterility (CMS) (Cosmides and Tooby, 1981; Burton *et al.*, 2013).

While sterility is commonly found in plant hybrids, few cases of hybrid sterility have been reported in *A. thaliana*. One of the rare examples of this is hybrid sterility found in recombinant inbred lines (RILs) between the Arabidopsis accessions Shahdara (Sha) and Colombia-0 (Col-0) (Durand *et al.*, 2012). In this case, a duplication event triggers *de novo* DNA methylation of the native copy of *AtFOLT1* to cause sterility. The transposition of *AtFOLT2*, a copy of *AtFOLT1*, causes a rearranged paralogous structure that triggers gene silencing of the native *AtFOLT1* by DNA methylation in Sha. As there is only one expressed copy of *AtFOLT* in Col-0, RIL individuals that contain loci combination of Col and Sha showed a lack of expression of *AtFOLT* in flowering tissues and as such, were sterile (Durand *et al.*, 2012).

CMS cases are relatively rare in *A. thaliana*; nevertheless, an F₁ CMS case between *A. thaliana* accessions Sha and Mr-0 has been reported (Gobron *et al.*, 2013). Cytological observations demonstrated pollen mortality in the F₁ generation when the mother was Sha, whilst genetic analysis showed that a novel mitochondrial genomic locus in Sha '*orf117Sha*' with two genomic loci on Chr1 and Chr3 from Mr-0 were the sterilizing factors when Sha was the mother. Crossing accessions similar to Mr-0 and Sha identified at least ten other occurrences of CMS in the F₁ generation. These ten accessions, which generated these events, shared the same cytoplasmic sterilizing factor with Sha. Interestingly, it was found that the locus '*orf117Sha*' is restricted to accessions from central Asia and Russia (Gobron *et al.*, 2013). Furthermore, it was confirmed that '*orf117Sha*' is a sterilizing factor by interacting with the nuclear loci of Mr-0 by developing cytolines through recurrent backcrosses. Furthermore, the previously identified loci from Chr1 and Chr3 from Mr-0 were involved in F₂ sterility when Mr-0 is the mother (Simon *et al.*, 2016). Repeating the scheme of crosses with similar accessions to Sha and Mr-0 and with QTL analysis for hybrids, it was found that the genetic basis of this case of CMS is rather complex with many identified QTLs (Simon *et al.*, 2016).

In rice, hybrids between cultivars of the *O. indica* × *O. japonica* were semi-sterile in the F₁ generation but individuals of the F₂ generation showed complete abortion of pollen (Long *et al.*, 2008). Genetic mapping revealed that the genetic basis of this sterility was due to one locus interaction between two adjacent genes that have different sequence variants between parents. One gene was found to encode a small ubiquitin-like modifier *SUMO E3*

ligase-like protein (*SaM*) and the other was found to encode an F-box protein (*SaF*). The locus *SaM⁺SaF⁺* in *O. indica* was shown to interact with *SaM⁻SaF⁻* in *O. japonica* where *SaM⁻* produces a non-functional protein and *SaF⁻* has an amino acid change. Segregants that harbor the heterozygous or homozygous combination of *SaM⁺SaF⁺* and *SaM⁻SaF⁻* showed a complete loss of fertility (Long *et al.*, 2008). In another independent study, a two-gene interaction caused hybrid sterility in a cross between rice cultivars Niponbare of *O. japonica* and Kasalash of *O. indica* (Mizuta *et al.*, 2010). Genetic analysis revealed that disruptions in two-gene interaction were the cause of this sterility. The first gene *DOPPELGANGER 1* in *O. japonica* had a loss of function due to a disruption in its sequence by a transposable element. The second gene *DOPPELGANGER 2* in *O. indica* had a loss of function caused by a mutation that terminates its translation (Mizuta *et al.*, 2010). The individuals that contained the two-gene combination (*indica/japonica*) exhibited pollen sterility due to the lack of expression of both genes in flowering tissues (Mizuta *et al.*, 2010). In another case, hybrids between *O. sativa* cultivars Tachisugata × H-193, showed fertile F₁ plants that segregated into individuals with reduced sterility and dwarf phenotypes in the F₂ (Matsubara *et al.*, 2015). Mapping and genetic analysis revealed the occurrence of eight significant epistatic interactions. However, the biggest contributor to this sterility was a recessive interaction between the two loci *HYBRID BREAKDOWN 4* on Chr1 of H-193 and *HYBRID BREAKDOWN 5* on Chr12 of Tachisugata. That was validated by analyzing F₃ progeny that harbor either locus in a heterozygous or homozygous manner (Matsubara *et al.*, 2015).

In a study by Yu *et al.* (2016), which used Aus-*japonica/indica* hybrids, female sterility was also observed between different varieties of rice. IR36, a variety of *O. indica*, and Cpslo17, a variety of *O. japonica* and Ingra belongs of the Aus variety. They have shown that hybrid sterility was due to epistatic interaction of different alleles in locus *S7* that encodes a tetratricopeptide repeat (TPR) that is highly expressed in the pistil. Down-regulation of this gene in hybrids derived from different parents rescued spikelet sterility and genetic complementation into respective parents also confirmed sufficiency of this locus to induce spikelet sterility (Yu *et al.*, 2016).

1.2.2 Hybrid necrosis

One of the most common types of post-zygotic hybrid incompatibility in plants is hybrid necrosis or weakness (Bomblies and Weigel, 2007; Chen *et al.*, 2016). Hybrid necrosis is associated with growth defects and necrotic lesions on leaves. So far, the identified causal genes of F₁ necrosis encode proteins involved in disease resistance. Thus, it has been suggested that hybrid necrosis evolved as a by-product of pathogen resistance mechanisms (Bomblies and Weigel, 2007; Bomblies *et al.*, 2007). It has been shown that 2% of intraspecific hybrids of *A. thaliana* exhibit temperature-dependent hybrid necrosis in the F₁

generation (Bomblies *et al.*, 2007; Chae *et al.*, 2014). Mapping of the first case of hybrid necrosis between *A. thaliana* accessions Uk-1 × Uk-3 showed that the phenomena may be linked to two loci: one on Chr3, *DANGEROUS MIX1 (DM1)* and one on Chr5, *DANGEROUS MIX2 (DM2)* (Bomblies *et al.*, 2007). Furthermore, it has been shown that both of these genes encode proteins belonging to the nucleotide-binding leucine-rich repeat (NLR) family of immune receptors (Bomblies *et al.*, 2007; Chae *et al.*, 2014). It was later found that the *DM2* locus containing a *RECOGNITION OF PERONOSPORA PARASITICA 1 (RPP1)* cluster of *NLR* may commonly cause hybrid necrosis in combination with different interacting factors (Chae *et al.*, 2014). In addition to NLRs, an allelic interaction of *ACCELERATED CELL DEATH 6 (ACD6)* has also been found to be a common cause of hybrid necrosis among global and local populations of *A. thaliana* (Todesco *et al.*, 2014; Świadek *et al.*, 2017). *ACD6* encodes an ankyrin repeat protein and has been described as a positive regulator of salicylic acid related defences against pathogens (Tateda *et al.*, 2014, 2015).

Other temperature-dependent hybrid necrosis cases have been reported in interspecific crosses in other plant species and genera (Chen *et al.*, 2016). Mino *et al.* (2002) showed that *F₁* lethality of *N.gosseii* × *N.tabacum* hybrids was associated with a prompt lysis of cells, DNA degradation and up-regulation of stress markers at 28 °C. In addition, it has been shown that the triggering factor of this lethality is transferred from cell to cell through the vasculature. However, these features were suppressed by growing the seedlings at 37 °C (Mino *et al.*, 2002). Another independent hybrid case is the interspecific *F₁* of *Nicotiana glauca* × *N.tabacum* that showed temperature-dependent programmed cell death associated with chromatin condensation and nuclear fragmentation in plant cells (Watanabe and Marubashi, 2004).

In rice, hybrids between two *O. sativa* cultivars, Nipponbare belongs to Japonica rice cultivars and the Peruvian rice cultivar Jamaica, showed a temperature-dependent dwarf phenotype, which was still fertile (Saito *et al.*, 2007). It was shown that the apical meristem in both roots and shoots lost their ability to perform cell division at temperatures below 29 °C. The genetic analysis of this phenomena revealed that the genetic basis of this hybrid case was the interaction between two complementary loci: *HYBRIDWEAKNESS1 (Hwc1)* derived from Jamaica and *HYBRIDWEAKNESS2 (Hwc2)* derived from Nipponbare (Ichitani *et al.*, 2001, 2007). *Hwc1* is specific to *O. rufipogon*, which harbours two leucine-rich repeat receptor-like genes *25L1* and *25L2* that are pathogen receptors. Similarly, *Hwc2* occurs exclusively in *O. sativa* and encodes a secreted putative subtilisin-like protease, which can act as a pathogen receptor (Figueiredo *et al.*, 2014). The temperature-dependent interaction between these two loci appears to activate the auto-immune response that impairs growth in both roots and shoot apical meristems (Chen *et al.*, 2014). Similarly, *F₁* hybrids between two *O. indica* lines (Taifeng-A and V1134) showed growth retardation at 20 °C that was associated with abnormal development of chloroplasts and mitochondria,

which could be recovered at 32 °C (Fu *et al.*, 2013). Genetic analysis linked this hybrid weakness to two dominant complementary loci named *HYBRIDWEAKNESS3* (*Hw3*) on Chr 11 and *HYBRIDWEAKNESS4* (*Hw4*) on Chr 7 that harbors *OS11G44310*, a putative calmodulin-binding protein. Calmodulin-binding proteins are key Ca²⁺ sensors that are involved in defence response (Reddy *et al.*, 2003). Therefore, as this gene has been found to be differentially expressed in F₁ hybrids, such genes may be interesting candidates for further study (Fu *et al.*, 2013).

1.2.3 Embryo lethality

Embryo lethality is a different type of BDM incompatibility that leads to problems in embryo establishment or development in the formed hybrids (Lafon-Placette and Köhler, 2016; Gehring and Satyaki, 2017). Embryo lethal hybrid cases have been widely reported and reviewed in plants (Stansfield, 2008; Chen *et al.*, 2016; Lafon-Placette and Köhler, 2016). For example, in the case of F₂ embryo lethality between hybrids of the *A. thaliana* accessions Columbia-0 (Col) and the Cape Verde Island (Cvi-0) (Bikard *et al.*, 2009), embryo lethality was due to the incompatible interaction between two paralogs of duplicated histidinol-phosphate aminotransferase genes (Bikard *et al.*, 2009). Individuals of the F₂ generation that inherited these two loci displayed complete abortion of the embryo.

In addition, it has been shown that endosperm abortion can be caused by multiple mechanisms but the paternal conflict is the main mechanism observed. It has been also found that gene imprinting can lead to endosperm abortion, as the endosperm is a dose-sensitive tissue to the increased contribution of either parental genome (Lafon-Placette and Köhler, 2016). As an example of interploidy hybridization, in a reciprocal cross of *A. thaliana* C24 (2x, 4x), *Ler* (2x, 4x) and Col-1 (6x), showed that endosperm development was inhibited by extra maternal genomes in the hybrid. In contrast, hybrids that inherited an extra dose of the paternal genome showed enhanced growth of the endosperm and embryo (Scott *et al.*, 1998). It has been suggested that these effects might be due to the dose of imprinting effects between paternal and maternal genomes (Scott *et al.*, 1998). Repeating this scheme of crossing with hypomethylated C24 plants that contained a methyltransferase I (*MET1*) antisense gene (silences a regulator of gene imprinting in the endosperm), it was found that there was a slight enhancement but not a full recovery in the number of embryo abortions. This finding suggests that maternal imprinting is necessary but not sufficient to explain endosperm failure (Adams *et al.*, 2000).

In another case of a reciprocal hybrid cross between *A. thaliana* accessions Col-1 and *Ler*, it was found that gene imprinting in the hybrid endosperm was mono-allelic and parent-of-origin-dependent, with dominance of maternally expressed genes (Raissig *et al.*, 2013). Genetic studies using transgenic parents silenced for genes regulating DNA methylation in the endosperm showed that *POLYCOMB REPRESSIVE COMPLEX* (*PRC2*) and not *MET1* was

responsible for regulating gene imprinting in the endosperm. However, in the resulting seedlings, genes from both parents were expressed, suggesting that this gene imprinting is endosperm-specific (Raissig *et al.*, 2013).

In *Oenothera*, Stubbe and Steiner, (1999) conducted 30 plastome-genome combinations of reciprocal interspecific hybrids between *O. elata*, *O. grandiflora*, and *O. argillicola*. In this study, it was shown that F₂ plants of 12 combinations showed normal vegetative growth, while the rest showed a wide spectrum of semi- and complete embryo lethality. Conducting a series of backcrosses between these incompatible hybrids and their parent showed that when the individuals were crossed back to their maternal lines, the viability of the resulting embryos was restored (Stubbe and Steiner, 1999).

1.3 Control of shoot architecture in plants

Plant shoot architecture is a complex trait controlled by many different factors (McSteen and Leyser, 2005; Bridge *et al.*, 2013). The body of the shoot is determined by different types of meristematic tissues (Figure 1.2 A) (Bridge *et al.*, 2013), which include the shoot apical meristem (SAM), that produces new cells and organs and supports vertical elongation of the main stem (McSteen and Leyser, 2005), axillary meristems (AM), which originate from the SAM and develops into axillary buds in leaf axils to give lateral branches and intercalary meristems (IM) that form at the base of internodes and promote stem elongation (McSteen and Leyser, 2005). The SAM itself, is composed of four cell zones: the central zone (CZ), peripheral zones (PZ), the rib zone (RZ) and the organizing center (OC), which is responsible for stem cell differentiation in PZ and the RZ (Sachs, 1965; Serrano-Mislata and Sablowski, 2018). The stem originates from the RZ that has a specific pattern of oriented cell division from central and organizing zones while lateral organs like leaves and floral buds they originate from PZ (Sachs, 1965; Serrano-Mislata and Sablowski, 2018).

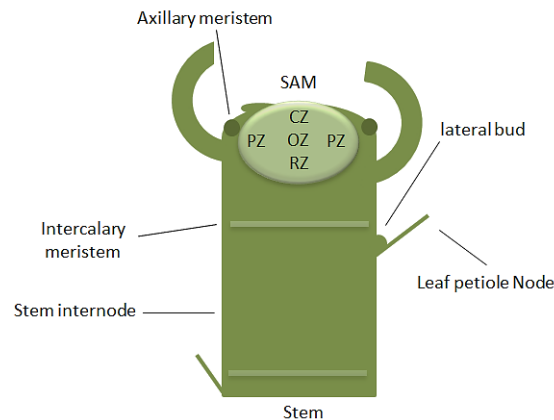


Figure 1.2 Schematic representations for different types of meristematic tissues on plant stem: Stem and shoot meristems. CZ: central zone; OC: organizing centre; PZ: peripheral zone; RZ: rib zone.

1.3.1 Genetic control of shoot architecture

The genetic basis of shoot architecture has been extensively studied by reverse and forward genetics in plants. Many conserved genetic players have been found to control or modulate shoot architecture through the balance of cell growth and differentiation in the SAM stem cells. The central regulatory signalling pathway of *WUSCHEL-CLAVATA3* (*WUS-CLV3*) is known to control stem cell proliferation and differentiation in the SAM through a negative-feedback loop (Schoof *et al.*, 2000). *CLV3* is a stem cell-specific protein expressed solely in SAM to limit the number of stem cells. Upon perception of the *CLV3* proteins by different receptors, the transcription factors *WUS* is suppressed, which in turn promotes cell differentiation in the SAM (Figure 1.3) (Schoof *et al.*, 2000). This regulatory pathway is responsible for maintaining stem cell identity during development and is regulated by hormones such as auxin and cytokinins (Schoof *et al.*, 2000; Somssich *et al.*, 2016; Wang *et al.*, 2018). In a study by Serrano-Mislata *et al.* (2018), it was shown that *DELLA* genes directly control stem elongation and size of the meristem by up-regulating the cell cycle inhibitor *KIP-RELATED PROTEIN 2* (*KRP2*) in the RZ, independent of *WUS-CLV3* pathway (Figure 1.3 A). However, in the *krp2 della* double mutant, meristem size but not stem elongation was restored, suggesting that *DELLA* control plant height and meristem size through independent pathways (Serrano-Mislata *et al.*, 2018).

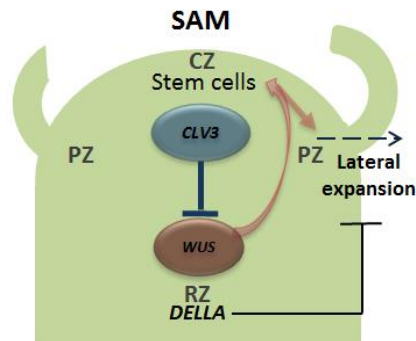


Figure 1.3 Schematic representations for shoot meristem maintenance by *WUS-CLV3* and *DELLA*. *WUS* in RZ (in red) positively regulate the expansion and differentiation of SAM while *CLV3* in stem cells (in blue) inhibits *WUS*, and *DELLA* (in black) in RZ inhibits SAM expansion independently of *WUS-CLV3*.

In addition to the *DELLA* and *WUS-CLV* pathways, many different genetic factors have been proposed as mediators of shoot meristem proliferation and differentiation (Weigel *et al.*, 1992; Long *et al.*, 1996; Conti and Bradley, 2007). Since the stem is built by a coordination

of different types of cells, a defect in cell growth orientation, proliferation or division can cause mechanical stress that may lead to abnormal stem morphogenesis (Galletti *et al.*, 2016). Growth and elongation of stem internodes are regulated by the relationship between cell proliferation and the orientation of cell division in the RZ (Hall and Ellis, 2012). Maeda *et al.* (2014) showed that the conflict between cell expansion and proliferation in SAM stem cells can create mechanical stress that affects stem organogenesis in *A. thaliana*. Similarly, Bencivenga *et al.* (2016) showed that when cells in the RZ failed to establish a distinct orientation pattern of cell division, severe dwarfism often resulted (Bencivenga *et al.*, 2016).

The growth of lateral branches is initiated from the axil of mature leaves in different manners. Axillary branches may grow acropetally, from base to apex, during vegetative growth or basipetally, from apex to base, after SAM differentiation (Grbić and Bleecker, 2000). Growth of axillary branches is controlled by different cascades of transcription factors such as the *LATERAL SUPPRESSOR (LAS)* transcription factors that accumulate specifically in axil primordia and promote initiation of auxiliary shoots (Greb *et al.*, 2003). Furthermore, *LAS* is down-regulated by other transcription factors that promote bud outgrowth like *REGULATORS OF AXILLARY MERISTEMS1 (RAX1)* (Wei *et al.*, 2012; Keller *et al.*, 2006). Recent studies have shown that the WRKY transcription factor *EXCESSIVE BRANCHES1 (EXB1)* is a positive regulator of shoot branching under stress condition by repressing auxin pathways and up-regulating *RAX* transcription factors (Guo and Qin, 2016). In addition, transcription factors, such as *SUPERSHOOT (SPS)* that functions in glucosinolate biosynthesis, has been found as a repressor of axillary branches by down-regulating cytokinin in buds (Tantikanjana *et al.*, 2001, 2004). Knockout of this gene showed significant increases in the number of rosette and cauline branches (Tantikanjana *et al.*, 2001).

Taken together, the genetic basis of shoot architecture is complex; however, it has been recently suggested that the *BRANCHED1 (BRC1)* encodes a TCP transcription factor has a central role in bud outgrowth through its involvement in multiple regulatory pathways (Figure 1.3 B) (Braun *et al.*, 2012; Gonzalez-Grandio *et al.*, 2013). *BRC1* is expressed and accumulated exclusively in lateral buds to inhibit outgrowth and has been found to be a positive regulator of abscisic acid (ABA) signalling by regulating ABA biosynthesis (Gonzalez-Grandio *et al.*, 2017). *BRC1* is up-regulated by different factors that suppress the bud outgrowth such as strigolactones, DELLA proteins and ABA (Dun *et al.*, 2012; Leduc *et al.*, 2014), while concomitantly, *BRC1* is down-regulated by the factors that promote bud outgrowth. For example, gibberellic acid regulates the expression level of *BRC1* by triggering the degradation of DELLA proteins (Davière and Achard, 2013; Davière *et al.*, 2014). Cytokinins are also known to negatively regulate *BRC1* by down-regulating strigolactone signalling as well as auxin signalling in the meristem (Leduc *et al.*, 2014).

Furthermore, independent of hormonal regulation, it has been shown that sucrose is a negative regulator of *BRC1* in buds (Mason *et al.*, 2014). *BRC1* has a major role in coordinating different interacting factor; however, by itself, *BRC1* it is not sufficient or necessary to regulate bud outgrowth (Seale *et al.*, 2017).

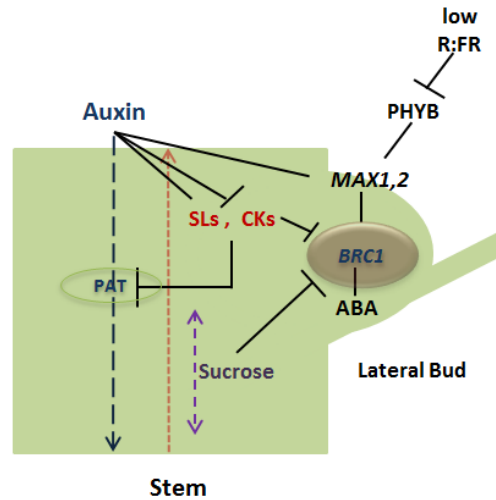


Figure 1.4 Schematic representation of the central coordinating role of *BRC1* in lateral bud outgrowth. Light-limiting conditions trigger the expression of *MAX1* and *2* and auxin through the photoreceptor phytochrome B (*PHYB*) and thus promote expression of *BRC1*. Increased expression of *BRC1* further promotes *ABA* biosynthesis in lateral buds. *BRC1* is expressed exclusively in lateral bud tissues and is suppressed by sucrose and cytokinin (*CKs*). Auxin enhances the expression of *MAX1* and *2* that positively regulate *SLs* and *BRC1*. Basipetal polar auxin transport (*PAT*) is inhibited by acropetally transported *SLs* and *CKs* that are antagonistic with auxin biosynthesis.

1.3.2 Hormonal control of shoot architecture

The early experiment of meristem decapitation in *Vicia faba* (field bean) (Thimann and Skoog, 1933) has since drawn attention on the pivotal role of auxin in apical dominance and inhibition of lateral branches. Auxin, to which indole-3 acetic acid (*IAA*) is the most active form, has been shown to have a pivotal role in a multitude of growth aspects in plants from germination to senescence. Biosynthesis of auxin is achieved by different pathways that recruit a wide range of genes (Sachs and Thimann, 1967; Bangerth, 1994; Li *et al.*, 1995; Li and Bangerth, 1999; Chandler, 2009; Normanly, 2010), which include transcription factors and enzymes that coordinate the interaction of auxin and other hormones (Rameau *et al.*, 2015; Wang *et al.*, 2008). *IAA* produced from the *SAM* must travel long distances from source to target in a directional manner by efflux and influx transport. Auxin basipetal polar transport, which occurs from cell to cell, is carried out by

PIN-FORMED that control the directional transport of auxin synergistically with ABC transporters. In contrast, P-glycoproteins facilitate long-distance auxin efflux through the plasma membranes (Petrásek *et al.*, 2006; Petrásek and Friml, 2009). In addition, auxin influx symporters (*AUX/LAX*) play an important role in auxin canalization (Yang *et al.*, 2006). There are two main models that explain how auxin regulates shoot branching (Rameau *et al.*, 2015). The first model explains how signalling pathways downstream of auxin modulate hormonal pathways and the second model explains how auxin canalization regulates branching downstream of other hormones (Sachs and Thimann, 1967; Bangerth, 1994; Li *et al.*, 1995; Rameau *et al.*, 2015).

According to the first model, cytokinins (CKs) and strigolactones (SLs) act downstream of auxin. The role of cytokinins (CKs) in regulating shoot branching was first discovered when exogenous application of CK unlocked dormant buds (Sachs and Thimann, 1967). One of the key enzymes of CK biosynthesis *ISOPENTENYL TRANSFERASE (IPT)* is regulated on transcriptional levels by endogenous levels of auxin. When auxin levels are low, CKs biosynthesis starts to increase in nodes and are then transported to axillary buds to initiate their outgrowth by downregulating *BRC1* (Tanaka *et al.*, 2006; Aguilar-Martinez *et al.*, 2007). Furthermore, it was observed by Tanaka *et al.* (2006) as well as Ferguson and Beveridge (2009), that when CKs levels are limited in dormant buds, even when auxin is very low, that buds did not grow, suggesting a crucial role of CKs in axillary bud growth (Tanaka *et al.*, 2006; Ferguson and Beveridge, 2009). In 2008, strigolactone-deficient mutants, which display an increased number of branches, have drawn much attention to SLs, such that they were considered a new class of hormones that inhibit lateral shoots (Umehara *et al.*, 2008). In contrast, many SL genes are positively regulated by auxin. For example, carotenoid cleavage dioxygenases and monooxygenases encoded by *MAX* have been shown to negatively affect strigolactone-mediated auxin transport, which in turn, suppresses the bud outgrowth by positively regulating *BRC1* (Hayward *et al.*, 2009; Dun *et al.*, 2012; Challis *et al.*, 2013). In summary, the first model proposes that auxin regulates both CK and SL biosynthesis in an opposing manner and both hormones act downstream of auxin to regulate *BRC1*, which in turn leads to bud outgrowth (Figure 1.3 B).

According to the auxin canalization model, the extent and direction of auxin transport control shoot branching (Harrison, 2017). It has been shown that the relationship between auxin basipetal transport and branching is governed by complex dynamics (Heisler *et al.*, 2005; Shinohara *et al.*, 2013; Harrison, 2017). This model suggests that at higher levels of auxin, CK and SL hinder auxin canalization by promoting the removal of PIN proteins from the plasma membrane. This inhibits the polar transport of auxin from and to axillary buds and thus decreases the chance of bud outgrowth (Shinohara *et al.*, 2013; Rameau *et al.*, 2015). Deficiency of either CK or SL increases auxin basipetal movement due to accumulated PIN proteins. For example, *A. thaliana max* SL-deficient mutant shows a fast

auxin transport but also a dwarf bushy phenotype (Shinohara *et al.*, 2013) (Figure 1.3 B). Moreover, flavonoids have also been shown as negative regulators of auxin polar transport. In *A. thaliana* flavonoid-deficient mutants, auxin canalization was shown to move faster and a greater number of lateral branches was observed (Brown *et al.*, 2001).

Besides the interrelation between IAA, CK, and SL, other hormones such as gibberellic acid (GA) and brassinosteroids (BR) also play a role in regulating internode elongation and shoot branching in plants. Analysis of GA-deficient mutants, which exhibit dwarf bushy phenotypes, present GA as a repressor of branching in plants. In contrast to SL, GA stabilizes the localization of PIN proteins to the plasma membrane. In addition, GA regulates the ratio of DELLA proteins to BRC1 transcription proteins in axillary buds (Willige *et al.*, 2011; Davière and Achard, 2013; Davière *et al.*, 2014). In the presence of GA, DELLA proteins are preferentially degraded, which then allows cell-cycle genes to promote meristem size. *BRC1* is then up-regulated to repress buds, which further promotes stem elongation and represses branching (Davière and Achard, 2013; Davière *et al.*, 2014). BR, on the other hand, promotes the growth of axillary buds through repressing the SL biosynthesis pathway, but do not always affect stem elongation (Wang *et al.*, 2013). As observed by Wang *et al.* (2013), enhanced expression of BR biosynthesis genes in *A. thaliana* mutants was associated with increased branches (Wang *et al.*, 2013). Contrastly, BR-deficient mutants in rice and pea often exhibit reduced branching but also dwarfism (Murfet and Reid, 1993; Murfet, 2003; Tong *et al.*, 2009).

While abscisic acid (ABA), jasmonic acid (JA) and salicylic acid (SA) are hormones known to mediate plant responses to different biotic and abiotic stresses (Tamaoki *et al.*, 2013; Gupta *et al.*, 2017), they also interact with IAA and CK to coordinate between growth and stress responses (Gupta *et al.*, 2017). Recently, it was shown that ABA suppresses bud outgrowth in response to shade conditions in *A. thaliana*. This response was mediated by *BRC1* that positively regulates ABA biosynthesis on a transcriptional level (Gonzalez-Grandio *et al.*, 2013). In another study, it was found that the level of ABA decreased in growing buds and was elevated in dormant buds. Analysis of knockout mutants of the auxin influx transporter, *MAX2* as well as *BRC1*, showed reduced levels of ABA and increased branching (Yao and Finlayson, 2015). Furthermore, the expression of ABA inhibited auxiliary bud outgrowth by suppressing local auxin biosynthesis and accumulation (Yao and Finlayson, 2015). In contrast, it was observed that ABA enhances the expression of *EXCESSIVE BRANCHES1 (EXB1)* that promotes bud growth under stress conditions (Guo and Qin, 2016). In the case of SA, exogenous application of SA analogues can repress a number of genes involved in auxin biosynthesis and enhance genes that convert free IAA into inactive forms (Staswick *et al.*, 2004, 2005; Wang *et al.*, 2006, 2007; Naseem *et al.*, 2018). However, other studies have shown that when plants are infected by pathogens, overexpression of auxin signalling F-box proteins can lead to reduced levels of SA in plants

(Robert-Seilaniantz *et al.*, 2011; Naseem *et al.*, 2018). For JA, the relationship between JA and auxin depends on level of stress and endogenous status of auxin in plants. As demonstrated by Qi *et al.* (2012), exogenous application of both auxin and methyl-JA enhanced the expression of JA responsive genes in *A. thaliana*. This is consistent with the analysis of knock out mutants of genes involved in auxin biosynthesis and transport (Sun *et al.*, 2009; Hentrich *et al.*, 2013), which show a higher susceptibility to pathogen infection. In addition, JA is known to regulate Flavin monooxygenase that is involved in auxin indole-3-pyruvic acid biosynthesis pathway (Sun *et al.*, 2009; Hentrich *et al.*, 2013), which demonstrates a positive relationship between auxin and JA (Sun *et al.*, 2009; Qi *et al.*, 2012). On the other hand, application of JA alone can lead to growth inhibition in *A. thaliana* and can cause interruption of auxin polar movement in roots (Sun *et al.*, 2011; Wasternack and Hause, 2013). Lastly, higher levels of auxin can inhibit JA by enhancing *JAZ1* expression, which is a jasmonate pathway repressor (Grunewald *et al.*, 2009).

Taken together, different hormonal signalling pathways work in a complex network to ensure the optimum shoot architecture for maximal growth, given developmental and environmental circumstances.

1.3.3 Sugars as regulators of shoot architecture

There is growing evidence suggesting an important role of sugars and sugar signalling in regulating shoot branching through a regulatory machinery includes hormones (Lunn and Rees, 1990; Morris *et al.*, 2005; Lunn *et al.*, 2006; Sairanen *et al.*, 2012; Wang and Ruan, 2013; Barbier *et al.*, 2015). The role of sugar in axillary bud outgrowth was investigated using intact and decapitated garden pea plants *Pisum sativum*. Supplying [¹¹C] CO₂ to the upper leaves of intact and decapitated plants showed a significant accumulation of photo-assimilates in node regions soon after decapitation (Mason *et al.*, 2014) and before any detected change in auxin levels. In addition, the total amount of sugar content in the axillary buds increased significantly within only 4 hours of decapitation. Accordingly, supplying ¹⁴C-sucrose to a single leaf node showed that within 2 hours of decapitation, the amount of sugar translocated from node to node doubled, which was significantly faster than the movement of IAA. This experiment showed that sugar supply to axillary buds is sufficient for bud release (Mason *et al.*, 2014). Furthermore, sugar deprivation in axillary buds inhibited bud growth even when hormones were in required levels for bud release (Mason *et al.*, 2014). Recently, it has been shown that trehalose 6-phosphate (Tre6P), a sugar-signalling molecule, has a major role in shoot architecture. *A. thaliana* mutants that overexpress the *E.coli otsA* (*Tre6P synthase-TPS*) gene have been shown to exhibit dwarfism with increased branching, while mutants of overexpression of *E.coli otsB* (*Tre6P phosphatase; TPP*) exhibit late flowering with reduced branching (Yadav *et al.*, 2014). Fichtner *et al.* (2017) have shown that when *Pisum sativum* plants are decapitated, there is

a rapid and sustained increase of Tre6P in newly formed buds, to which the rate of increase is correlated with a bud's growth rate. These results clearly show a positive correlation between sugar signalling pathways and bud outgrowth (Fichtner *et al.*, 2017).

1.3.4 Role of flavonoids in shoot architecture

Flavonoids have emerged as modulators of auxin transport by influencing the activity of P-glycoproteins that are ATP-binding cassette transporters, which in turn can compete with auxin for these transporters (Peer and Murphy, 2007; Zhao *et al.*, 2010). For example, *A. thaliana* *Transparent Testa tt4* mutants with flavonoid deficiency show decreased apical dominance and increased branching as a consequence of faster auxin transport (Brown *et al.*, 2001). Furthermore, such mutants also show that the regulatory role of flavonoids in auxin canalization can be a tissue-specific, such as within shoot apices (Peer and Murphy, 2007; Zhao *et al.*, 2010). In addition, flavonoid derivatives, such as kaempferol and quercetin act downstream of auxin either by inhibiting auxin transport or by responding to accumulated auxin (Besseau *et al.*, 2007; Zhao and Dixon, 2010). Upon silencing a key gene in lignin biosynthesis in *A. thaliana*, mutants showed a dwarf bushy phenotype, alterations in leaf vasculature and the accumulation of flavonoids and auxin (Besseau *et al.*, 2007). However, silencing flavonoids in this mutant by chalcone synthase repression or by crossing such mutants with flavonoid deficiency mutants restored the wild-type phenotype without altering the lignification pattern of the vasculature (Besseau *et al.*, 2007). Thus, it has been suggested that the dwarf bushy phenotype of these mutants may be due to the disruption of auxin transport by the accumulation of flavonoids (Besseau *et al.*, 2007). This is consistent with another study that showed that *p-glycoprotein4* *A. thaliana* mutants with blocked auxin polar transport accumulate flavonoid derivatives (Terasaka *et al.*, 2005). Double mutants of auxin transporters *multidrug resistanc1* and *p-glycoprotein1* exhibited reduced auxin transport coupled with curled leaves, a dwarf bushy phenotype and the accumulated of flavonoids (Noh *et al.*, 2001). These results show that shoot branching is controlled, not just by availability or depletion of auxin, but also by its altered distribution, transportation and accumulation.

1.3.5 Environmental factors controlling shoot architecture

Several environmental factors such as light, temperature, nutrient availability, soil condition and wind influence plant shoot architecture (McSteen and Leyser, 2005; Wang *et al.*, 2018). Usually, plants have to deal with a combinatorial effect of several environmental factors that determine the fate of shoot growth (Jackson, 2009; Leduc *et al.*, 2014). One of the major determinants of shoot branching in plants is light quality. A well-studied example is shade avoidance syndrome. In *A. thaliana*, a decreased red to far-red (R:FR) ratio is perceived by phytochrome B (PHYB) and phytochrome-interacting factors (PIF) that are major light integrators and negative regulators of *MAX2* and auxin (Leduc *et al.*, 2014;

Wang *et al.*, 2018). It has been shown that phytochrome B and PIF co-degrade as a response to a low R:FR, which up-regulates *MAX2* and *BRC1* to inhibit bud outgrowth and promote stem elongation. This phenotype is characteristic of shade avoidance syndrome (Leduc *et al.*, 2014).

Ambient temperature is also a major factor affecting plant branching (Wang *et al.*, 2018). One of the widely known effects of temperature is the necessary exposure to low temperatures for a prolonged time to overcome dormancy and promote the transition from vegetative growth to flowering. Djennane *et al.* (2014) have shown that the exposure of buds to darkness and cold temperature (5 °C) before transfer to ambient temperature (20 °C) can lead to bud growth. In addition, it was shown that strigolactone pathway genes, which include *MAX2*, may regulate this effect in a gradient and tissue-specific manner (Djennane *et al.*, 2014). Furthermore, Antoun *et al.* (2013) have shown that in *A. thaliana*, growth temperatures below or above the control temperatures (22 °C) can affect the number and length of branches. Specifically, stem elongation of cauline branches was reduced by the lower temperature (17 °C) and were increased in plants grown at 27 °C (Antoun *et al.*, 2013).

Soil temperature also affects shoot branching by influencing the availability of water and nutrients such as nitrogen to the root system. This can, in turn, have a dramatic effect on biomass partitioning such that the shoot to root ratio may be altered (López-Ráez *et al.*, 2008). It has been shown that low levels of nitrogen in the soil cause restricted shoot growth through cytokinins-strigolactone pathways that are antagonistic to auxin. Also, the low levels of inorganic phosphate can promote strigolactone biosynthesis and restrict cytokinin biosynthesis in roots (López-Ráez *et al.*, 2008; Ito *et al.*, 2015; Wang *et al.*, 2018).

Mechanosensing factors like wind, rain or wounding by herbivore attack can also dramatically affect the shoot architecture (Braam and Davis, 1990; Chehab *et al.*, 2008). Wind, as an example of mechanical stress, can trigger a strong response in plants, whereby stems become shorter and thicker: a process known as thigmomorphogenesis (Grace, 1988; Braam and Davis, 1990; Braam, 2005). It has been shown that these mechanosensing factors regulate the expression of touch-induced genes that encode calmodulin that is involved in the transduction of environmental signals (Braam and Davis, 1990; Braam, 2005).

1.4 *Arabidopsis thaliana* as a model to study hybrid incompatibilities

The *Arabidopsis* genus has been widely accepted as a model for studying various plant molecular and development pathways. Importantly, this genus, with its characterized species *A. lyrata* and *A. arenosa*, also provide a valuable opportunity to answer key questions about evolution and hybrid incompatibility between species (Bombliès and

Weigel, 2010; Hunter and Bomblies, 2010). The fully sequenced 1000 *A. thaliana* accessions (“1001genomes.Org”), which possesses accessions from very different geographies and microclimates, provides a plethora of information to better understanding hybrid incompatibility in context of intraspecific hybrids (Hunter and Bomblies, 2010). The *Arabidopsis* genus is very amenable to advanced molecular tools such as proteomics, genome editing, comparative genomics and bioinformatics which makes it highly achievable to conduct a wide range of experiments (Bownam, 1994; Hayashi and Nishimura, 2006; Norman and Benfey, 2009; Ossowski *et al.*, 2008; James *et al.*, 2013; Staiger, 2015). Furthermore, a short life-cycle of *A. thaliana* gives a valuable opportunity to conduct comprehensive genetic studies in a relatively short period of time in comparison with other plant taxa. Due to these reasons, *A. thaliana* has been a very successful model so far to study hybrid incompatibilities (Alcázar *et al.*, 2009; Todesco *et al.*, 2014; Świadek *et al.*, 2017; Plötner *et al.*, 2017).

1.5 Altered shoot branching in BG-5 x Kro-0 F₁ hybrids

F₁ hybrids between BG-5 and Kro-0 parents, exhibiting a temperature-dependent F₁ dwarf-bushy stature, were first identified in the laboratory to Prof. Dr. Detlef Weigel (Figure 1.1 A). In addition, it was observed that F₂ generations segregate with multiple classes of reproductive failure. Mapping of F₂ 190 parental-like individuals and 190 F₁-like individuals resulted in linkage to two loci (Boldt, 2009): one locus (700 kb) on chromosome 2 (5.90-6.50 Mb), and one locus (920 kb) on chromosome 3 (21.63-23.05 Mb) (Figure 1.1 B). Since these intervals are relatively large, however, fine-mapping and an amiRNA approach were used to narrow-down such intervals (Boldt, 2009; Muralidharan, 2015). The final size of each interval was a 220 kb region (20 protein-coding genes on chromosome2, 22.44-22.60) and a 160 kb region (12 protein-coding genes on chromosome3, 5.93-6.14).

1.6 Aims of this study

In this thesis, I further investigated the case of hybrid incompatibility between BG-5 x Kro-0 accessions of *A. thaliana*. The following aims that were addressed include:

1. Detailed phenotyping and physiological analysis of the F₁ phenotype
2. Investigation of candidate genes
3. Phenotypic and genetic analysis of the F₂ hybrid breakdown
4. Analysis of the genetic architecture of the hybrid abnormality using backcrosses

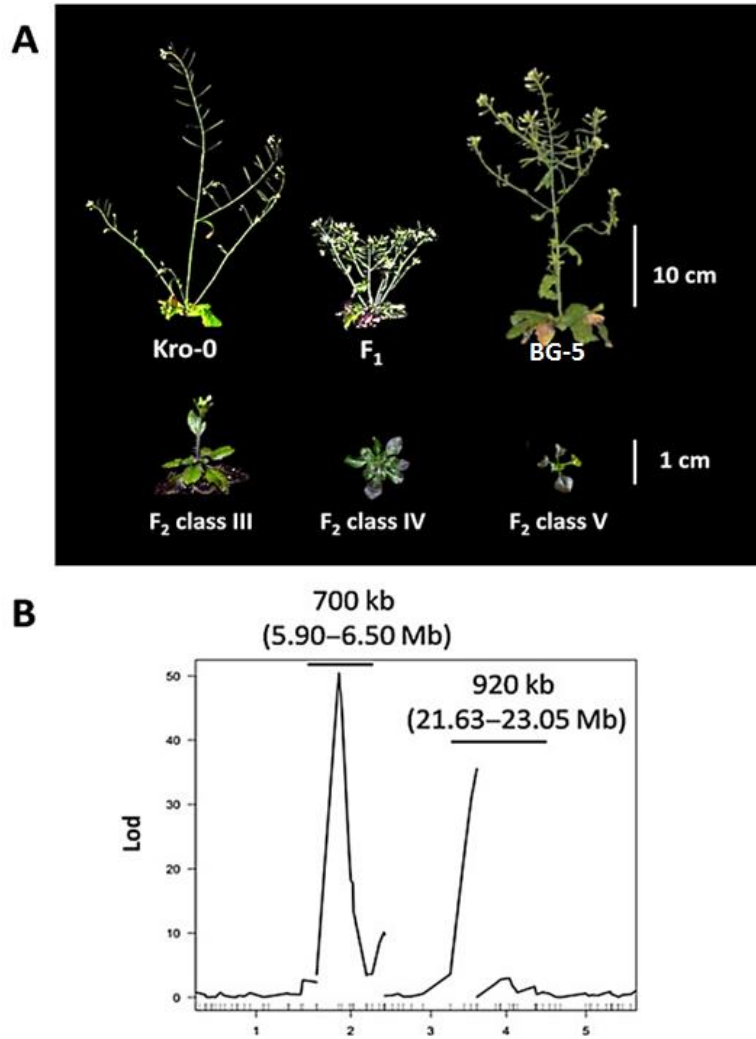


Figure 1.5 *A. thaliana* BG-5 × Kro-0 hybrid phenotypes and genetic mapping. **A:** BG-5 × Kro-0 F₁ and F₂ phenotypes at 17°C. **B:** Lod-scores of QTL analysis showing peaks of two loci (Chr2 and Chr3) associated with F₁-like phenotype.

2. Material and Methods

2.1 Plant growth conditions

Seeds of all plants were first stratified in 0.1% agarose for 2 days at 4°C to ensure a higher rate of germination. Seeds were then transferred to soil before thinning into individual replicates. For phenotypic evaluation all transformed and non-transformed BG-5, and Kro-0 plants and their hybrid progenies (F₁, F₂s, F₃s and backcross populations) were grown on soil under long day conditions (16 h/8 h light/dark regime with ~250 μmol m⁻² s⁻¹ irradiance and a relative humidity of 65%) with a constant temperature of either 17 °C or 21 °C. Transformed (amiRNA lines) and non-transformed plants used for crossing, were grown under greenhouse conditions (16 h/8 h light/dark regime with 150-350 μmol m⁻² s⁻¹ irradiance and a relative humidity of 65%). For selection of T₀ transformants on plates, seeds were suspended and washed with 0.02% sodium hypochlorite for surface-sterilization. Sterilized T₀ seeds were put on MS-plates (Murashige and Skoog) containing BASTA herbicide (10 μg/ml Glufosinate-ammonium), incubated for 2 days at 4 °C in the dark and then shifted to a 21 °C growth chamber, before being finally transported to the greenhouse.

2.2 Accessions

All accessions used in this study are listed in Table 2.1.

Table 2.1 Accessions that were used in this study.

Ecotype	Country	Latitude/ Longitude	STOCK NUMBER
Kro-0 (parent)	Germany	50.0742/8.96617	CS22342
Kro-0_Salk	Germany	50.0742/8.96617	CS76533
BG-5 (parent)	USA	N47/W122	CS76533
BG-2	USA	N47/W122	CS22342
Ragl-1	UK	54.3512/-3.41697	CS22558
Sq-8	UK	51.4083/-0.6383	CS76604
Stw-0	Russia	52/36	CS76605
Bor-4	Czech Republic	49.4013/16.2326	CS22591
Do-0	Germany	50.7224/8.2372	CS1112
Kelsterbach-4	Germany	50.0597/8.5298	CS6041
T1090	Sweden	55.6575/13.2386	CS78043
Est-1	Russia	58.3/25.3	CS1151
CIBC-5	United Kingdom	51.4062/0.6756	CS22602
NFA-10	United Kingdom	51.4083/-0.6383	CS22599
TDR-17	Sweden	55.771/14.1206	CS76246
ALST-1	United Kingdom	54.8/-2.4333	CS22550

2.3 Phenotyping

Phenotyping of F₁ hybrids and parental lines was performed at a number of developmental stages. Traits measured in this study included: days to the onset of bolting, days to the onset of cauline branching, days to the onset of rosette branches and primary stem development, primary stem length, 1st internode length, total number of shoot branches, rosette branch length, number of cauline branches, number of rosette branches, number of internodes, rosette diameter, number of seeds, flower diameter and root length. For measurement of traits such as stem length and rosette diameter plants were photographed with a reference ruler and scored using ImageJ (Collins, 2007). For seed counting, a random number of seeds was taken in five replicates from each sample (F₁ and parents) or each individual (e.g. the successive generations) and counted using automatic cell counting with ImageJ. The total number of seeds from each sample was then weighed to calculate the total number of seeds.

2.4 Confocal laser Scanning microscopy

After bolting, shoot apical meristems (SAM), were dissected by removing flower buds, and followed by staining with propidium iodide solution. SAM of four independent plants from each genotype (stained similarly with PI) was imaged by Leica confocal SP8 using Z-stacks step size of 0.5 µm with a 40X water immersion objective. ImageJ was used to process and visualize the microscopy images (Collins, 2007).

2.5 Metabolite measurements

To compare metabolites of F₁ hybrids with their respective parents whole rosettes were harvested at 10-leaf stage before the development of altered inflorescence architecture. To analyze temperature-induced changes in F₁ hybrids, plants were grown until the 10-leaf stage, to which half of the plants were moved to 17 °C (LD), while the other half remained at 21 °C. Whole rosettes were harvested at 24 h intervals (24, 48, 72 and 96 h) after the temperature switch. The harvested tissues were frozen immediately in liquid nitrogen and ground using a mixer mill (Retsch GmbH) at 30 hertz (Hz) for 35 sec.

2.5.1 Measurement of Tre6P, phosphorylated intermediates and organic acids

For sugars and sugar intermediates, 18 mg of leaf powder was aliquotted from the ground tissue. Phosphorylated intermediates and organic acids were extracted with ice-cold chloroform-methanol solution (3:7 (v/v), with thorough mixing using a vortex, followed by incubation at -20°C for approximately 2h. After incubation, 350 µl of ice-cold water was added, followed by a 10 minute centrifugation at 4 °C. This step was repeated twice. All extracts were dried using a speed vacuum at room temperature. All dried extracts were dissolved in 350 µl water and an aliquot of 125 µl was filtered by the ultracel membranes.

This final filtrate was used to measure sugar molecules. For Tre6P, the filtrate was diluted 1:10 with water, and then 35 μ l of the diluted filtrate was mixed 1:1 with the internal standards (D_2 Tre6P, 4 nM). The final extract was measured by high-performance anion-exchange chromatography coupled to tandem mass spectrometry as described by Lunn *et al.*, (2006) with modifications as described in Figueroa *et al.*, (2016). Soluble sugars were measured enzymatically as described in Stitt *et al.*, (1989).

2.5.2 Secondary metabolites

For secondary metabolites, 25 mg leaf powder was aliquotted of the ground tissue. Metabolites were extracted with 80% methanol (v/v). The extracts were analyzed using a UPLC system coupled to an Exactive Orbitrap mass detector according to Giavalisco *et al.*, (2009). MS recorded spectra of the UPLC gradient was from 0 to 19 minutes. The captured peak areas were normalized by internal standard isovitexin (CAS29702-25-8) and fresh weight.

2.6 Hormone measurements

To identify if the phenotype of Kro-0 x BG-5 F_1 hybrids was associated with hormonal interplay, levels of phytohormones were measured in F_1 plants and their parents at two temperatures 17 °C and 21 °C. Leaves, the first internode and the second internode were harvested after the induction of cauline branches when plants had reached the third internode. The samples were frozen immediately in liquid nitrogen then ground with a mixer mill (Retsch GmbH) at 30 hertz (Hz) for 40 sec. At least 50 mg of the ground tissues was aliquotted and phytohormones were extracted using 0.5 mL of 2-propanol: H₂O: HCl solution (2:1:0.002 v/v). After thorough vortexing, the samples were incubated on an orbital shaker at 4 °C for 30 minutes. 1 mL of dichloromethane was added and samples were further incubated for 30 minutes on an orbital shaker at 4 °C. Samples were then centrifuged at 13,000 x *g* at 4 °C for 5 minutes for phase separation. One milli-liter of the extract from the dichloromethane layer was dried using a speed vacuum at room temperature and the extract was re-dissolved in 100 μ L of methanol: water (1:1 v/v). Phytohormones, abscisic acid (ABA), indole-3-acetic acid (IAA), indole-3-carboxylic acid (ICA), jasmonic acid (JA), 12-oxo-phytodienoic acid (OPDA) and salicylic acid (SA), were analyzed by ultra-performance liquid chromatography coupled to tandem mass spectrometry (UPLC-MS/MS) and measured as described by Trost *et al.*, (2014) and quantified as described by Pan *et al.*, (2011).

2.7 Genotyping

For genotyping, genomic DNA was isolated from leaves. Samples were harvested in Eppendorf tubes containing 5 mm stainless steel grinding balls and flash frozen in liquid nitrogen. Samples were immediately ground with a mixer mill (Retsch GmbH, Retsch,

Germany) at 25 hertz (Hz) for 15 sec. DNA was extracted by incubating the ground tissue in CTAB buffer [500 µl of 2x CTAB buffer (2% (w/v) cetyltrimethylammonium bromide, 100 mM Tris-HCl, 1.4 M sodium chloride, 20 mM EDTA)] for 40 minutes at 65 °C. For aqueous phase separation, 500µl CI solution (chloroform: isoamyl alcohol 24:1 (v/v)) was added and samples were vortexed thoroughly, before being centrifuged at 14000 rpm for 7 minutes. The aqueous layer was aspirated and genomic DNA was precipitated by adding an equal volume of 100% ethanol followed by centrifugation at 14000 rpm for 10 minutes. The DNA pellet obtained was dissolved in sterilized water and stored at -20 °C (Doyle 1991). Polymerase chain reaction (PCR) was used to amplify the targeted sequence using Dream Taq Polymerase (Thermo Scientific™, Waltham, Massachusetts, USA) according to the manufacturer's protocol. PCR products were mixed with 1µl nucleic acid staining dye GelRed™ (Biotium, 1:100 diluted) then loaded on 1% to 3% agarose gel for electrophoresis (voltage of 80-100 V) A 100 bp DNA ladder (Thermo Scientific™ Waltham, Massachusetts, USA) was used to determine the size of the products. DNA bands were visualized using A BIOVISION™1000 imaging system (Peqlab, Erlangen, Germany).

Four SSLP markers and four CAPS markers were used to investigate the heterozygosity of F₁ hybrids and to identify the genotype of F₂ individuals in each genetic interval and for the candidate genes inside these intervals (Table 2.2). For genotyping of amiRNA transformants, 35S promoter and amiRNA sequence-specific primers were used. SSLP primers were used to confirm heterozygosity of F₁ hybrids (Table 2.2). A combination of CAPS and SSLP markers were used to genotype segregants of the F₂ generation, thus identifying their genotype at the targeted interval. Genotyping was performed for:

1. F₁ shifted and non-shifted plants at early stages (8 leaves) from/to conditions, for phenotyping and metabolic/hormonal measurements.
2. F₁ individuals grown at 21 °C.
3. A recombinant line from backcrosses and successive generations that were selected by genotyping and temperature selective pressure at 17 °C.
4. AmiRNA-*Gene*-F_{1, 2} were genotyped to confirm heterozygosity and the presence of the construct.

Table 2.2 marker type, name, sequence for the forward (F) and reverse (R) primers and position for the markers that were used for genotyping in this study.

Chr2 Markers		Sequence 5',3'	Position (Mb)
SSLP	NGA1126	F: CGCTACGCTTTTCGGTAAAG	11696314 bp
		R: GCACAGTCCAAGTCACAACC	
	MSAT2.11	F: GATTTAAAAGTCCGACCTA	8220762 bp
		R: CCAAAGAGTTGTGCAA	
CAPS	AT2G14120	F: CACAACCGCAAAGAGAAACA	5955744 bp
		R: TTGGGATATCATTTGTGGTCTTC	EcoRI in Kro-0
	AT2G14160	F: TGACCTGTGAATCAAAGATAAACAT	5976615 bp
		R: AGATCGTTAACTTTGACTTTGATGA	
	AT2G14440	F: TATGTCTCCGGTCATGCAAA	6145043 bp
		R: CAAAGCCTCCTTTACCGAGA	
Chr3 Markers		Sequence 5',3'	Position (Mb)
SSLP	CIW21	FOR: TGATTTGAAGAGTTGAAACC	2195367 bp
		REV: TTGAGCAAAGACACTACTGAA	
	NGA6	FOR: ATGGAGAAGCTTACACTGATC	23031050 bp
		REV: TGGATTCTTCTCTCTTCAC	
CAPS	AT3G60970	FOR: TGATGCAAACGGAAGAGTG	22558940 bp
		REV: ACACACACTTGCCAAGCAAC	ScaI in BG-5
35S promoter (CAMV)		F: GAACTCGCCGTAAAGACTGG	T-DNA INSERT
		R: CGTGGTTGGAACGTCTTCTT	

2.8 Construction of artificial microRNA constructs

Cloning of amiRNA constructs for targeting various genes was performed as previously described ('WMD3 - Web MicroRNA Designer'; Schwab *et al.*, 2006; Ossowski *et al.*, 2008). Briefly, candidate gene sequences and AGI codes were submitted to the online server WMD3-Web MicroRNA Designer, which chooses target regions specific for the candidate gene while minimizing off-targets throughout the genome (Table 2.3). The chosen targets were checked manually for off-targets and further submitted for primer design with the option to design four primers (sense1, antisense2, sense3, antisense4) with homologous overhangs with plasmid pRS300. As this program is mainly based on the *A. thaliana* accession Col-0, parental accessions chosen for the study may have had polymorphisms at the target region. Thus target regions were checked manually by comparing the target sequence with the gene sequence from Kro-0 and BG-2 using the 1001 genome browser (atg1001/3.0/gebrowser.php) (Table 2.3). The BG-2 accession was chosen instead of BG-5, as the latter had not been fully-sequenced; however, the sequenced genome of BG-2 (a close relative to BG-5) was available. More importantly, BG-2 x Kro-0 also displays F₁ phenotype.

Cloning of amiRNA constructs was achieved according to Schwab *et al.*, (2006) and using the web designer 'WMD3 - Web MicroRNA Designer'. Briefly, three overlapping fragments

containing regions of amiRNA (target sequence + hairpin loop) were generated by PCR using HiFi Phusion Polymerase (Thermo Scientific™, USA) and the plasmid pRS300 as a template. PCR products with the correct size were excised from the agarose gel and purified using either the Invisorb Fragment CleanUp kit (Stratec, Birkenfeld, Germany) or Wizard® SV Gel and PCR Clean-Up System (Promega, Madison, Wisconsin, United States). Using these three overlapping extracted fragments as templates (in 1:1:1 ng) the final product was generated. The product was digested by EcoRI and BamHI and run on an agarose gel before being purified and ligated to the (EcoRI and BamHI digested) donor plasmid pJLBlue using T4 DNA Ligase (Roche).

The transformation of the ligation mix was carried out in chemically competent *E.coli* (DH5 α) cells, by heat-shock (30 s at 42 °C and then moved immediately on ice, followed by a 1h recovery in LB media at 37 °C). Plasmids from positive transformants were checked by PCR, extracted from the bacteria (PureYield™ Plasmid Miniprep System, Promega; Invisorb Spin Plasmid Mini Two, Stratec) and verified by sequencing. Confirmed products then used for sub-cloning to the pGreen-IIS vector (pFK210) (Hellens *et al.*, 2000). pFK210 contains (CaMV) 35S constitutive promoter upstream of multiple restriction sites and plant selection marker (BASTA, containing phosphinothricin). The sub-cloning was done by recombination using LR Gateway® LR Clonase® II enzyme mix (Invitrogen Darmstadt, Germany).

Destination vectors were extracted and confirmed by restriction enzyme digestion and sequencing. Positive vectors were co-transformed with pSOUP helper plasmid into *Agrobacterium tumefaciens* (GV3101) by electroporation. Genetically modified *Agrobacteria* were used to transfer the amiRNA constructs to plants by floral dipping (Clough and Bent, 1998).

Table 2.3 Chr2/Chr3 candidate genes and their amiRNA target sequence.

AGI	Gene annotation on Tair	amiRNA Target region 5'→3'
AT2G14090.1	f-box protein	TAAACAAGTAGGAAGGTCCTC
AT2G14100.1	cytochrome p450	TTACAAAGATGCAAGTGACTG
AT2G14110.1	haloacid dehalogenase-like hydrolase (had)	TTCTCGTTTCGAAAGGCACTT
AT2G14120.1	dynammin gtpase effector domain	BCAAATGAATGAGBCATGCGA
AT2G14150.1	mutator-like transposase family	TATACCCTGTGACAGCACCTG
AT2G14160.1	rna-binding family protein	TAGAATGTATAACGBCACCAG
AT2G14260.1	proline iminopeptidase	TTTTGTGATACGCGTBCACAA
AT2G14270.1	cytochrome c oxidase polypeptide vib family	TGBCATAGCTACABCGGACTA
AT2G14285.1	small nuclear ribonucleoprotein family protein	BCACATAACATABCATGGCBC
AT2G14300.1	similar to the putative helicase	TTATATGAGTTACBCCGGCGC
AT2G14310.1	a 70 kda dna-binding	TGAACAGTACABCATAGGCTG
AT2G14320.1	mutator-like transposase family	TGCTTTCACAAATTGGGCTG
AT2G14330.1	domain of unknown function	TCAATATGAGGCCGAAGTCGA
AT2G14340.1	transposable element gene	TAATCCGACCCCATATCGCTT

AT2G14350.1	pseudogene of unknown protein	TAAACCTGTACATTGGGCCTT
AT2G14365.1	lcr84	TACACAATGGCTTACATGCAG
AT2G14390.1	unknown protein	TATTGTCTCGTTAAAGGTCGA
AT2G14405.1	pseudogene	TATTTACGGGACCGAAAACAT
AT2G14410.1	pseudogene	TATTACGGTAAAAAGGAGCTA
AT2G14440.1	leucine-rich repeat protein kinase	TTTTTCAGTCTACCAGGGCAA
AT3G60720.1	pdlp8	TAATCGTTTGTTCGTAGCGT
AT3G60730.1	plant invertase	TTATCCTTTGAAACTACGCCG
AT3G60750.1	transketolase 1	TCAGAAATGTATATCGACCC
AT3G60840.1	map65-4	TAATTCGCTTTACCCCGACTC
AT3G60870.1	at-hook motif nuclear-localized protein	TGAGTTAATTAATTCGGCGG
AT3G60890.1	little zipper 2	TTTATGTTTGATATGGTGCGC
AT3G60900.1	fasciclin-like arabinogalactan-protein 10	TTAAATCGTATTTACTGGCGC
AT3G60966.1	ring/u-box superfamily protein	TTAGTACATCTGAGTACACTG
AT3G60970.1	multidrug resistant gene 15	TAATGGGTAGTTGCAACCCAT
AT3G61010.1	ferritin/ribonucleotide reductase-like	TTATGTAATAGGATGGTGCGT
AT3G61035.1	cytochrome p450	TGATACGTGAAAAAGAGGCTA
AT3G61070.1	integral to peroxisome membrane	TAATCTAGTGTAGTGATGCTT

SNPs were identified by comparing Kro-0 and Bg-2 sequences with the Col-0 sequence.

2.9 Analysis of amiRNAs hybrids

Parents transformed with amiRNAs constructs against target genes were selected using BASTA. The selected lines of amiRNA-*Gene*-BG-5 and amiRNA-*Gene*-Kro-0 were shifted to grow on the soil in greenhouse condition. Three of these amiRNA lines were used as pollen donors and crossed with parental accessions. At least 20 individuals of the resulting F₁ generation were grown on soil at 17 °C without BASTA selection. If the amiRNA rescued the phenotype, segregation of hybrids with the F₁ phenotype as well as wild type phenotypes was expected. If the amiRNA did not rescue the phenotype, all F₁ individuals would show the F₁ dwarf bushy phenotype. To verify that the rescued hybrids were real heterozygotes, the F₁ hybrids that exhibited a rescued phenotype were genotyped for nga1126 or CIW21 flanking markers. The presence of the amiRNA construct was confirmed using (CaMV) 35S constitutive promoter-specific primers or a combination of promoter-specific and amiRNA specific primers. Silenced genes that reversed the F₁ phenotype were considered necessary for the phenotype and needed further confirmation. Knock-down genes that exhibited a dwarf-bushy phenotype were considered not necessary and were excluded. The procedure of amiRNA crosses - from T₁ independent line selection to checking the F₁ phenotype - was repeated two times independently.

2.10 Gene expression assay

RNA expression levels were measured in leaves and roots of amiRNA lines and in parental accessions. For leaf tissues, three biological and two technical replicates were used for each line. For root tissues, four biological replicates with two technical replicates were used. Harvested tissue was immediately frozen in liquid nitrogen and then ground with a mixer mill (Retsch GmbH) at 30 hertz (Hz) for 35 sec. RNA extraction was done using the InviTrap Spin Plant RNA mini kit (Stratec Biomedical, Birkenfeld, Germany) and cDNA was synthesized by using 4 µg of the extracted RNA using SuperScript III Reverse Transcriptase (Invitrogen, USA) and RiboLock RNase inhibitor (Thermo Fischer Scientific Waltham, MA, USA). Maxima SYBR Green/ROX qPCR Master Mix (Thermo Fischer Scientific) was used for the qPCR reaction by using 50–200 ng of the synthesized cDNA as a template. Expression levels were measured with One Step Plus real-time PCR system (Applied Biosystems, Life Technologies, Carlsbad, CA, USA) and normalized against the geometric mean of two reference genes, *UBIQUITIN 10* (*AT4G05320*) and *ELONGATION FACTOR 1* (*AT5G60390*). Primers used for qRT-PCR are given in Table 2.4. The significance of these results was determined using a Kruskal-Wallis test to compare the hybrid to each parent separately.

Table 2.4 List of primers used for quantitative RT-PCR

AGI	Forward primer	Reverse primer
<i>AT4G05320</i>	GGCCTTGATAATCCCTGATGAAT	AAAGAGATAACAGGAACGGAAACA
<i>AT5G60390</i>	TGAGCACGCTCTTCTTGCTTCA	GGTGGTGGCATCCATCTTGTACA
<i>AT3G60840</i>	CGCTTAACTCGTTGTGCTCG	TCTTGAACCTTCTGCATTCCG
<i>AT3G61035</i>	CGTCGTCTCGTTGGAGGTTA	CCTTACGGACTTCGTGGCTT
<i>AT2G14120</i>	TCGTCCAGTTTACAGCGGTC	GAAGAGCTCCTTGACCACCC
<i>AT2G14100</i>	TGGTATGGACCTGATGGATGT	AAGGATAAGCTCCACGAACAAG

2.11 Cloning of the genomic constructs

To investigate the causality of the candidate genes, genomic constructs were cloned using NEB Gibson Assembly Master Mix (New England Biolabs Inc.) or In-Fusion (Clontech Laboratories, Inc.). Genomic DNA from Kro-0, BG-5 and Col-0 accessions were separately used as templates for each target gene. Gene-specific oligos with overhangs that align with the vector sequences after digestion with EcoRI and BamHI or SmaI were designed (Table 2.5). To clone a large gene, the gene was initially amplified in ~ 3 fragments of distinguishable size on 1% agarose gel, in such a way that amplicons could then be assembled into a larger fragment utilizing homologous overhangs at their ends. PCR was carried out using HiFi Phusion Polymerase (Thermo Scientific™, Waltham, Massachusetts, USA) to amplify the correct size of the full length of the targeted genes with the intergenic

region containing the promoter, CDS, introns and a 1 kb downstream sequence. Some of the targeted genes had big intergenic regions (15 kb in the case of *AT2G14100*, for which only 1.5 kb upstream of the targeted gene was included (online tools were used to detect the promoter and their TFs; PlantRegMap). However, in other cases like *AT2G14120*, the intergenic region was only 539 bp (promoter analysis vector was used to confirm the expression). PCR amplicons of the correct size were extracted from the gel and purified. The assembly mix ~5 µl (vector, mix and fragments) was used to transform chemically competent *E. coli* cells as previously described (Section 2.8). All antibiotic-resistant clones were first screened by PCR and then confirmed by sequencing. Following confirmation, one vector of each gene was then co-transformed with the pSOUP helper plasmid into *Agrobacterium tumefaciens* (GV3101) by electroporation. The positive genetically modified *Agrobacterium* was checked by PCR for the gene of interest and was then used to transfer the genomic constructs to plants by floral dipping (Clough and Bent 1998). T₀ seeds were selected on BASTA plates and positive T₁ transformants for each clone were transferred to soil and grown at 17 °C for phenotypic evaluation.

Table 2.5 Forward (F) and reverse (R) primers designed for the genomic constructs of the candidate genes.

AGI	Sequence
<i>AT2G14100</i>	F:gatatcgaattcctgcagcccGGTTGAACACGCCAAGAAAT
	R:cgctctagaactagtgggaTcccCACCCCTCTCTGACCCAAAAT
<i>AT2G14120</i>	F ₁ :cactatagggcgaattgggtacGCCTTTGGTTTGAGGATGAA
	R ₁ : GGCTATTTGCACGGAAGG
	F ₂ :GAACTGCAAACATGCCACAC
	R ₂ : CCCTCTACGCAAGGCAATAA
	F ₃ :TAAGCAGAAGAGTCAAGGAAAAG
	R ₃₍₁₎ :tcgacctcgagggggggcccAGGCAATGCAAGGATTTTCCAC
	R ₃₍₂₎ :tcgacctcgagggggggcccCTCTCTGAATCCATCTGCAAAA
	R ₃₍₃₎ :tcgacctcgagggggggcccCACTCTCTGAATCCATCTGCAA
<i>AT3G60840</i>	F:cactatagggcgaattgggtacCAACTCGGACCGGAAGAAT
	R:tcgacctcgagggggggcccGGTTTCGTCGTCCTTTATCCA
<i>AT3G60970</i>	F:gatatcgaattcctgcagcccAATCCAGCGGAATCACAGAG
	R:cgctctagaactagtgggaTCCCTCGATGCACCATGCTTCTAA
<i>AT3G61035</i>	F:gatatcgaattcctgcagcccGAAAAATGGGGTTTCTTTTGTG
	R:cgctctagaactagtggatcccTGCACATACCCAGATAGATCG
<i>AT3G61070</i>	F:cgctctagaactagtggatcTGGCCAGCTTAGGTCAAAT
	R:tatcgataagcttgatcgCTGATTTCTCGGGTGTGGT

2.12 GUS staining assay

Genomic constructs of plasmid pFK202 were used to re-clone the same genomic segments into the donor vector pJLBlue, before being subcloned into the gateway destination vector pKGWFS7,0 (non-promoter with *beta-glucuronidase* (*GUS*) and kanamycin resistance) (Karimi *et al.*, 2002) for promoter analysis. Positive clones were identified by PCR and

sequencing and then co-transformed with the pSOUP helper plasmid into *Agrobacterium tumefaciens* (GV3101) by electroporation. The positive genetically modified *Agrobacterium* was used to transfer the pKGWFS7,0 harboring the cloned genes to plants by floral dipping (Clough and Bent, 1998). At least 10 independent T₁ transformants were selected on kanamycin MS-plates and used GUS staining. Two-week-old plants were incubated overnight at 37 °C in GUS assay solution (1 mg/ml X-Gluc, 5 mM potassium ferrocyanide, 5 mM potassium ferricyanide, 0.2% Triton X-100 in 100 mM sodium phosphate buffer pH 7.4). Incubated samples were then washed and 70% ethanol solution was added. Samples were incubated for 5-10 minutes at 80 °C until all chlorophyll was removed.

2.13 Segregation analysis in successive hybrid generations and backcrosses

Hybrid breakdown in F₂, F₃ and backcrossed plants was evaluated for quantitative characterization and segregation ratio at 17 °C. Backcrossed populations were generated by crossing F₁ hybrids to both parents as a pollen donor. All lines that were selected from backcross populations were genotyped and evaluated phenotypically at 17 °C. A scheme of this work is illustrated in Figure 2.1. Genotyping was done using markers flanking the intervals to monitor any recombination and CAPS markers for identified genes inside the interval (Table 2.2).

2.14 Statistical analysis

All data managing and statistical analyses were done using R version 3.3.3. (R Development Core Team 2012). For statistical analysis of the comparison of phenotypes between hybrids and parents, data were first tested for normality using Shapiro-Wilk test. If the data was not normally distributed, Kruskal-Wallis one-way analysis was conducted. This test was followed by post-hoc (post-hoc Tukey's HSD) analysis using the CRAN - Package (PMCMR) ('Thorsten, 2018). For statistical analysis between hybrids, a Student's t-test was used to calculate the significant differences between means of genotypes. Boxplots were used to visualize the sample statistics with the 95% confidence intervals (Krzywinski and Altman, 2014). Bar plots were produced by R package ggplot2 (Wickham, 2009). Pearson's chi-squared tests (χ^2) were used to test the distribution of the observed phenotype in comparison with the expected one. Heat-maps were generated using Excel. The correlation analysis was performed after denoting the phenotypes of F₂ from I to V according to the phenotypic classification to see whether a specific trait might show significant correlation with phenotypic differences.

2.15 Boxplot diagrams

All morphological quantified data was visualized using boxplots (Krzywinski and Altman, 2014). The hinges of the box are the versions of the 1st and 3rd quartiles while the upper whisker = 3rd quartile+1.5×IQR and the lower whisker = 1st quartile -1.5×IQR and IQR= 3rd

quartile-1st quartile. The dot above or below whiskers represents the data point which lies beyond the extremes of the whiskers. The box is the interquartile range (IQR) and notches are the 95% confidence interval (CI) calculated as $\pm 1.58 \times \text{IQR} / \sqrt{n}$ between two medians.

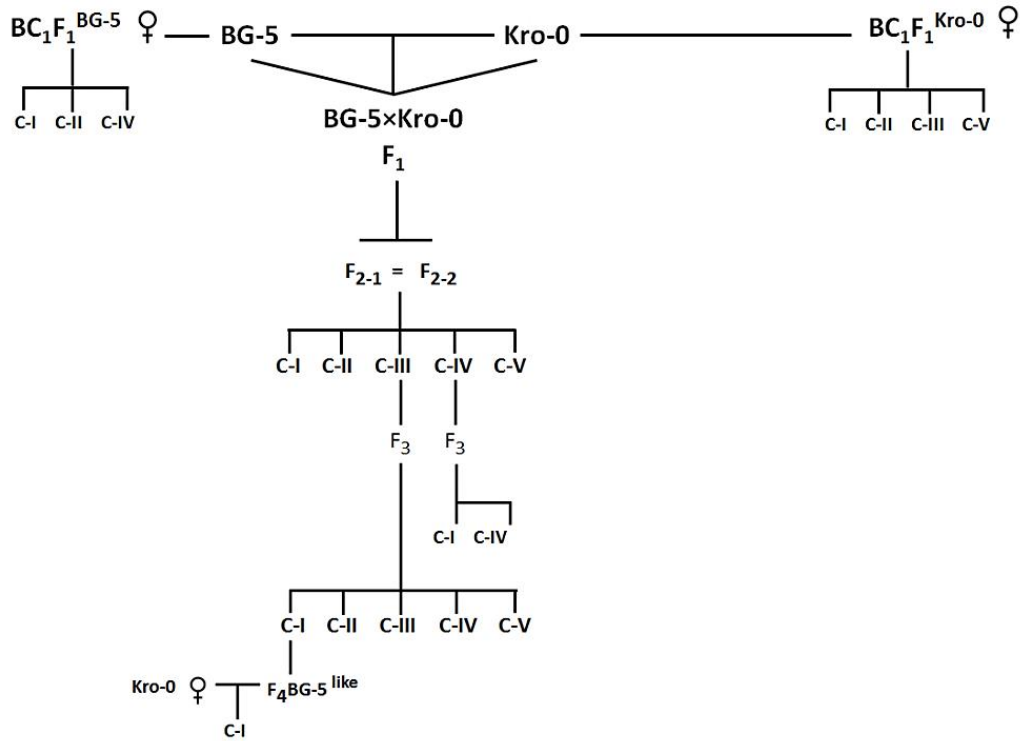


Figure 2.1 Scheme illustrating the studied segregating generations and their phenotypic classes. $F_{(i)}$ = generation populations, BC_1F_1 =Backcross first generation, Phenotypic classes: C-I=parental-like, phenotype. C-II= F_1 -like phenotype, C-III= dwarf phenotype, C-IV= stunted growth (6-8 leaves) and C-V= stunted growth (2-4 leaves).

3. Results

3.1 Temperature-dependent BG-5x Kro-0 F₁ phenotype

F₁ hybrids of *A. thaliana* accessions BG-5 (Seattle, USA) and Kro-0 (Krotzenburg, Germany) had a dwarf and bushy habit in comparison to their parents when grown at 17 °C (Figure 3.1 A and C). Interestingly, F₁ hybrids resembled their parental accessions when grown at higher temperatures $\geq 21^{\circ}\text{C}$ (Figure 3.1 B and D), thus, the F₁ dwarf bushy habit appears to be temperature dependent. In addition, the rosette of F₁ hybrids exhibited a purple coloration at 17 °C, which is indicative of anthocyanin accumulation (Figure 3.1 E).

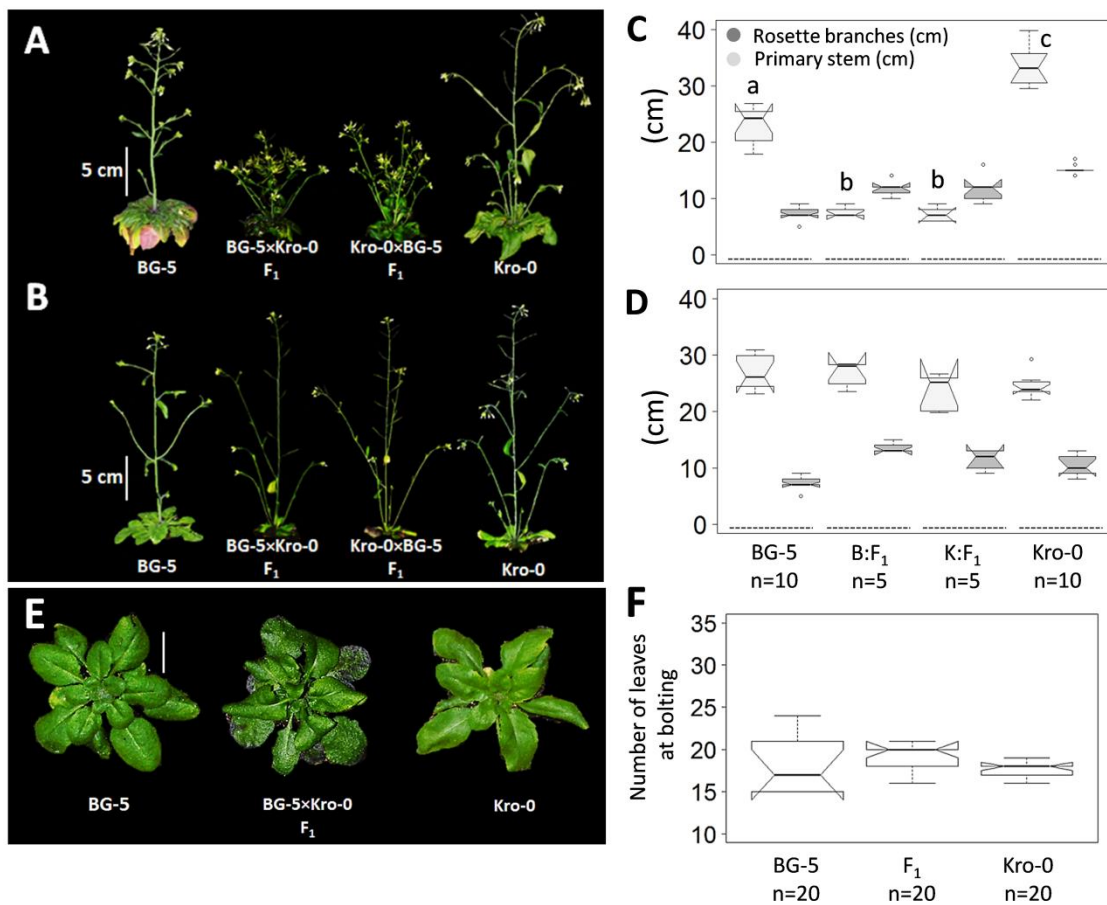


Figure 3.1 Phenotypic analysis of the temperature-dependent F₁ phenotype. **A:** an altered shoot phenotype in F₁ hybrids compared with the parental accessions at 17 °C and **B:** F₁ shoot phenotype with the parental accessions at 21 °C. **C:** stem length (cm) compared to the length of the rosette branches (cm) at 17 °C and **D:** at 21 °C. **E:** rosettes of F₁ and parents at 17 °C four weeks after germination. **F:** number of rosette leaves at bolting. Different lowercase letters denote significantly different means. p-values were calculated by Kruskal-Wallis followed by post-hoc Kruskal nemenyi test. B:F₁= BG-5xKro-0 F₁, K:F₁= Kro-0xBG-5 F₁.The dash lines specify genotypes.

For further understanding the F₁ dwarf bushy phenotype, the phenotype of F₁ hybrids and parents was quantitatively characterized at 17°C and at 21 °C, followed by a ratio analysis of characterized traits. Hybrid individuals were reciprocally shifted between 17 °C and 21 °C to identify the decisive developmental stage of the F₁ phenotype. The following 15 traits were assessed: days to onset of bolting, days to onset of cauline branching, days to onset of rosette branches and stem development, stem length, 1st internode length, total number of shoot branches, rosette branch length, number of cauline branches, number of rosette branches, number of internodes, rosette diameter, number of seeds, flower diameter and root length. To investigate the integrity of cell division in apical meristems in F₁ hybrids and parental lines, shoot and root apical meristems were observed under electron microscopy at 17 °C. The statistical significance of the data between hybrids and parents was analyzed using a Kruskal-Wallis test followed by a Kruskal nemenyi post-hoc test. Furthermore, to see how F₁ hybrids and their parental accessions responded to changing temperatures, a ratio of data at 17 °C to 21°C was calculated.

3.1.1 Quantification of F₁ and parental phenotypes at 17 °C

Days to the onset of bolting, days to onset of cauline branching and days to onset of rosette branches in the F₁ phenotype were intermediate to the parental accessions but significantly different from both (Figure 3.2 A). This shows that the timing of axillary branches growth is not affected in F₁ hybrids. However, the initial growth of stem in the F₁ was significantly slower compared to parents and stopped one week after bolting (Figure 3.2 B). This indicates an early stem growth arrest that takes place one week after bolting in F₁ hybrids, which leads to a final stem length that was significantly shorter than the parents (Figure 3.2 C). The strongest reduction in stem elongation was observed in the first internode (Figure 3.2 D). Length of rosette branches was intermediate to both parents (Figure 3.2 F); however it was further found that the bushy architecture in the F₁ generation at 17°C was associated with significantly more branches than in parental lines (Figure 3.2 E). When the number of rosette and cauline branches was investigated, it was observed that the parents, BG-5 and Kro-0, showed different branching architecture from each other. BG-5 had very few rosette branches (~ 1) but more cauline branches than Kro-0, while Kro-0 had significantly more rosette branches than BG-5 (Figure 3.2 G and H). Furthermore, F₁ plants had a similar number of rosette branches as Kro-0 and a similar number of cauline branches as BG-5, resulting in significantly more branches in total (Figure 3.2 G, H and E). The other scored traits did not show significant differences in the F₁ (Figure S1 A to D). For example, seed number was not significantly different in the F₁ hybrids compared to both BG-5 and Kro-0 (Figure S1 A to D). Interestingly, after two weeks of growth, root length was significantly higher in F₁ hybrids (Figure S1 E).

Analysis of cell division in the apical meristems (SAM and RAM Figure 3.3 A to E) in the F₁ generation did not show any visible difference compared to parents. Consequently, arrested growth in the F₁ hybrids was not due to changes in apical meristems.

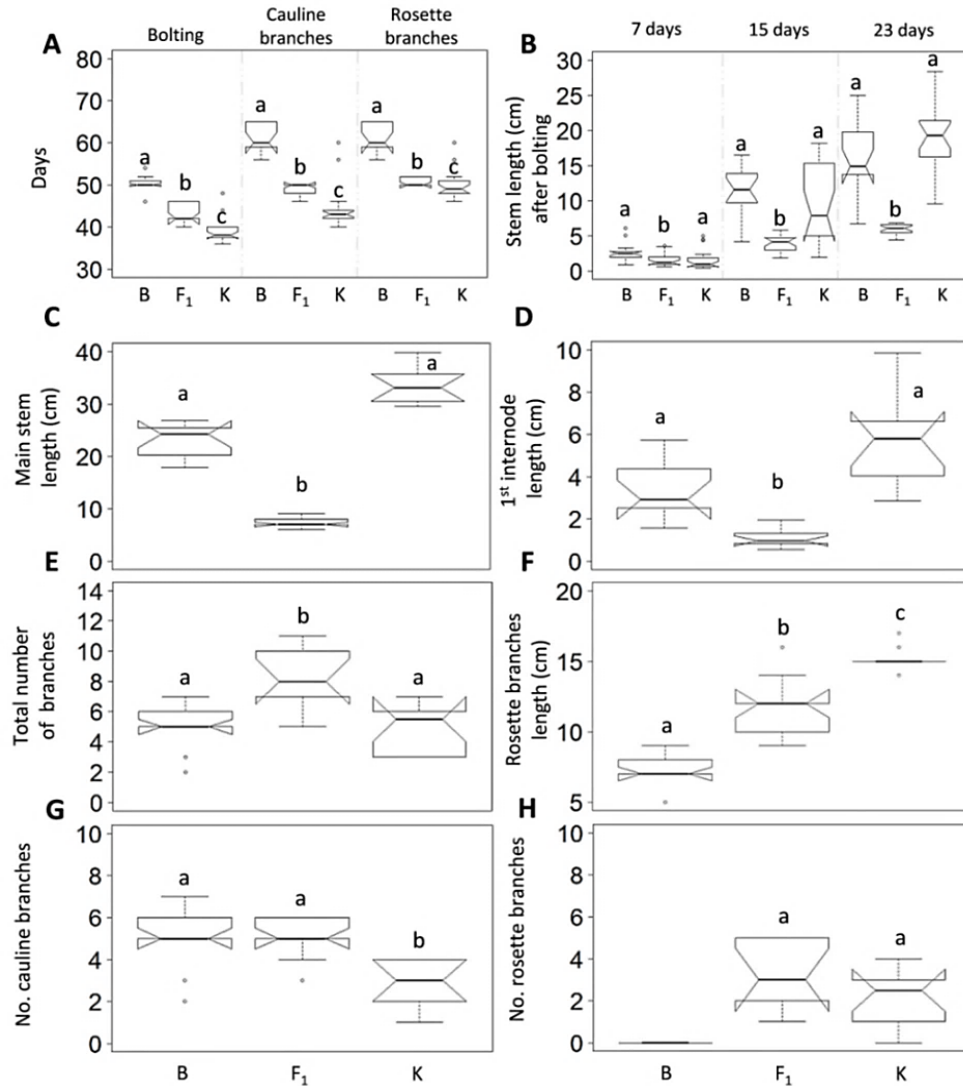


Figure 3.2 Characterization of shoot architecture in F₁ hybrids at 17 °C. **A:** days to the onset of bolting, cauline branches and rosette branches, **B:** stem length growth per week (cm) after bolting, **C:** the stem length (cm) 4 weeks after bolting, **D:** arrested growth in the 1st internode (segment of stem between the rosette and the first cauline node), **E:** the total number of branches, **F:** rosette branches length (cm), **G:** number of cauline branches and **H:** number of rosette branches in F₁ hybrid compared with the parental accessions. Different lowercase letters denote significantly different means. p-values were calculated by Kruskal-Wallis followed by post-hoc Kruskal nemenyi test. B: BG-5, K: Kro-0 and F₁: BG-5×Kro-0 first generation hybrid. the number of biological replicates B=18, F₁=20 and K=17.

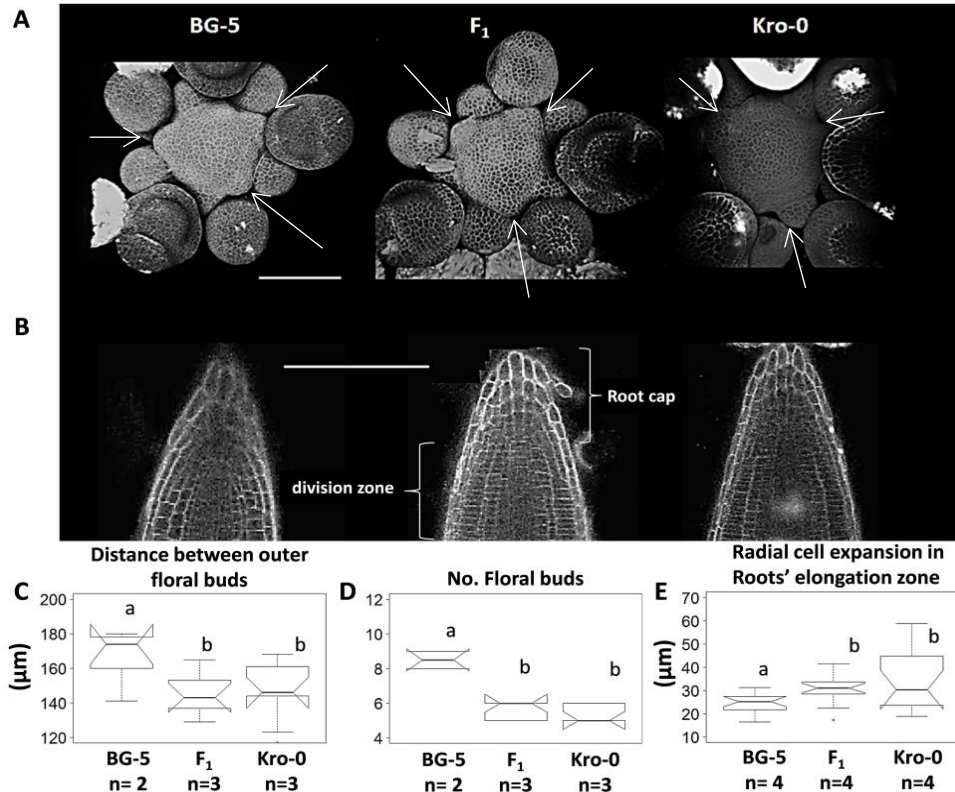


Figure 3.3 Shoot apical meristem (SAM) at bolting and root apical meristem (RAM) two-weeks after germination of F₁ and parents at 17°C. Bar= 100μM. A: scanning microscopy of a young inflorescence meristem of F₁ and parents. **B:** scanning microscopy of root tips including the root elongation zone of F₁ and parents. **C:** mean of three different measured distances between outer floral buds (white arrows) on SAM of F₁ and parents (based on bar scale unit). **D:** number of floral buds on SAM that did not differentiate of F₁ and parents (visual scoring). **E:** radial cell expansion of the first 6 cells in the elongation zone of roots for each replicated for each genotype. Different lowercase letters denote significantly different means. p-values were calculated by Kruskal-Wallis followed by post-hoc Kruskal nemenyi test. F₁: BG-5×Kro-0 first generation hybrid.

3.1.2 Response of shoot architecture related traits to temperature in F₁ hybrids and parents

In order to highlight which traits were affected by temperature, ratio analysis was performed for each trait and for each genotype. The ratio analysis was consistent with previous results in terms of stem growth rate, specifically, the first internode. However, it was shown that F₁ cauline branches were specifically affected by temperature, while the length and number of rosette branches did not show any difference across conditions (Figure 3.4 C and D; S1, S2). Interestingly, parental branching architecture was not influenced by temperature (Figure 3.4 A, B; S1, S2).

Both Kro-0 and BG-5 showed similar branching architecture when grown at 21 °C as when grown at 17 °C. BG-5 showed no rosette branches while Kro-0 developed more rosette branches (Figure 3.4 A to E; S1, S2). Since branching architecture directly affects seed number, seed number was also investigated in parents and F₁ hybrids. Interestingly, the parental lines showed significant differences in seed number between the two temperature condition; although, the aspects of their branching architecture were not significantly different (Figure 3.4 F; S1, S2). In contrast, F₁ hybrids had similar numbers of seeds at both temperatures, despite showing a dramatic change in their shoot phenotype (Figure 3.4 F). This indicated that differences in flower number and silique capacity may give F₁ hybrids the ability to maintain fitness capacity. F₁ hybrids at 17 °C displayed a greater number of cauline branches and flowers but silique length was comparatively small (data not shown). Therefore, seed number was increased in F₁ hybrids as a result of a greater number of shorter siliques. Altogether, the dwarf bushy phenotype of F₁ hybrids at 17 °C is characterized by a shorter main stem with a greater number of cauline branches.

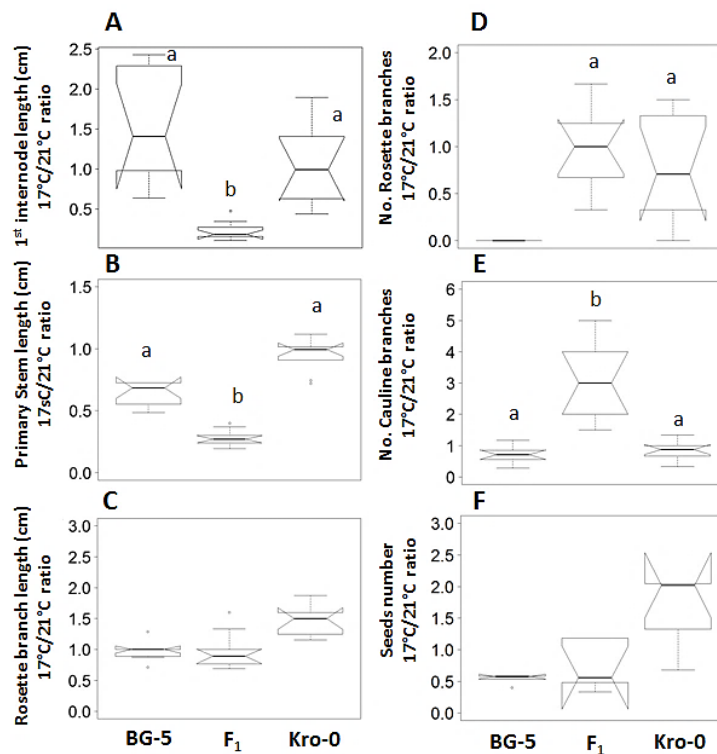


Figure 3.4 Response of shoot architecture related traits to temperature in F₁ hybrids and parents. **A:** first internode length (cm) **B:** stem length (cm), **C:** the length of basal branches (cm), **D:** number of basal branches, **E:** number of cauline branches, **F:** number of seeds. Different lowercase letters denote significantly different means. p-values were calculated by Kruskal-Wallis followed by post-hoc Kruskal nemenyi test. F₁: BG-5×Kro-0 first generation hybrid. N = 20 for each genotype.

3.1.3 Developmental control of temperature induced F₁ phenotype

Previous findings show that stem growth and cauline branches were affected by temperature. However, timing of axillary shoot growth did not change. To investigate the role of growth development in the F₁ phenotype, a reciprocal transfer experiment between 17 °C and 21 °C was conducted. Two groups of F₁ plants were grown at two constant temperatures (17 °C and 21 °C) until the six-leaf stage. Groups were divided into five sub-groups containing five biological replicates each. In the first experiment, four sub-groups of the F₁ hybrids grown at 21 °C were transferred to 17 °C at four developmental stages, while one sub-group was kept at 21 °C as a control. Sub-groups were transferred at the eight-leaf stage (stage I), at the onset of bolting (stage II), after the formation of the first internode (stage III) and after the formation of the second internode (stage IV, Figure 3.5). In a similar manner, the second experiment was performed in the opposite manner to the first, with plants being grown first at 17 °C and then transferred to 21 °C.

F₁ hybrids that were transferred from 21 °C to 17 °C before the formation of the first internode (stages I and II) exhibited a dwarf bushy phenotype similar to hybrids grown at 17 °C (Figure 3.5 A). When hybrids were transferred after the formation of first internode (stage III and IV), the phenotype appeared similar to the F₁ hybrids grown at 21 °C, with no appearance of the dwarf bushy phenotype (Figure 3.5 A). For rosette leaves, the shifted plants at stages III and IV did not accumulate anthocyanins in their leaves like those grown constantly at 17 °C.

In line with these findings, F₁ hybrids that were transferred from 17 °C to 21 °C before formation of the first internode (stages I and II), exhibited a primary stem that was similar to the F₁ hybrids grown at 21 °C (Figure 3.5 B). Similarly, plants that were transferred after the formation of first internode (stage III and IV) exhibited the dwarf bushy phenotype (Figure 3.5 B). Interestingly, the total number of branches did not change significantly when hybrids were transferred from 21 °C to 17 °C (Figure 3.5 C). However, all F₁ hybrids transferred from 17 °C to 21 °C after the eight-leaf stage (stage II, III and IV) exhibited more branches than control plants. Also, all shifted plants had a striking purple rosette. This experiment shows that the dwarf bushy phenotype is controlled before formation of the first internode. Once hybrids have reached the first internode stage, temperature does not appear to influence this phenotype. This result is consistent with the previously mentioned intact SAM cell division at bolting in F₁ hybrids at 17 °C and one can exclude that this phenotype is from SAM.

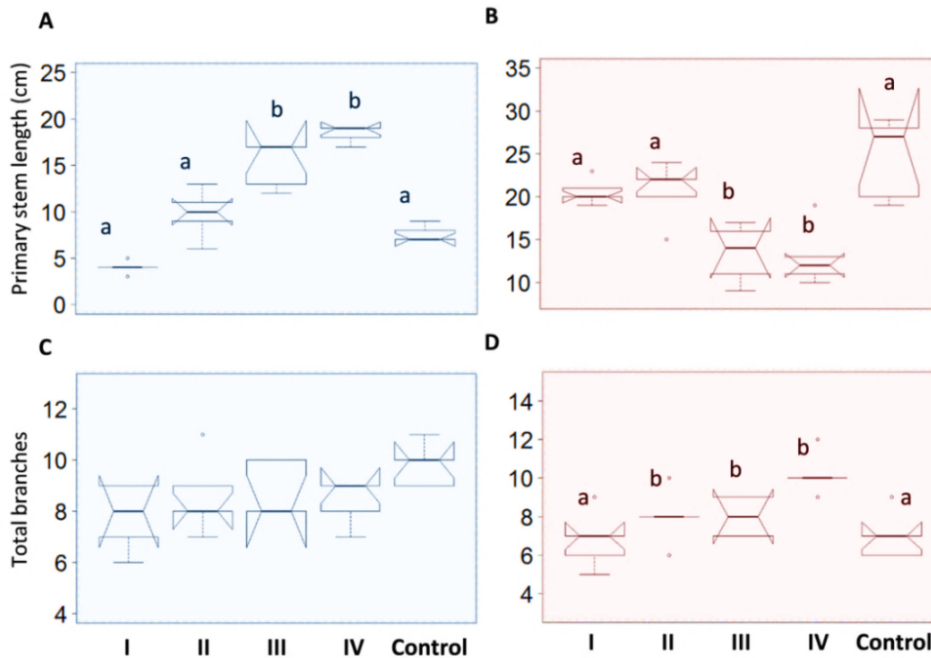


Figure 3.5 Developmental-dependence of the F₁ phenotype. **A:** primary stem length (cm) of individuals that were shifted from 21 °C to 17 °C at four different developmental stages (I to IV) **B:** primary stem length (cm) of individuals that were shifted from 17 °C to 21 °C at four different developmental stages (I to IV) **C:** total number of branches of individuals that were shifted from 21 °C to 17 °C at four different developmental stages (I to IV) **D:** total number of branches of individuals that were shifted from 17°C to 21°C at four different developmental stages (I to IV). Blue coloration of the box indicate experiments where the plants were switched to 17°C and red coloration experiments in which plants were switched to 21°C. Lowercase letters denote significantly different means. p-values were calculated by Kruskal-Wallis followed by post-hoc Kruskal nemenyi test. This experiment was conducted using only F₁: BG-5×Kro-0 genotype and N = 5. I: 8 leaves stage, II: Bolting stage, III: first internode stage, IV: second internode stage, Control: F₁ hybrids grown at constant temperature.

3.2 Analysis of compounds associated with the F₁ phenotype

3.2.1 Sugar and secondary metabolites analysis

Sugars and metabolites, especially flavonoids, are factors known to influence shoot architecture in plants (Peer and Murphy 2007; Barbier *et al.*, 2015). To find out if changes in metabolites were associated with the F₁ hybrid phenotype, two experiments were conducted using rosette leaves tissues of eight-leaf and ten-leaf stages. These two developmental stages were chosen as previous experiment showed that the decisive developmental stage of F₁ phenotype is before formation of the first internode (Figure 3.5). In the first experiment, sugar and secondary metabolites were measured in F₁ and parental accessions at 8 leaves stage at constant 17 °C. In the second one, F₁ were grown at constant

21 °C until they reached the 10 leaves stage. Then F₁s were divided into two groups, one kept at constant 21 °C and used as a reference, and the second group was transferred to a constant 17 °C. Leaf tissues of 8 biological replicates of both conditions were harvested consecutively each 24 hours for four-time points (24h, 48h, 72h and 96h) after the shifting time point.

For sugar and sugar intermediates, F₁ hybrids showed no significant change in such compounds in comparison to parental lines. Levels of Tre6P, sucrose and ratio of Tre6P to sucrose was not correlated with the F₁ phenotype in either of the performed experiments (Figure 3.6 A to C; Figure 3.7). For secondary metabolites; cyanidin glycosides, anthocyanin^(A9) and anthocyanin^(A11), were significantly greater in F₁ hybrids compared to their parents (Figure 3.7). It is known that cyanidin glycosides and other anthocyanins are derived from the shikimate pathway using phosphoenolpyruvic acid (PEP); however these metabolites were not significantly different in F₁ plants (Figure 3.7). For the second experiment, derivatives of anthocyanin, kaempferol and quercetin significantly increased from the 72 h time-point to the 96 h time-point in F₁ hybrids transferred from 21 °C to 17 °C (Figure 3.7). These results indicate that altered shoot branching in hybrids may be associated with increased flavonoid content but not with altered sugar levels.

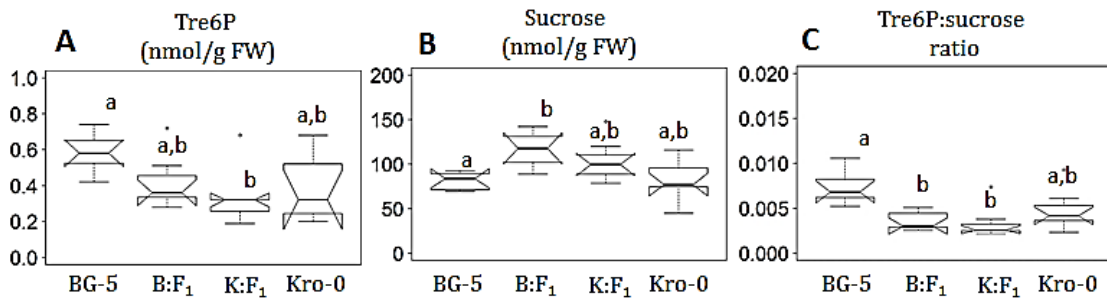


Figure 3.6 The role of Tre6P in the F₁ phenotype at 17 °C. A: Tre6P concentration (nmol/g FW) in reciprocal F₁ and parents. C: Sucrose (nmol/g FW) in reciprocal F₁ and parents. D: Tre6P: Sucrose ratio in reciprocal F₁ and parents. Different lowercase letters denote significantly different means. p-values were calculated by Kruskal-Wallis followed by post-hoc Kruskal nemenyi test. B:F₁= BG-5×Kro-0 first generation hybrid, K:F₁= Kro-0×BG-5 first generation hybrid. This experiment was done using rosette tissues at 8 leaves stage at constant 17°C, N=7 . The Tre6P: Sucrose ratio was calculated individually for each replicate in each genotype.

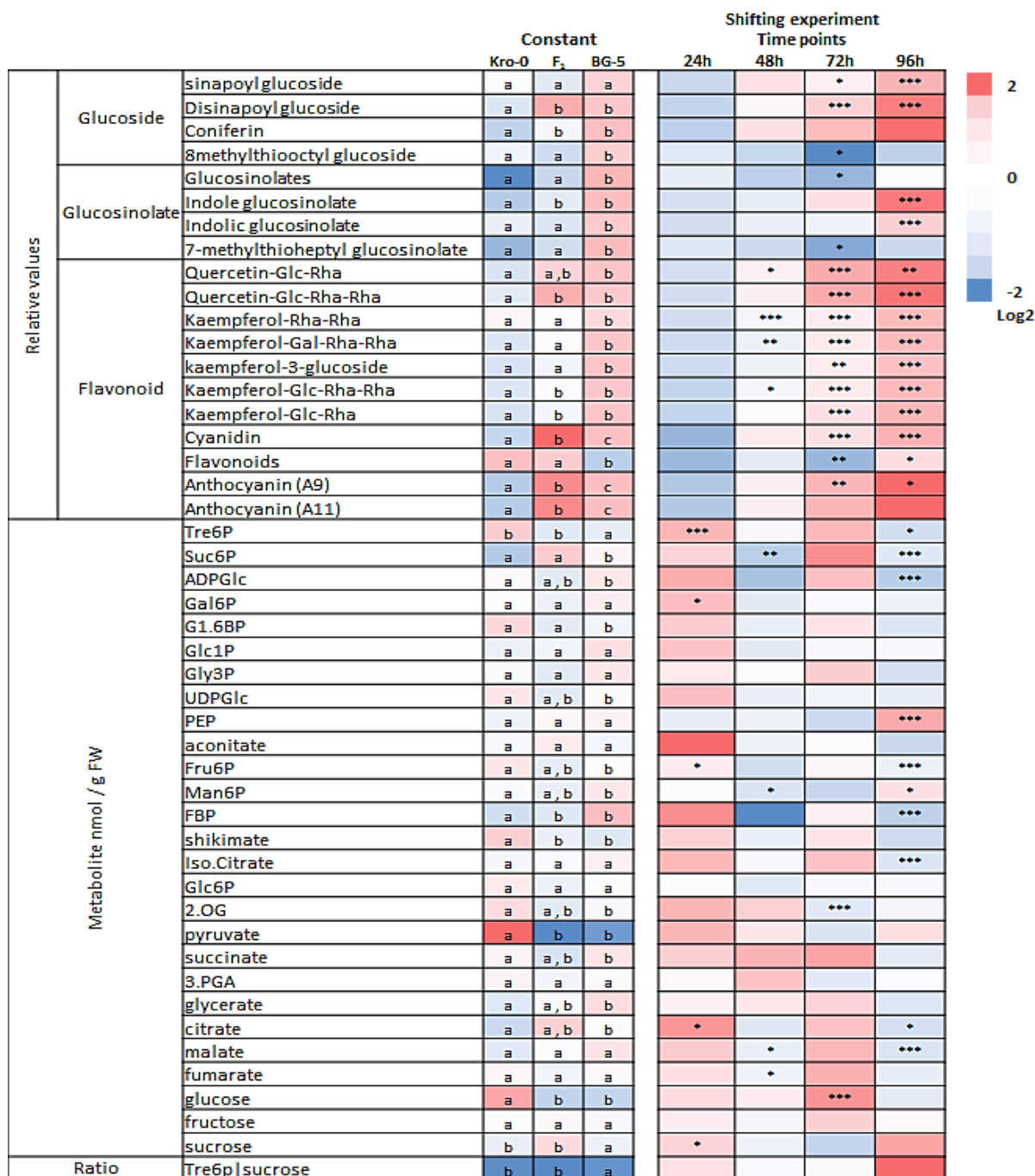


Figure 3.7 Analysis of metabolites in F₁ hybrids, BG-5 and Kro-0. The data was scaled on the average value of parents for each metabolite for the first experiment then calculated log₂ fold values are visualized in heat map. For the second experiment the data was scaled on 21°C values for each metabolite and each time point then the calculated log₂ fold changes are visualized in heat map. Different lowercase letters denote significantly different means. p-values were calculated by Kruskal-Wallis followed by post-hoc Kruskal nemenyi test. Asterisks denote statistically significant differences between two conditions for each variables at each time-point (p-value <0.05 * <0.01 ** and <0.001***) p-values were calculated by t-test. N=7 for sugar analysis and N=4 for secondary metabolites. The Tre6P: Sucrose ratio was calculated individually for each replicate in each genotype.

3.2.2 Hormone analysis

To elucidate the potential role of hormones and their alterations in the F₁ phenotype, hormones were measured in F₁ hybrids and their parents grown at 17 °C and 21 °C. While hormones involved in shoot branching are known to accumulate in rosette leaves, auxin is known to be synthesized in the SAM and transferred basipetally to the stem (Vernoux *et al.*, 2010). As such, Indole-3-acetic acid (IAA), salicylic acid (SA), abscisic acid (ABA), jasmonic acid (JA), indole-3-carboxylic acid and 12-oxo-phytodienoic acid were measured in rosette leaves and stem internodes in five biological replicates in both F₁ hybrids and their parents. All tissues were harvested at one developmental stage, after formation of the second internode and before the initiation of axillary branches.

At 17 °C, the level of IAA in F₁ plants was similar to BG-5 parents at the first internode but significantly lower than both parents at the second internode (Figure 3.8 A). SA, ABA and JA showed comparable levels in F₁ hybrids and parents in leaves, while hybrid plants displayed a significant increase in such compounds in stem internodes (Figure 3.8 B-D). In leaves, IAA was not detected (Figure 3.8 A).

At 21 °C, the level of IAA in F₁ hybrids was similar to the BG-5 parent at the first internode and similar to the Kro-0 parent in leaves and at the second internode (Figure 3.8 H-M). SA, ABA and JA showed comparable levels at 21 °C in leaves and at both stem internodes between hybrids and parents.

Interestingly, the ratio of IAA levels at 17 °C and 21 °C showed that IAA was significantly higher at the first internode of F₁ hybrids compared to their parents. This suggests that IAA transport could be slightly inhibited in this section of stem at 17 °C (Figure 3.8 G). Altered hormone levels could be due to several reasons including an activated stress response or imbalance in hormonal homeostasis in F₁ hybrids at 17 °C that was absent in parents.

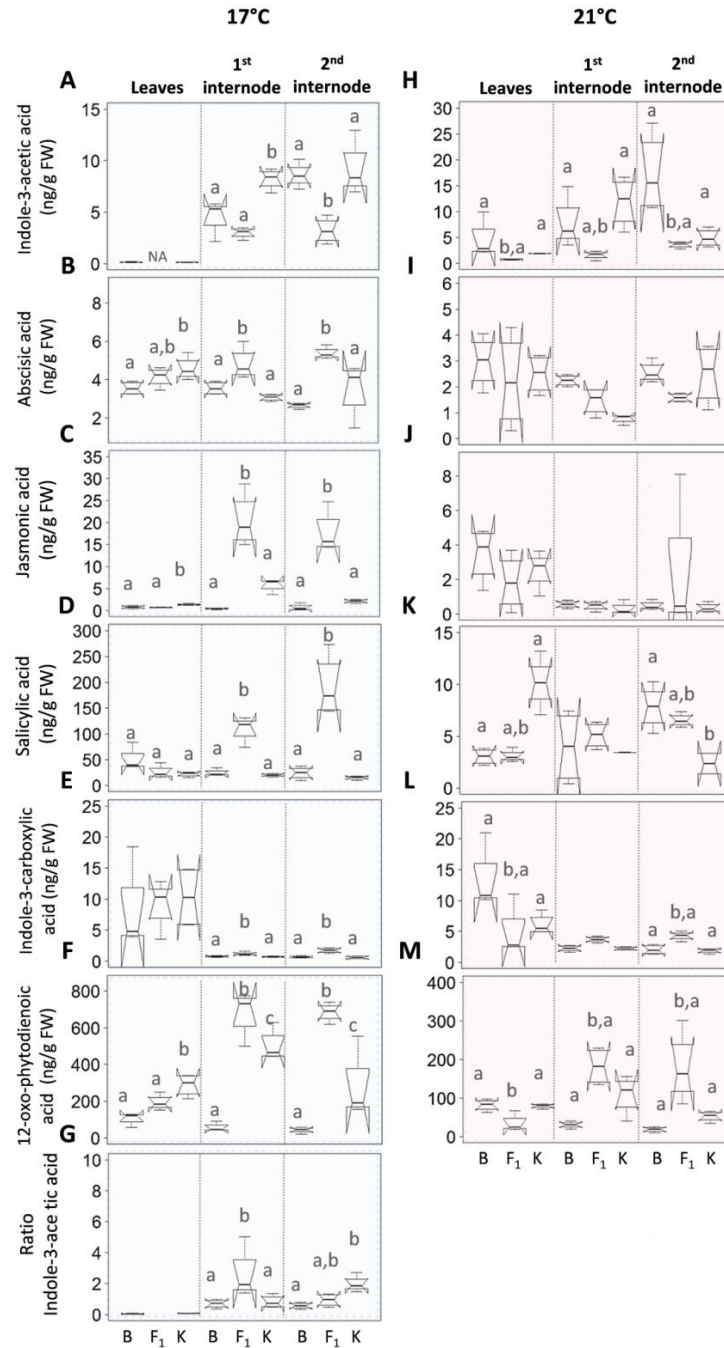


Figure 3.8 Analysis of hormones in leaves, the first internode and the second internode at 17 °C and 21 °C of F₁ hybrids, BG-5, and Kro-0. A: indole-3-acetic acid, **B:** abscisic acid, **C:** jasmonic acid, **D:** salicylic acid, **E:** indole-3-carboxylic acid, and **F:** 12-oxo-phytyldienoic in F₁s and parents grown at 17°C. **G:** Graph showing the ratio (Indole-3-acetic acid at 17°C/ Indole-3-acetic acid at 21°C). The ratio was calculated individually for each replicate. **H:** indole-3-acetic acid, **I:** abscisic acid, **J:** jasmonic acid, **K:** salicylic acid, **L:** indole-3-carboxylic acid and **M:** 12-oxo-phytyldienoic acid in F₁s and parents grown at 21°C. Different lowercase letters denote significantly different means. p-values were calculated by Kruskal-Wallis followed by post-hoc Kruskal-Nemenyi test. N= 5, B: BG-5, K: Kro-0 and F₁= BG-5×Kro-0 F₁ hybrid.

3.3 Genetic analysis of genes underlie the F₁ phenotype

Genetic mapping was previously performed at Max Planck Institute of Developmental Biology in the laboratory of Prof. Dr. Detlef Weigel. Linkage to two loci was shown by mapping 190 parental-like and 190 F₁-like individuals from an F₂ population. One locus was a 700 kb interval on Chr2 (5.90-6.50 Mb), and the other was a 920kb region on Chr 3 (21.63-23.05 Mb). Since the intervals were relatively large, fine-mapping and sequencing were used to narrow-down these intervals (Boldt, 2009; Muralidharan, 2015). Before starting my work, the final size of Chr2 interval was 220 kb (5.93-6.14 Mb) and Chr3 interval was 160 kb (22.44-22.60 Mb). Additionally, some of the candidate genes were further studied using an amiRNA approach (Muralidharan, 2015). One of the silenced Chr3 genes was shown to be necessary to the phenotype, but causal genes had not been identified (Muralidharan, 2015). In my work, I used an amiRNA approach to test the remaining candidate genes on Chr2 and Chr3 and then further developed genomic constructs for the narrowed-down genes that were found to be necessary for F₁ dwarf bushy phenotype.

3.3.1 Artificial microRNAs approach (amiRNAs) to identify candidate genes

To know which gene(s) within the intervals described were necessary for the F₁ phenotype, 20 candidate genes on Chr2 and the 12 candidate genes on Chr3 were knocked down individually using an artificial microRNA approach (see Table 2.3 section 2.6) ('WMD3 - Web MicroRNA Designer'; Schwab *et al.*, 2006; Ossowski *et al.*, 2008). For Chr2, three independent T₁-Kro-0 lines (amiRNA-T₁) were crossed with BG-5 using the former as a pollen donor (BG-5×amiRNA-*Gene*-Kro-0). Similarly, for Chr3, three independent lines of T₁-BG-5 were crossed to Kro-0 using the former as the pollen donor (Kro-0×amiRNA-*Gene*-BG-5). If the amiRNA targeted gene was necessary for F₁ phenotype, knockdown of this gene could reverse the F₁ phenotype to parental-like phenotype. Since T₁ lines would be hemizygous and contain only one copy of the insert, the amiRNA-*gene*-F₁s should segregate such that the F₁ phenotype and parental-like phenotypes occurred in a 1:1 ratio at 17 °C.

Utilizing this logic, for Chr2 candidate genes, 18 out of the 20 amiR-*gene*-F₁s showed 100% F₁ phenotype with no phenotypic reversions, indicating that these genes were not likely to be causal genes. Three lines of the amiR-Chr2-*gene* cross did not give any F₁ seeds, probably due to gamete lethality caused by gene silencing (Figure S3). Two amiR-*gene*-F₁ lines showed 50% parental-like phenotype, one containing amiRNA against *AT2G14100* (*CYP705A13*) and one amiRNA against *AT2G14120* (*DRP3B*), making these genes likely candidates for the F₁ phenotype within the Chr2 interval. Similarly, for Chr3 candidates, 10 out of 12 amiR-*gene*-F₁ hybrids showed comparable phenotypes to the F₁ phenotype (Figure S4); while hybrids with amiRNA against two target genes, namely *AT3G60840* (*MAP65-4*) and *AT3G61035* (*CYP76C8*) displayed a parental-like phenotype in comparison

with the F₁ control. Besides the visual scoring of *amiR-Gene-F₁*s, primary stem length, rosette branches length, first internode length, and the number of branches were scored for *amiRNA-AT2G14120-F₁* and *amiRNA-AT3G60840-F₁* at 17 °C (Figure 3.9 A). Indeed, knock-down of these genes in F₁ hybrids restored apical dominance and branching architecture to parental- like patterns (Figure 3.9 B, C and D).

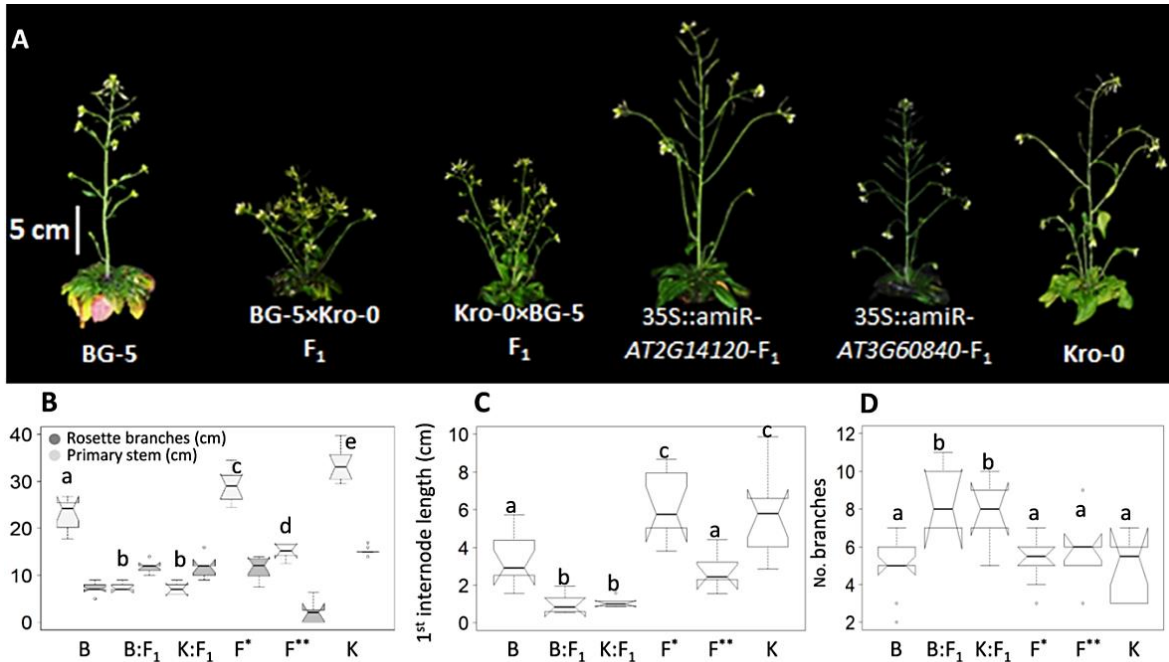


Figure 3.9 Characterization of *amiRNA-gene-F₁* in comparison to parents and the F₁ phenotype at 17 °C. A: altered phenotype of *amiRNA-AT2G14120-F₁* and *amiRNA-AT3G60840-F₁* compared to F₁ and parents. **B:** stem length (cm) compared to the length of the rosette branches (cm). **C:** 1st internode length (cm). **D:** Total number of branches. Different lowercase letters denote significantly different means. p-values were calculated by Kruskal-Wallis followed by post-hoc Kruskal nemenyi test. N=5, B: BG-5. B: F₁= BG-5xKro-0 F₁. K: F₁= Kro-0xBG-5 F₁. F*= 35S::amiR-*DRP3B* F₁. F**= 35S::amiR-*MAP65* F₁.

To confirm that the *amiRNA* construct silenced the targeted genes, expression analysis of candidate genes in leaves and roots was performed. Both genes, *DRP3B* and *MAP65-4* were detected in leaves and other tissues, however, *CYP705A13* and *CYP76C8* were only detected in roots. Silencing of the targeted genes was confirmed by expression analysis. All of the targeted candidate genes showed reduced expression in *amiR-Gene*-accessions than in parental lines (Figure 3.10 A-D). It should be noted however, that although *amiRNA* constructs were designed to be specific to target genes, one cannot fully rule out silencing of possible off-targets especially in case of *CYPs*.

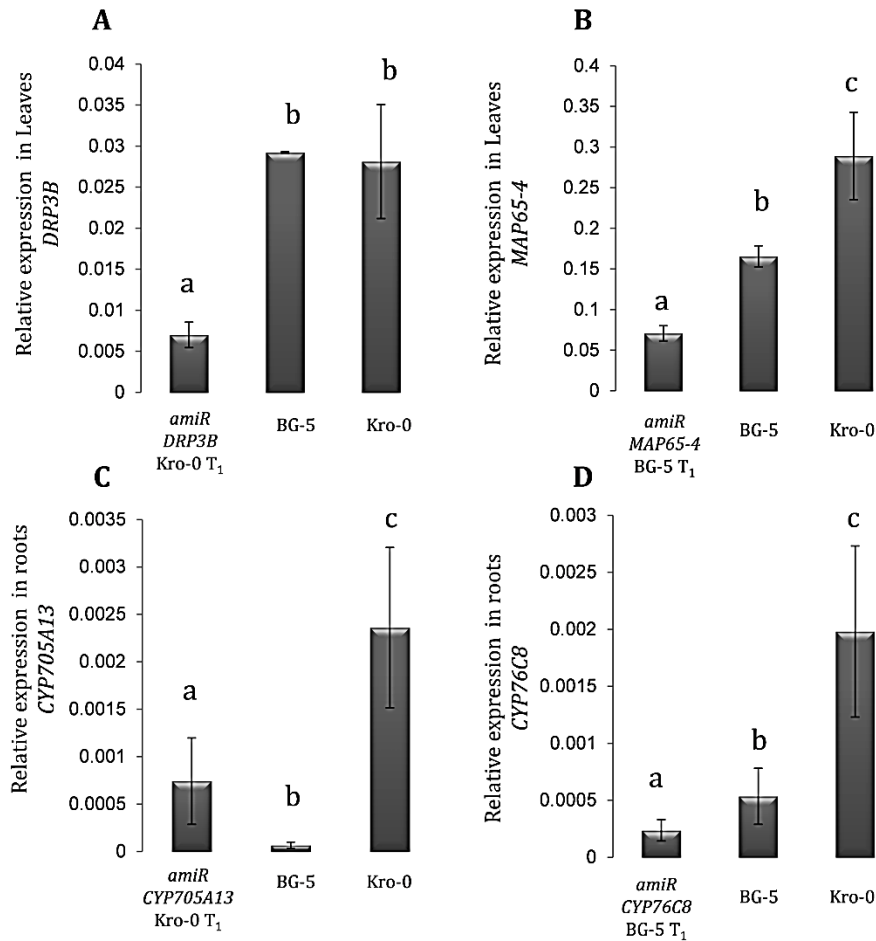


Figure 3.10 Relative expressions of the targeted genes in amiRNA-lines and parental accessions. A: relative expression of *AT2G14120* in amiRNA-*AT2G14120*-Kro-0 and parents in leaves. **B:** relative expression of *AT3G60840* in amiRNA-*AT3G60840*-BG-5 and parents in leaves. **C:** relative expression of *AT2G14100* in amiRNA-*AT2G14100*-Kro-0 and parents in roots. **D:** relative expression of *AT3G61035* in amiRNA-*AT3G61035*-BG-5 and parents in roots. Barplots represent mean \pm SD and different lowercase letters denote statistically significant differences between means calculated by Kruskal-Wallis test followed by post-hoc Kruskal nemenyi test. Data was normalized against the geometric mean of two reference genes, *UBIQUITIN 10* (*AT4G05320*) and *ELONGATION FACTOR 1* (*AT5G60390*). N = 4.

3.3.2 Genetic complementation of parental accessions

The amiRNA approach showed that four genes, two from Chr2: *AT2G14100* (*CYP705A13*) and *AT2G14120* (*DRP3B*) and two from Chr3: *AT3G60840* (*MAP65-4*) and *AT3G61035* (*CYP76C8P*) were necessary for the reversion of the F₁ dwarf bushy phenotype. To investigate whether these genes were sufficient to cause the F₁ phenotype, genes on Chr2 from Kro-0 were cloned and introduced into BG-5. Similarly, identified genes on Chr3 were cloned from BG-5 and introduced to Kro-0. It should be noted that the gene *AT2G14120* (*DRP3B*) undergoes alternative splicing that can produce three isoforms. As the third

version retains an intron and overlaps with a natural antisense gene, an additional construct was made for this gene to include the natural antisense gene (*DRP3B_antisense*).

In addition to these genes, two additional genes on Chr3 were also considered for genetic complementation. These two genes were chosen based on SNPs that were identified by comparing the sequence of each gene on Chr3 (of BG-2) to the same in Kro-0. The non-synonymous SNPs were found only in one gene, *AT3G60970* which encodes an ABC transporter protein (*MRP15*) that is known to be involved in flavonoids and auxin transport. The other gene was *AT3G61070*, which encodes a protein known to be involved in peroxisome elongation (*PEX11*) and displays alternative splicing as well.

The whole genomic length of these mentioned genes was cloned with additional upstream sequences to insure that the native promoter was included (*pGene::Gene-accession*). The intergenic region that might contain the promoter of *AT2G14120* (*DRP3B*) was only 539 bp while for *AT2G14100* it was ~ 11.921bp. Based on this, for long intergenic region only 1.5 kb was included and for short intergenic region the entire region was included for cloning.

In addition, the cloned genes were re-cloned into a new vector that contains *Escherichia coli beta-glucuronidase* gene (*GUS*) as a gene fusion marker on the C-terminal end. This was performed to check the validity of promoters and whether such constructs were expressed *in vivo*. For *GUS* staining experiments, 10 independent individuals of BG-5 T₁ lines that were transformed with three constructs (*pATDRP3B::ATDRP3B::GUS*, *pATMAP65-4::pATMAP65-4::GUS*, *pATMRP15::ATMRP15::GUS*) were used to check the expression of these constructs. All stained plants showed that the *GUS* gene was expressed by the native promoter of the cloned genes (Figure 3.11).

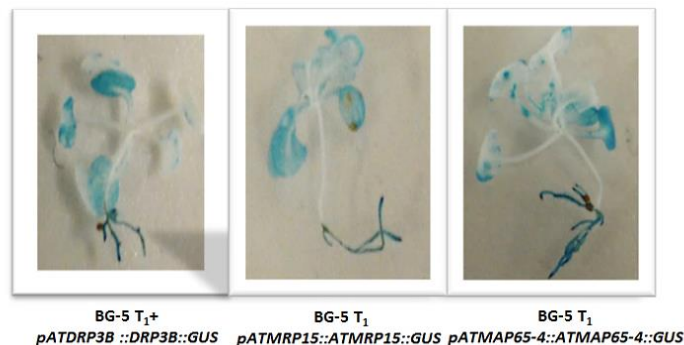


Figure 3.11 *GUS* staining showing the expression of cloned candidate genes by native promoters. In BG-5 T₁ lines for *pATDRP3B::ATDRP3B::GUS*, *pATMAP65-4::ATMAP65-4::GUS* and *pATMRP15::ATMRP15::GUS* one week old plants after germination.

T₁ plants carrying the transgene were selected on basta MS-plates. For large constructs like dynamin genomic constructs (9-11 kb) only 15 T₁ plants were analyzed and for the small constructs more than 20 T₁ lines were analysed. In the T₁ generation, none of the lines showed the altered shoot branching (Figure 3.12).

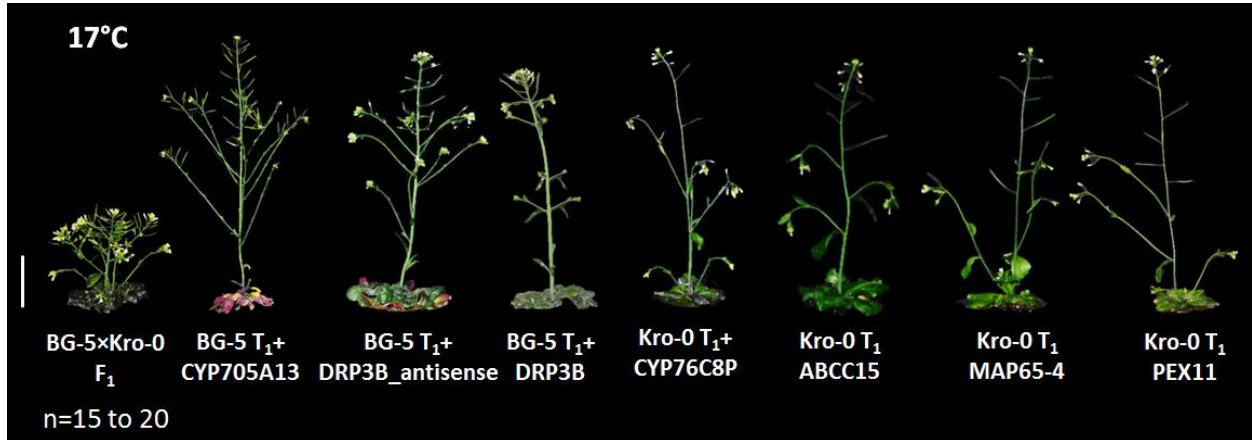


Figure 3.12 Phenotypes of T₁ pGene::Gene transformants with parental alleles at 17 °C. bar=5cm.

3.3.3 Polymorphisms among parental accessions in candidate genes

As BG-5 has not been fully sequenced, cloned genomic constructs from both parents were fully sequenced to identify non-synonymous SNPs in the found candidate genes between parents. The BLASTP program in NCBI (www.ncbi.nlm.nih.gov) was used to predict potential function of protein sequences. To identify whether there were non-synonymous SNPs, the sequences of the cloned candidate genes of the genomic DNA of Kro-0 and BG-5 were assembled using Benchling (<https://benchling.com>). To identify any possible substrate for the found genes, SWISS-MODEL (<https://swissmodel.expasy.org/>) was used to model the protein and to find potential ligands. Interestingly, none of the predicted protein structures of these genes specified any potential substrate or binding site on a target protein.

Dynamin-related protein, *AT2G1412*, consists of 20 exons and 19 introns (5763bps) and undergoes alternative splicing to form three isoforms. The direction of translation of this gene is from 3' to 5' and as such, shares the promoter region with a pseudo transposable element. This intergenic region was 539 bp only (including the promoter). The third copy of this gene has retains an intron and overlaps with a natural antisense gene, which suggest a non-functional copy. The protein blast showed this dynamin-related protein consists of only three domains (GTPase domain, a middle domain, GTPase effector domain). Since this protein is missing two domains, pleckstrin homology (PH) and proline-rich domains that are necessary for endocytosis, this protein appear to be incapable of transporting substrates. Therefore, a potential function of this protein may be in membrane fission

during cytokinesis. This prediction is consistent with previous studies showing that *DRP3B* in Col-0 is involved in peroxisome and mitochondrial fission (Fujimoto *et al.*, 2009; Aung and Hu, 2012). Sequence analysis of *AT2G14120* Kro-0 showed that more than one non-synonymous SNP exists between Kro-0 and BG-5 sequence, most of them in non-coding regions. Only one non-synonymous SNP was found in exon 20 (position: 5954296), which causes an amino acid change from glutamic acid in Kro-0 to Glutamine in BG-5 (E743Q). This SNP exists in a GED domain which is responsible for proper assembly with the GTP assembly domain.

The microtubule-associated gene, *AT3G60840* (*MAP65-4*) from BG-5, consists of 11 exons and 10 introns (2892 bp). This gene also belongs to a conserved family of microtubule protein genes. A protein blast showed that this protein might function in peroxisome stability and/or localized to phragmoplast during cytokinesis. The sequence of *AT3G60840* (*MAP65-4*) in BG-5 had three synonymous SNPs in introns and one non-synonymous SNP in exon 10 (position: 22478053) in comparison to Kro-0. This non-synonymous SNP causes an amino acid change from lysine in BG-5 to asparagine in Kro-0 (K516N) at the C-terminal end of the protein.

The cytochrome P450 gene (*AT2G14100*) consists of two exons and one intron (1639 bp). The potential function of this gene is in the lignin pathway and/or as an oxidoreductase localized to the plasma membrane. Two non-synonymous SNPs were found in exon 1 in *AT2G14100* (*CYP705A13*). The first (position: 5935548) causes a change in amino acid sequence from tyrosine in BG-5 to phenylalanine in Kro-0 (Y129F). The second non-synonymous SNP (position: 5935983) causes an amino acid change from methionine in BG-5 to leucine in Kro-0 (M274L). Also, it is not known how these changes can affect functionality of the protein or may potentially cause an epistatic interaction with the Kro-0 allele.

The other cytochrome P450 gene (*AT3G61035*) consists of four exons and three introns (1398 bp). This gene undergoes alternative splicing, resulting in three isoforms and functions in the indole glucosinolate pathway by tryptophan catabolism (TAIR). *AT3G61035* localizes to the plasma membrane (similar to *AT2G14100*). One non-synonymous SNP was found in *AT3G61035* (*CYP76C8P*) in exon 1 (position: 22593529) that causes an amino acid change from valine in Kro-0 to leucine in BG-5 (V40L). Also, it is not known how this SNP can affect functionality of this protein or even cause an epistatic interaction with the Kro-0 allele.

3.3.4 Characterization of crosses among parental-like accessions

For additional confirmation of the genetic architecture of the F₁ phenotype, crosses with other accessions that share SNPs with either of the parental lines used were performed. The assumption was that if the SNPs in the candidate genes (for example, SNPs in Chr2

candidates from Kro-0) were the genetic cause of the F₁ phenotype, then crossing accessions that share these SNPs with the other parent (in this case, BG-5) would recapitulate the F₁ phenotype.

When the Kro-0 sequence was compared with the available accessions within the atg1001 genome browser (1001genomes.org), nine accessions sharing SNPs with the two candidate genes (including coding, non-coding and promoter SNPs) on Chr2 with Kro-0 were selected. It should be noted here that the BG-5 accession has not been fully sequenced. Since crossing Kro-0 with BG-2, a closely related accession to BG-5, also produces the F₁ phenotype (Figure 3.13 A), five accessions sharing SNPs with the two candidate genes and the additional one *AT3G60970* on Chr3 were selected based on sequencing data from BG-2 instead of BG-5.

Once accessions of interest were chosen, Kro-0-like accessions were crossed with BG-5. Similarly, BG-2-like accessions were crossed with Kro-0. The F₁ crosses that were produced were then screened at 17 °C (Table 3.1). From 15 crosses, only one cross between BG-5 and Ragl-1 showed the F₁ dwarf bushy phenotype at 17 °C (Figure 3.13 A). These F₁ plants were scored for stem length (cm) and total number of branches and were similar to BG-5×Kro-0 F₁ phenotype (Figure 3.13 C and D). Furthermore, the segregating plants in the F₂ generation of BG-5 and in the F₁ generation of Ragl-1 exhibited similar dosage-dependent hybrid breakdown to those scored for Kro-0-BG-5 hybrid (Figure 3.13 B). To find out if Ragl-1 and Kro-0 shared a unique SNP in the targeted interval in comparison to accessions that did not show the F₁ dwarf bushy phenotype, SNPs within the Chr2 interval were investigated; however, none were unique to Ragl-1 and Kro-0. This indicated that SNPs in the coding and non-coding sequence might not be the only cause of the F₁ phenotype.

Table 3.1 Selected accessions, the genes they shared SNPs with and the phenotype of their F₁ hybrids.

Accession	Shared SNPs	crossed to	F ₁ phenotype
Kro-0_Salk	<i>AT2G14120</i> Kro-0	BG-5	NO
BG-2	BG-5 is not sequenced	Kro-0	YES
Filet-1	<i>at2g14120</i> Kro-0	BG-5	NO
Ragl-1	<i>at2g14100, at2g14120</i>	BG-5	YES
Sq-8	<i>at2g14120</i>	BG-5	NO
Stw-0	<i>at2g14100, at2g14120</i>	BG-5	NO
Bor-4	<i>at2g14100, at2g14120</i>	BG-5	NO
Do-0	<i>at2g14100, at2g14120</i>	BG-5 /CIBC-5/TDR-17	NO/NO/NO
Kelsterbach-4	<i>at2g14100, at2g14120</i>	BG-5 /ALST-1/CIBC-5	NO/NO/NO
T1090	<i>at2g14120</i> Kro-0	BG-5	NO
Est-1	<i>at3g61035</i> BG-2	Kro-0/Do-0	NO/NO
CIBC-5	<i>at3g60840</i> BG-2	Kro-0 /Bor-4	NO/NO
NFA-10	<i>at3g60970</i> BG-2	Kro-0	NO
TDR-17	<i>at3g60970</i> BG-2	Kro-0 /Do-0/ Bor-4	NO/NO/NO
ALST-1	<i>at3g60970</i> BG-2	Kro-0 /Do-0	NO/NO

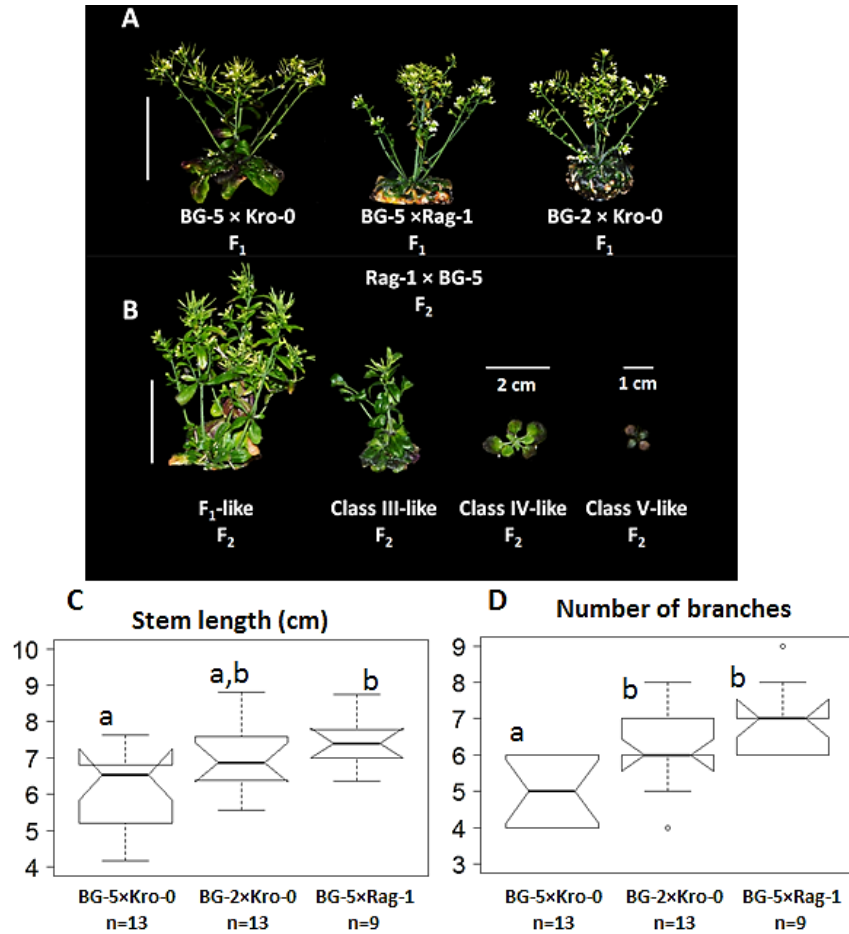


Figure 3.13 Additional crosses with BG-5- and Kro-like accessions that show the F₁-like phenotype at 17 °C. A: dwarf-bushy phenotypes in F₁ hybrids of BG-2×Kro-0 and BG-5× Rag-1. **B:** F₂s of BG-5× Rag-1 hybrid segregated HB classes' phenotypes. **C:** stem length (cm) of F₁ hybrids of BG-2×Kro-0 and BG-5× Rag-1. **D:** number of branches of F₁ hybrids of BG-2×Kro-0 and BG-5× Rag-1. Different lowercase letters denote significantly different means. p-values were calculated by Kruskal-Wallis followed by post-hoc Kruskal nemenyi test. Numbers in parenthesis in the X-axis denote the number of biological replicates for each phenotype.

3.4 Characterization of F₂ phenotypes

Hybrid breakdown (HB) by definition is any type of reproductive failure in the F₂ and successive generations (Fishman and Sweigart, 2018). The F₂ progeny of BG-5×Kro-0 F₁ produced more severe phenotypes, some of which, exhibited reproductive failure. The different phenotypes observed were initially classified into five groups according to the severity of their phenotype and inability to reproduce (Figure 3.14 A). Unlike the F₁ temperature-dependent phenotype, the most severe phenotype in the F₂ generation manifested as a stunted growth habit at 17°C that affected the ability of these plants to

recover when shifted to 21 °C (Figure 3.14 A and B). The fine mapping that was performed using F₂ hybrids, using markers flanking the F₁ phenotype associated loci, revealed that these classes were linked to the same loci in a dose-dependent manner (Boldt, 2009). Thus a model of two interacting loci was considered to explain the HB classes in the F₂ generation. In this study, hybrid breakdown in such hybrids were further characterized and the validity of the two gene model in F₂ hybrids was tested. In addition, the candidate gene on Chr2, *AT2G14100*, according to the gene expression analysis indicated that this gene was expressed exclusively in roots in both Kro-0 and BG-5. Thus, root phenotypes in three F₂ hybrids and one F₃ hybrid were investigated of to see if changes in root phenotype may be linked to the different shoot phenotypic classes observed.

3.4.1 Classification of F₂ phenotypes

Hybrid breakdown that appeared in successive generations of Kro-0 and BG-5 hybrids was reported earlier; however, no quantitative measurements were made. In order to characterize HB, three F₂ populations were grown at 17 °C to measure the number of leaves, rosette diameter (cm) (three weeks after germination), number of branches, stem length (cm), number of seeds and the rate of germination. This characterization showed that the stem length, rosette diameter and number of seeds were the most significant traits to separate the segregants into five different classes. The class-I showed a parental-like phenotype, class-II plants exhibited an F₁-like phenotype and class-III plants showed a short stem and sometimes did not make branches. Finally two different HB classes showed the stunted growth habit at two different growth stages (Figure 3.14 C-H; Figure S 5 and 6). The F₂ classes II and III showed significantly shorter stem length while rosette diameter separated the other small plants into two classes, class-IV and class-V. In terms of branching, as mentioned earlier, F₁ hybrids showed an increased number of branches and similar number of seeds with parents. However, in F₂ populations, F₁ like segregants showed significantly fewer branches and seeds compared to the parental-like segregants (Figure 3.14 F and G; Figure S 5 and 6). This indicates that the F₁-like phenotype (class-II) becomes more severe in successive generations. The class-III showed a drastic loss of fitness; however, it maintained a high percentage of seed viability (Figure 3.14 H, Figure S 5 and 6). HB class-IV and class-V showed premature death without reaching the flowering stage (Figure 3.14 C-H; Figure S 5 and 6). To know whether the HB classes showed any changes in root phenotype, the root length and lateral root number were measured for all segregants in the F₂ population and in one F₃ and then Pearson correlation analysis was done to see whether the root phenotype would explain the classes or their other traits. The analysis showed that root length and lateral root number had no significant correlation with either of the different phenotypes or with the other scored traits used for F₂ classification (Figure 3.15 A and B; S 7).

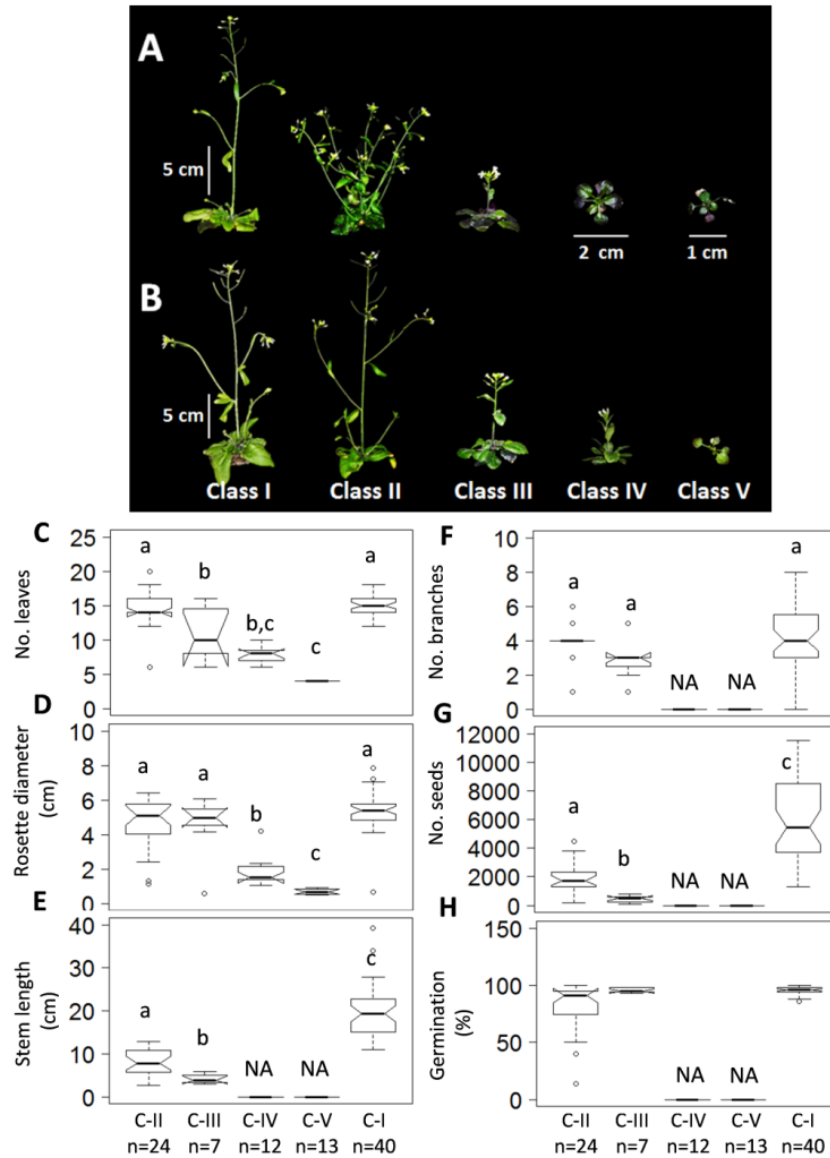


Figure 3.14 Phenotypic characterizations of F_2 hybrids at 17 °C. Five classes of phenotypes shown by F_2 hybrids derived from Kro-0 x BG-5 F_1 hybrids **A:** at 17 °C and **B:** at 21 °C. **C:** number of leaves, **D:** rosette diameter (cm), **E:** primary stem length (cm), **F:** total number of branches, **G:** number of seeds, and **H:** germination rate (%). Different lowercase letters denote significantly different means. p-values were calculated by Kruskal-Wallis followed by post-hoc Kruskal nemenyi test. C-I= parental-like, C-II= F_1 -like, C-III= dwarf plant class-III, C-IV= stunted growth 6-8 leaves class-IV, C-V=stunted growth 2-4 leaves class-V. Numbers in parenthesis in the X-axis denote the number of biological replicates for each phenotypic class.

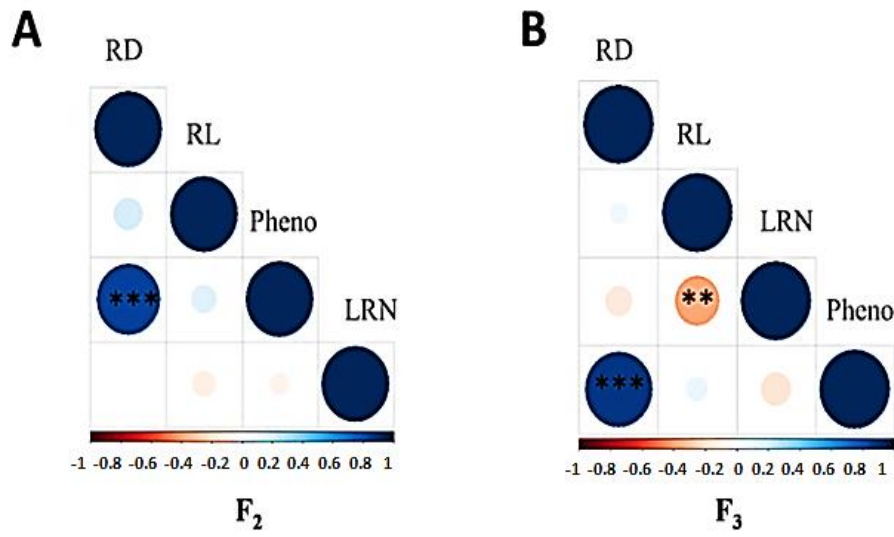


Figure 3.15 Correlation analyses between root and shoot phenotypes in F₂ and F₃ hybrids grown at 17 °C. A: correlation coefficient matrix between root and shoot phenotypes in F₂. **B:** correlation coefficient matrix between root and shoot phenotype in F₃. Asterisks denote statistically significant correlation between two traits (p-value <0.05 * <0.01 ** and <0.001 ***) with 95% confidence interval. The colour scale denotes the correlation coefficient as Red = -1, and Blue=1. RD: rosette diameter (cm), MSL: Primary stem length (cm), BN: Branches number, RL: root length (cm), LRN: lateral root number, Pheno: denotes the five different classes of phenotypes. The scale is from -1 (red) to +1 (blue).

3.4.2 Testing the two-locus model for F₂ segregations

Extensive genotyping done previously (more than 4000 plants) showed that HB classes in the F₂ may be linked to the same loci associated with the F₁ dwarf bushy phenotype (Boldt, 2009; Muralidharan, 2015). Nonetheless, no phenotypic frequency analysis was performed to test the two loci model. Thus, after the classification of F₂ phenotypes, genotyping of two F₂ populations was achieved using markers flanking the identified intervals on Chr2 and Chr3 and the candidate genes they contained (Table 2.2). This was followed by a chi-square test to test the two loci model.

To further analyze the segregation of the different F₂ phenotypes, 192 F₂ plants were genotyped using SSLP and CAPS markers (Table 2.2). The genotyping showed that the most severe phenotypes in successive generations were related to the same identified intervals in a dose-dependent manner (Table 3.2). Interestingly, the plants of class-II and III were both heterozygous for the two intervals. If the class-II (F₁ like phenotype) and class-III (dwarf without little branching) were basically the same genotype at these loci, the difference of their phenotypes could be explained by another genetic locus that was unknown or missed in the QTL analysis and genotyping. This was first investigated by

scoring the segregating phenotypes of two F₃ hybrids that were genotyped in the F₂ generation as heterozygous and phenotyped as a class-III. Then a backcross was performed to see how the locus of one parent affected the genetic background of the other. Five plants of the class-IV were shifted to 21 °C to collect some seeds and follow their segregations in F₃. However, in this thesis, the two phenotypes of the same genotype (class-II and III) will be separated and not joined in figures to investigate their differences.

Table 3.2 Phenotypic classification of F₂ progeny and their expected numbers.

Class	Phenotype	Total number of leaves	reproductive ability (Seeds)	Genotype		Expected number of individuals
				Chr2	Chr3	
Class-I	parental-phenotype	after flowering	4000-12000	KK	KK	42
				BB	BB	
				KB	KB	
				BB	KB	
				BB	KB	
Class-II	F ₁ -like	after flowering	1000-3000	KB	KB	24
Class-III	dwarf main stem	after flowering	0-100	KB	KB	
Class-IV	stunted growth	6-8 leaves	0	KB	BB	12
Class-V	stunted growth	2-4 leaves	0	KK	KB	12

K= locus from Kro-0, B=locus from BG-5

A χ^2 test showed that two F₂ populations followed that suggested model; however, one population did not (Table 3.3). It could be that the third population did not follow the model due to human error; however, a backcross of the F₁ to its parental accessions could reveal more about the correct genotype of each class of HB.

Table 3.3 χ^2 test of a two-gene model for observed phenotypes of three F₂s populations.

Filial	Phenotype	Class-I	Class-II	Class-III	Class-V	Sum
F ₂₋₁	Observed number of individuals	40	31	12	13	90
	Expected number of individuals	42	24	12	12	90
	$(O - E)^2/E$	0.095	2.041	0	0.08	2.216
	<i>p</i> -value	0.68				
F ₂₋₂	Observed number of individuals	39	32	10	13	90
	Expected number of individuals	42	24	12	12	90
	$(O - E)^2/E$	0.214	2.66	0.33	0.08	3.28
	<i>p</i> -value	0.44				
F ₂₋₃	Observed number of individuals	31	23	23	19	90
	Expected number of individuals	42	24	12	12	90
	$(O - E)^2/E$	2.88	0.041	10.08	4.083	17.08
	<i>p</i> -value	0.006				

Degree of freedom=3

The segregating phenotypes of 96 individuals derived from one plant possessing a class-III phenotype produced hybrids of all phenotypic classes (Figure 3.16 A). This result showed that this class was not homozygous at one of the targeted loci, but rather was heterozygous for both. The 39 segregating plants of phenotypes class-IV included only two phenotypes, one that was classified as class-I (parental-like) and the other like class-IV (Figure 3.16 B). The result of the segregating phenotypes of class-IV is consistent with this genotype (KB/BB).

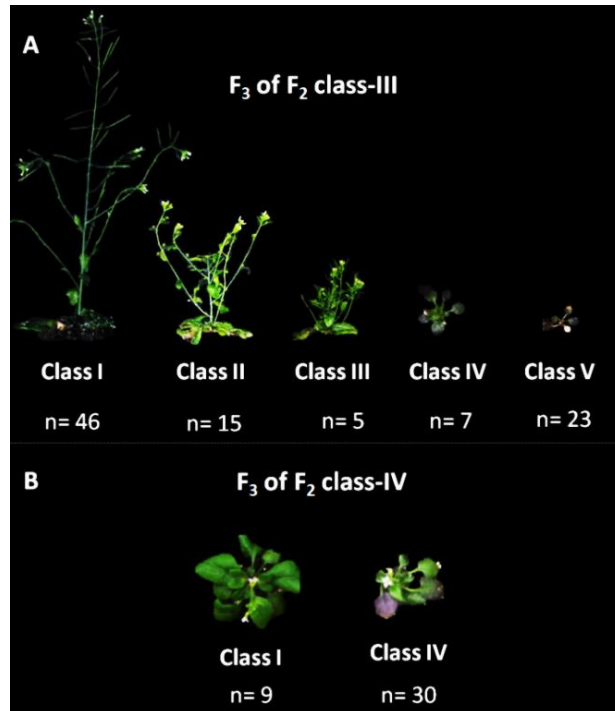


Figure 3.16 Phenotypic segregation of F₃ plants of F₂ class-III plant and plant class-IV grown at 17 °C. **A:** the phenotypic segregations of F₃ plants of F₂ class-III with their frequencies. **B:** the phenotypic segregations of F₃ plants of F₂ class-IV with their frequencies

Interestingly, no individuals of HB in F₂s were homozygous for both intervals which suggest that the homozygosity of these loci had a lethal effect that either prevented germination or caused premature death directly after germination. Such an explanation could explain why these plants were not scored. Based on this, the frequencies of the phenotypes were analysed taking into account the result of the genotyping data (Table 3.2).

To know whether any of the amiR-F₁s that showed F₁ phenotypic reversion into a parental-like phenotype would also reverse the severe phenotypes observed, F₂ segregations of these hybrids were followed. Only F₂ hybrids of the amiR-*DRP3B* F₁ did not show any severe segregants in comparison to the F₂ of wild-type hybrid.

Table 3.4 Expected and observed phenotypes of amiR-*DRP3B* F₂s based on their genotyping.

amiR- <i>DRP3B</i> F ₂ s	Expected phenotypes	Class-I	Class-II	Class-IV	Class-V
	Genotyped individuals		28	10	13
Observed phenotype		Class-I			

In addition, F₂ segregations of Rag-1 crossed to Kro-0 showed the dose-dependent hybrid breakdown (Figure 3.13 B). Altogether, the causal genes of the F₁ phenotype appear to participate in F₂ phenotypes in a dose-dependent manner with evidence for another segregating element that makes the F₁ phenotype more severe.

3.5 Analysis of backcrosses

Previous results showed that F₂ phenotypes were linked to two loci known to cause the F₁ phenotype. However, the phenotypic analysis suggested that there might be an additional genetic factor influencing the F₁-like phenotype in F₂ generations. Hence, a backcross was performed to dissect the contribution of the Kro-0 and BG-5 alleles to the F₂ phenotypes observed. In addition, segregation ratios of the backcrosses were evaluated to further investigate the involvement of additional genetic factors in the F₂ generation. Backcrosses (BCs) were performed using the F₁ as the pollen donor to avoid errors such as obtaining selfed-seeds of the F₁. For example, to create the first generation of the backcrossed lines, one F₁ (BG-5 (Mother) × Kro-0 (Father)) was used as a pollen donor to cross with BG-5 (BC₁F₁^{BG-5}) and with Kro-0 (BC₁F₁^{Kro-0}).

In the first generation of the BC₁F₁^{BG-5} population, BG-5 alleles were both homozygous and heterozygous, while alleles of Kro-0 are always heterozygous. In the first generation of the BC₁F₁^{Kro-0} population, alleles of Kro-0 were both homozygous and heterozygous, while BG-5 alleles are always heterozygous.

3.5.1 Phenotypic characterization of backcrosses

To evaluate backcrosses, phenotyping was performed for 96 individuals of each one of the first generation progeny in both backcrosses with BG-5 and Kro-0 parents. In BC₁F₁^{BG-5}, the observed phenotypes could be grouped based on their phenotypic characteristics at 17 °C into three classes according to Table 3.2, namely class-I, class-II and class-IV (Figure 3.17 A) while the observed phenotypes in BC₁F₁^{Kro-0} were classified into class-I, class-II, class-III and class-V (Figure 3.17 B). All classified phenotypes in these backcrosses were

characterized for the traits associated with F₁-like phenotype and HB (Figure 3.17 C-J). In both backcrossed populations, the HB classes showed stunted growth as expected (Figure 3.17 C, D, G and H). In BC₁F₁^{BG-5}, class-II plants exhibited similar traits to the F₁ dwarf-bushy phenotype such as a shorter stem length and more branches in comparison to class-I (parental-like) plants (Figure 3.17 C and E). However, BC₁F₁^{Kro-0} class-II plants showed similar numbers of branches with class-I but a more reduced stem length similar to class-III (Figure 3.17 D, F). In fact, plants of class-II and class-III are very similar in the backcross with Kro-0. In addition, root length did not show any significant difference among the different phenotypic classes in both backcrosses (Figure 3.17 I and J).

In order to investigate how different combinations of the parental alleles may influence different phenotypic classes, the phenotypic classes that were scored in BCs were compared to the similar classes of F₁, F₂, and F₃ and to parental phenotypes. This comparison showed that the class-I (parental-like) plants exhibited positive and negative transgressive phenotypes for stem length and rosette diameter respectively, but not for the number of branches (Figure 3.18 A-C). Comparing class-II (F₁-like phenotype) from BCs with class-II of F₂s, F₃ and F₁ showed that BC₁F₁-K-class-II exhibited a significant reduction in primary stem length and in the number of branches (Figure 3.18 D). Furthermore, this result showed that the number of branches in class-II is significantly reduced in the successive generation (Figure 3.18 D). Interestingly, both classes IV and V did not show any significant differences when compared with same classes from different generations. Altogether, first generation backcrosses indicate that the BG-5 allele has a stronger effect on the hybrid phenotype than the Kro-0 allele.

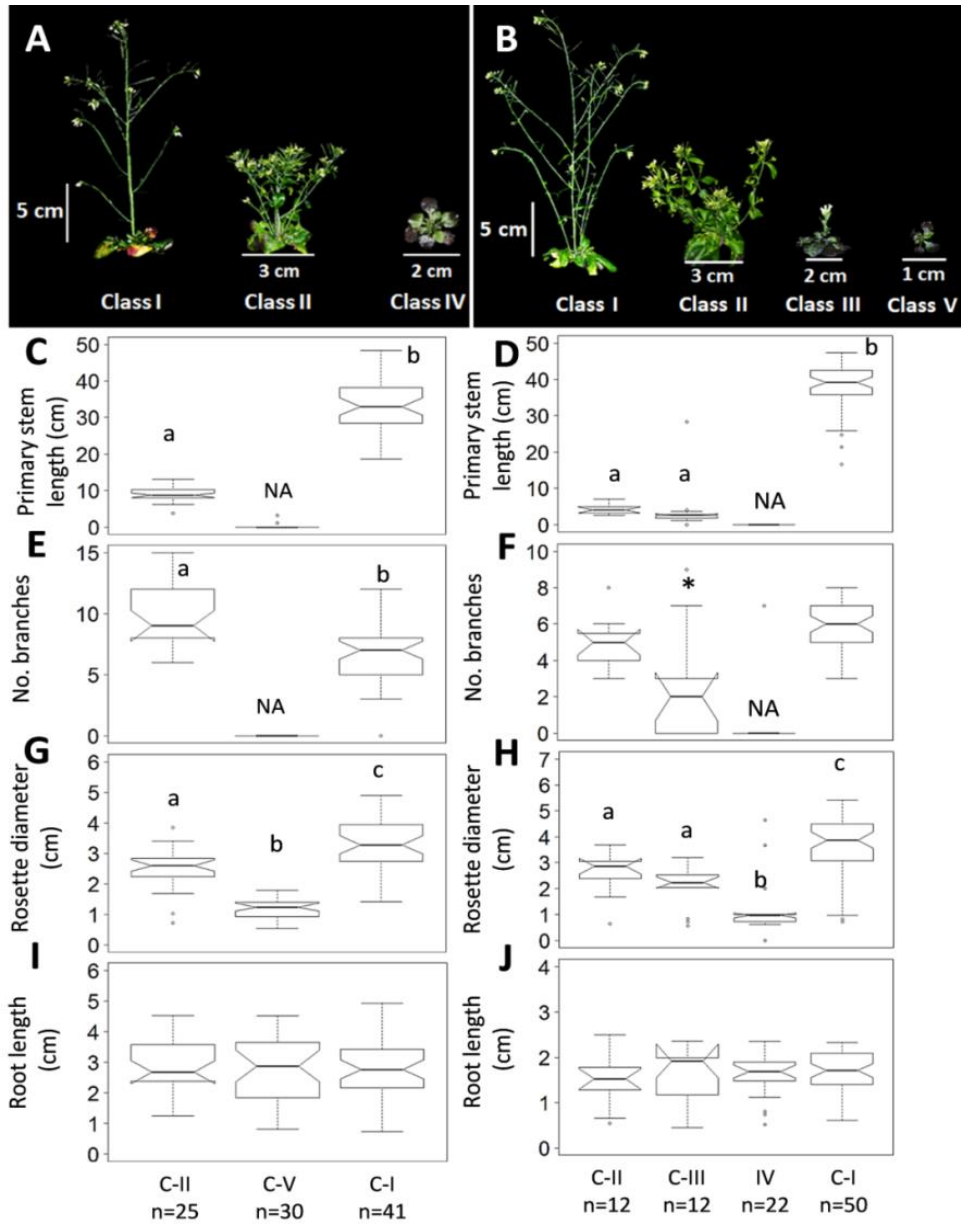


Figure 3.17 Phenotypic characteristics of backcrosses grown at 17 °C. **A:** Three difference classes of $BC_1F_1^{BG-5}$ phenotypes. **B:** $BC_1F_1^{Kro-0}$ different 4-classes of phenotypes. **C:** stem length (cm) in three different classes of $BC_1F_1^{BG-5}$ phenotypes. **D:** primary stem length (cm) in $BC_1F_1^{Kro-0}$ different 4-classes of phenotypes. **E:** the total number of branches in $BC_1F_1^{BG-5}$ different 3-classes of phenotypes. **F:** the total number of branches in $BC_1F_1^{Kro-0}$ different 4-classes of phenotypes. **G:** rosette diameter (cm) in $BC_1F_1^{BG-5}$ different 3-classes of phenotypes. **H:** rosette diameter (cm) in $BC_1F_1^{Kro-0}$ different 4-classes of phenotypes **I:** root length (cm) in $BC_1F_1^{BG-5}$ different 3-classes of phenotypes. **J:** root length (cm) in $BC_1F_1^{Kro-0}$ different 4-classes of phenotypes. Different lowercase letters denote significantly different means. p-values were calculated by Kruskal-Wallis followed by post-hoc Kruskal Conover test. C-I= parental-like, C-II= F₁-like, C-III= dwarf plant class-III, C-IV= stunted growth 6-8 leaves class-IV, C-V=stunted growth 2-4 leaves class-V. Numbers in the X-axis denote the number of biological replicates for each phenotypic class.

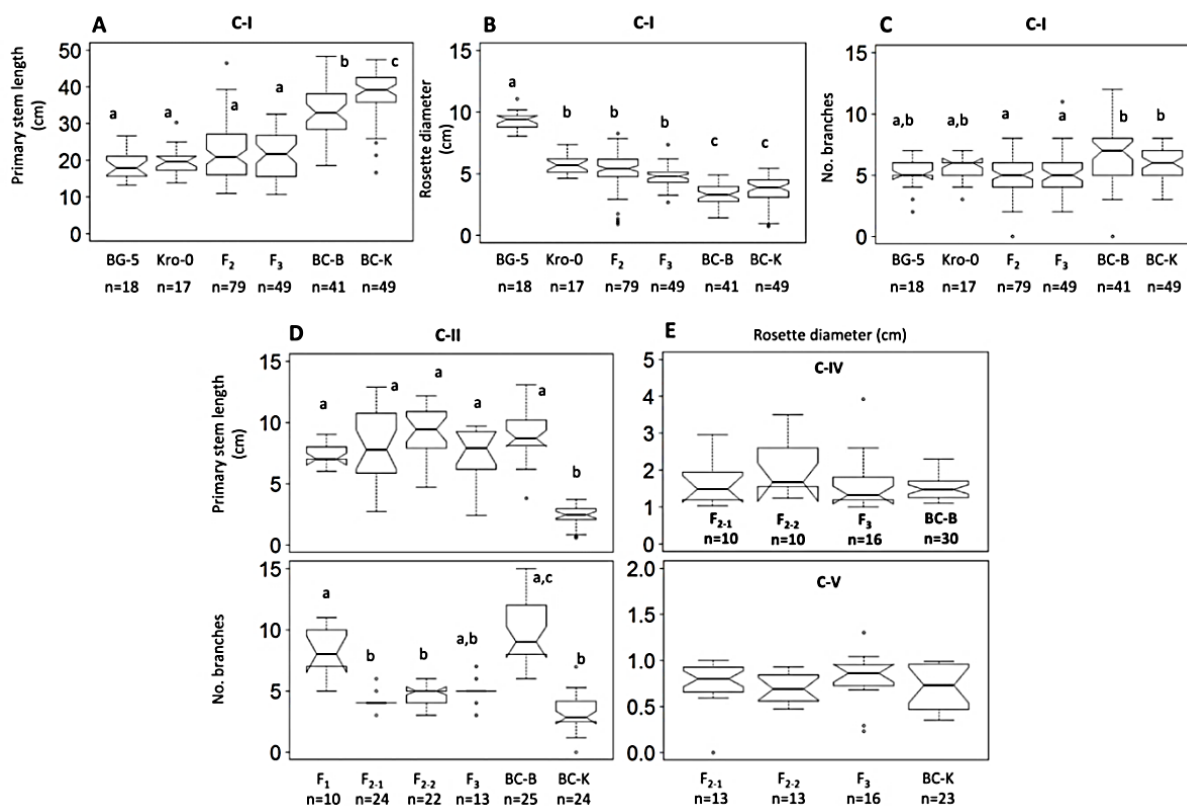


Figure 3.18 Comparison of different segregating phenotypic classes with F₁ and parents grown at 17 °C. **A:** stem length (cm). **B:** rosette diameter (cm). **C:** the total number of branches. **D:** primary stem length (cm). **E:** rosette diameter (cm). Different lowercase letters denote significantly different means. p-values were calculated by Kruskal-Wallis followed by post-hoc Kruskal Conover test. C-I= parental-like, C-II= F₁-like, C-III= dwarf plant class-III, C-IV= stunted growth 6-8 leaves class-IV, C-V=stunted growth 2-4 leaves class-V. Numbers in the X-axis denote the number of biological replicates for each phenotypic class.

3.5.2 Analysis of phenotypic ratios in backcrosses

To further investigate the frequencies of the different phenotypes that were found in both backcross populations, a χ^2 test was performed. In BC₁F₁^{BG-5}, a χ^2 test showed that the observed phenotypes at 17 °C matched the phenotypic ratio expectations (Table 3.5). Moreover, the residuals of the test showed that there was no significant deviation in each observed class from the expected one.

Table 3.5 χ^2 test of two-gene model for BC₁F₁^{BG-5} observed phenotypes.

Phenotype	Class-I	Class-II	Class IV	Sum
Observed number of individuals	41	25	30	96
Expected number of individuals	48	24	24	96
(O - E) ² /E	1.02	0	1.5	2.52
p-value	0.28			

Degree of freedom=2

However, in BC₁F₁^{Kro-0}, the phenotypic ratio of class-II to class-III was 1:1 (while in the F₂ it was 3:1) which supports that this heterozygous genotype of the loci of interest was influenced by another unknown element (recessive one). This result suggested that this unknown element may come from a Kro-0 genetic background since this difference was not observed in BC₁F₁^{BG-5}. Generally, a χ^2 test of BC₁F₁^{Kro-0} showed that the observed frequencies support the expected model for two genes with an evidence of a third locus affecting the F₁ like phenotype (Table 3.6). However, to further confirm the genetic architecture and to find out the additional genetic factor, genetic mapping using the different classes of F₂ phenotypes and backcrosses is required.

Table 3.6 χ^2 test of two-gene model for BC₁F₁^{Kro-0} observed phenotypes.

Phenotype	Class-I	Class-II	Class IV	Sum
Observed number of individuals	50	24	22	96
Expected number of individuals	48	24	24	96
(O - E) ² /E	0.08	0	0.16	0.24
<i>p</i> -value	0.81			

Degree of freedom=2

3.5.3 Crosses between backcross recombinant lines

In addition to characterizing and analyzing the first generation of backcrosses, individuals of the first generation of BC₁F₁^{BG-5} and BC₁F₁^{Kro-0} were crossed to each other and to parents (Table 3.7; 3.8). The first generations of backcrossed lines were recombinant lines of BCs. Here the assumption was that if the two loci, one on Chr2 and one Chr3, were the only ones responsible for the F₁ phenotype, independent of any other elements in the parental genomic background, then all crosses that harbour these two loci similar to the parents should result in an F₁ phenotype. For example, when crossing the parental-like phenotype line of BC that had the genotype e.g. KB/KK with BG-5 accession BB/BB then the F₁ seeds of this cross would segregate two genotypes as 1:1 i.e. KB/KB and BB/KB would manifest as an F₁-like phenotype and parental-like phenotype. In addition to these crosses, three F₄ lines of F₃ seeds of a plant that showed homozygous BG-5 allele were crossed to Kro-0.

In BC₁F₁^{Kro-0}, 12 lines of class-I were selected and genotyped, using one flanking marker for Chr 2 and Chr 3 and one marker on one of the candidate genes on Chr 2 and Chr 3, to know whether recombination takes place. These lines were then crossed with BG-5 and lines of the first generation of BC₁F₁^{BG-5} parental-like individuals (class I). In a similar manner, six lines of parental-like (class I) individuals from the first generation of BC₁F₁^{BG-5} were selected and genotyped and then crossed with Kro-0 and class-I from of BC₁F₁^{Kro-0}. In those cases in which there was a recombination event between the used markers, the scenarios of expected phenotypic ratios were presented (Table 3.7 and 3.8). In total, 20 crosses were

done that are summarized in Table 3.7 and 3.8. At least 20 individuals of each cross were grown and evaluated at 17 °C with F₁ plants as a control. Interestingly, only three crosses out of 20 showed the expected phenotype with the expected ratios (Table 3.7, 3.8). The progeny from line 6 of BC₁F₁^{Kro-0} parental-like individuals, when crossed with BG-5, gave the expected F₁ dwarf-bushy phenotype with the expected ratio, but when crossed to BC₁F₁^{BG-5} parental-like individuals, the hybrid individuals showed in addition to the dwarf-bushy phenotypes more severe phenotypes (class III). None of the BC₁F₁^{BG-5} with parental phenotype showed the F₁-like bushy-dwarf phenotype when crossed to Kro-0. These results suggest an involvement of a third locus in the F₁ phenotype or that the recombination events in these lines change the whole endogenous transcriptomic status. Also taking into account the result of crosses between and with other accessions, his result supports the assumption that F₁ phenotype has a strong dependency on the interaction between natural genetic and transcriptomic configuration of the parental accessions.

Table 3.7 Genotypes of BC₁F₁^{Kro-0} C-I lines and the lines they were crossed with and their hybrid phenotypes.

BC ₁ F ₁ ^{Kro-0}							
Phenotype	Genotype chr2		Genotype chr3		Crossed with	F ₁ phenotype	Expected phenotype
	nga1126	AT2G14120	CIW21	AT3G60970			
BC ₁ -K-CI-1	K	H	K	K	F ₄ BG-5-like, BG-5	Parental	1:1 WT, F ₁ -like
BC ₁ -K-CI-2	K	H	H	K	BG-5	Parental	1:1 WT, F ₁ -like
BC ₁ -K-CI-3	K	H	K	K	BG-5	Parental	1:1 WT, F ₁ -like
BC ₁ -K-CI-4	K	K	K	H	BG-5	Parental	1:1 WT, F ₁ -like
BC ₁ -K-CI-5	K	H	K	H	BC ₁ -B-CI-1	Parental	1:1 WT, F ₁ -like
BC ₁ -K-CI-6	K	H	K	H	BC ₁ -B-CI-6	C-III, F ₁ -like	1:1 WT, F ₁ -like
BC ₁ -K-CI-6	K	H	K	H	BG-5	WT, F ₁ -like	1:1 WT, F ₁ -like
BC ₁ -K-CI-7	K	H	K	K	BC ₁ -B-CI-2	Parental	25% Class IV 25% F ₁ -like and 50% Parental
BC ₁ -K-CI-8	K	H	K	K	BC ₁ -B-CI-4	Parental	1:1 WT, F ₁ -like
BC ₁ -K-CI-9	K	H	K	K	BC ₁ -B-CI-6	Parental	1:1 WT, F ₁ -like
BC ₁ -K-CI-10	K	K	K	H	BG-5	Parental	100% F ₁ -like
BC ₁ -K-CI-11	K	K	-	K	BG-5	Parental	100% F ₁ -like

Table 3.8 Genotypes of BC₁F₁^{BG-5} C-I lines and the lines they were crossed with and their hybrid phenotypes.

BC ₁ F ₁ ^{BG-5}							
Phenotype	Genotype chr2		Genotype chr3		Crossed with	F ₁ phenotype	Expected
	nga1126	AT2G14120	CIW21	AT3G60970			
BC ₁ -B-CI-1	B	B	B	B	Kro-0	Parental	100% F ₁ -like
BC ₁ -B-CI-2	H	B	B	H	BC ₁ -K-CI-2	Parental	1:1 WT, F ₁ -like
BC ₁ -B-CI-3	B	B	B	H	BC ₁ -K-CI-8	Parental	1:1 WT, F ₁ -like
BC ₁ -B-CI-4	H	B	B	H	Kro-0	Parental	1:1 WT, F ₁ -like
BC ₁ -B-CI-5	B	B	B	H	BC ₁ -K-CI-12	Parental	1:1 WT, F ₁ -like
BC ₁ -B-CI-6	B	B	B	B	BC ₁ -K-CI-6	1:1 F _{1T} , F ₁ -like	1:1 WT, F ₁ -like
F ₄ B-like	B	B	B	B	Kro-0	Parental	100% F ₁ -like
BC ₁ -K-CI = class-I showing parental phenotype in BC ₁ F ₁ ^{Kro-0}							
BC ₁ -B-CI = class I showing parental phenotype in BC ₁ F ₁ ^{BG-5}							
F ₄ B-like = lines of F ₃ seeds linked to BG-5 like genotype							
K= homozygous to Kro-0 locus, B= homozygous to BG-5 locus, H= hybrid to both loci.							

4. Discussion

In recent years, studies in *A. thaliana* have contributed to our understanding of genetic mechanisms of post-zygotic hybrid incompatibility. In *A. thaliana* the most common type of post-zygotic hybrid incompatibility is hybrid necrosis and many of them have shown to have a simple genetic basis e.g. linkage to one or three loci (Bomblies *et al.*, 2007; Alcázar *et al.*, 2009; Chae *et al.*, 2014; Todesco *et al.*, 2014; Świadek *et al.*, 2017). However, less is known of the other mechanisms of hybrid incompatibility in plants. In my thesis, I investigated a novel hybrid phenotype, in which the F₁ hybrid between *A. thaliana* accessions BG-5 and Kro-0 showed altered shoot architecture and hybrid breakdown in successive generations. This hybrid case was characterized and showed that the dwarf bushy F₁ phenotype depends on both temperature and developmental stage and is associated with hormonal and metabolic changes. Additionally, four genes to be necessary for the F₁ phenotype were identified.

4.1 F₁ phenotype depends on temperature and developmental stage

As BG-5×Kro-0 F₁ exhibited a dwarf bushy phenotype at 17 °C and parental-like phenotype at 21 °C, detailed characterization of the F₁ generation in comparison to parents at these temperatures revealed that the phenotype was due to restricted growth in the stem coupled with an increased number of cauline branches at 17 °C. The major effect on the stem was observed at the first internode and manifested as an extreme reduction of internode elongation. Reduction of stem elongation could be due to a defect in SAM growth or orientation of cell division (Maeda *et al.*, 2014; Bencivenga *et al.*, 2016). However, it was shown that the SAM was intact in F₁ plants at 17 °C at the bolting stage. This is consistent with previous work that compared the SAM in BG-5×Kro-0 F₁ after the stem stopped growing and before branching between 17 °C and 21°C, to which no significant differences were observed (Muralidharan, 2015). In addition, rosette and cauline branches grew in F₁ hybrids at both temperatures, suggesting that the axillary meristems were intact. Furthermore, it was shown that the F₁ dwarf bushy phenotype can be induced before bolting and that after this stage, the F₁ phenotype cannot be induced or reversed by a temperature shift. However, it is possible that F₁ suffers a defect in RZ or intercalary meristems, both of which have shown to control stem elongation (Van der Knapp *et al.*, 1999) and no experiment was done to check these meristematic tissues in F₁s.

There are several other hybrid incompatibility cases that are controlled by temperature. For example, in several cases of hybrid necrosis, the activation of an immune response and necrotic phenotype was only visible at the lower temperature (Todesco *et al.*, 2014; Świadek *et al.*, 2017). So far, how temperature is inducing hybrid necrosis is not yet known. In contrast to BG-5 x Kro-0 F₁, temperature-dependent necrosis cases are not developmental-dependent. So far, we do not have evidence that altered inflorescence

architecture in F₁ is due to an activated pathogen response or not. Therefore, it is believed that this hybrid case is due to a novel mechanism yet to be unravelled. In addition, the necrotic phenotype was associated with significantly reduced fitness at the lower temperature (Watanabe and Marubashi, 2004; Świadek *et al.*, 2017). Although temperature had a major effect on shoot architecture in BG-5 x Kro-0 F₁ hybrids, it did not affect the final number of seeds. On the other hand, parents did show a significant change in seed number across conditions, in spite of the robust shoot architecture they possessed.

Taking together F₁ hybrids at 17 °C suffer restricted stem growth and more cauline branches but have an intact SAM and produce a robust number of seeds.

4.2 Metabolic and hormonal changes are associated with F₁ phenotype

4.2.1 Flavonoids are increased by temperature in hybrids

Analysis of sugars and secondary metabolites did not reveal any significant changes of sugar molecules like sucrose or the sugar signalling molecule, Tre6P, in F₁ hybrids in comparison to parents. However, it was found that flavonoids, including kaempferol(s), quercetin(s) and derivatives of indole glucosinolate accumulated in response to the temperature switch from 21 °C to 17 °C.

In addition, when F₁ hybrids were compared to their parents at 17 °C, three classes of anthocyanins were significantly up-regulated. Although higher levels of flavonoids in leaves do not directly explain the dwarf bushy phenotype of BG-5×Kro-0 F₁, many *A. thaliana* mutants that showed accumulation of kaempferol(s) and quercetin(s) also showed dwarf bushy phenotypes (Brown *et al.*, 2001; Besseau *et al.*, 2007; Peer and Murphy, 2007). It is also known that indole glucosinolates (GLS) are linked to auxin homeostasis and mutants blocked in indole glucosinolates pathway show severe growth defects due to auxin changes (Boerjan *et al.*, 1995; Mikkelsen *et al.*, 2000, 2004, 2009; Bak and Feyereisen, 2001; Tantikanjana *et al.*, 2004; Skirycz *et al.*, 2006).

4.2.2 Hormonal changes are associated with the altered stem growth

Hormonal analysis was performed at two temperatures and showed that ABA, JA and SA were significantly up-regulated in F₁ hybrids at 17 °C in stem tissues but not in leaves. Although the parental accessions had a completely different branching architecture to each other, they had comparable auxin levels in stem internodes and at both temperatures. For their F₁ progeny at 17 °C, IAA levels were lower than both parents but significantly lower than Kro-0. At 21 °C however, the F₁ generation showed comparable auxin levels to their parents. Interestingly, the ratio of auxin levels between the conditions showed a significant difference in the first internode, indicating a higher accumulation of auxin in this segment

of the stem at 17 °C. This is consistent with the observation that the critical stage of the F₁ phenotype is in the range of before or during bolting.

The result of lower IAA in dwarf bushy F₁ hybrids was expected and it is known that lower auxin levels induce CK levels to initiate buds outgrowth (Wang *et al.*, 2018). It is worth mentioning here, that our in-house facility could not measure CKs, SLs or other hormones. Thus, gene expression analysis for the responsive gene for each of IAA, cytokinins, gibberellic acid, abscisic acid and ethylene was performed for leaves, stems and the SAM at 17 °C for F₁ hybrids and parents at different developmental stages (Alhajturki *et al.*, 2017). The analysis showed that the expression of IAA responsive genes was higher at the eight-leaf stage and lower at the first internode of hybrids compared to parental accessions. Furthermore, the expression level of two auxin transporter genes *PIN* and *AUXIN RESISTANT 1 (AUX1)*, the influx symporter, showed that the expression of these genes was not significantly reduced at the first internode and was significantly reduced in the SAM of F₁ hybrids (Alhajturki *et al.*, 2017). This result suggests that the SAM in F₁ hybrids produces less auxin before branching. Furthermore, at the first internode of F₁ hybrids, CK responsive genes showed higher expression levels while GA responsive genes showed lower expression levels compared to both parents (Alhajturki *et al.*, 2017). These findings are consistent with what is known about the hormonal regulation of branching, that is, CKs are known to induce axillary bud growth at lower levels of auxin, while GA inhibits bud growth and promotes stem elongation (Tanaka *et al.*, 2006; Wang *et al.*, 2014).

ABA, JA and SA are known to mediate abiotic and biotic stress responses in plants and act antagonistically with auxin (Gonzalez-Grandio *et al.*, 2013; Wasterneck and Hause, 2013; Yao and Finlayson, 2015; Gupta *et al.*, 2017). Although higher levels of JA and SA might explain the lower levels of auxin seen in F₁ hybrids, it is not known whether they are the major cause of the F₁ phenotype or a secondary effect of the mechanism controlling this phenotype. Although ABA has been shown to suppress branching (Gonzalez-Grandio *et al.*, 2013; Yao and Finlayson, 2015), it has been also shown that ABA is a positive regulator of *EXB1* that promotes shoot branching under stress conditions by repressing auxin. Interestingly, *EXB1* has been suggested as a coordinator between JA and SA pathways (Li *et al.*, 2004; Guo and Qin, 2016).

Altogether, F₁ hybrids at 17 °C produce less IAA in the SAM and accumulate CKs and other stress-related hormones that act antagonistically to auxin.

4.3 Four genes are necessary for F₁ phenotype

Genetic mapping of 190 F₁-like individuals and 190 parental-like individuals in the F₂ generation was performed and revealed a linkage of the F₁ phenotypes to two loci on Chr2 and Chr3. Fine mapping was used narrow down the intervals to 220 kb (5.93-6.14 Mb) on Chr2 and 160 kb (22.44-22.60 Mb) on Chr3 (Boldt, 2009; Muralidharan, 2015). In my PhD,

20 genes on Chr 2 and 12 genes on Chr 3 were silenced using amiRNA to investigate candidate genes. Out of the 20 silenced genes on Chr2 from Kro-0, two genes reversed the F₁ phenotype to a parental-like phenotype at 17 °C. These include *AT2G14100* the monooxygenase CYP705A13 and *AT2G14120* encodes the dynamin-related protein DRP3B. Out of 12 silenced genes on Chr 3, *AT3G60840*, which encodes a microtubule-associated protein MAP65-4 was found, which is consistent with previous findings of Muralidharan (2015). Also, *AT3G61035*, which encodes a monooxygenase CYP76C8, was necessary for the F₁ dwarf bushy phenotype. None of these genes have been previously linked to controlling shoot branching *per se* and their function is also largely unknown.

It has been shown that the DRP3B protein encoded by *AT2G14120*, is a self-assembling GTPase involved in mitochondria and peroxisome fission and fusion (Fujimoto *et al.*, 2009; Aung and Hu, 2012; Kao *et al.*, 2018). Although single mutants do not exhibit a phenotype, the double mutant *drp3a drp3b-1* exhibits a dwarf statue (Fujimoto *et al.*, 2009; Aung and Hu, 2012). *DRP3B* is expressed at different developmental stages but mainly at the second stem internode as well as the SAM in Col-0 (eFP browser; Figure S 8). The expression level of this gene in leaves and in the stem of F₁ hybrids was similar to Kro-0 at 17 °C (Alhajturki *et al.*, 2017). Interestingly, this gene had only one non-synonymous SNP in its coding sequence causing an amino acid change from glutamic acid in Kro-0 to glutamine in BG-5 (E743Q). This SNP is in the C-terminal or GTPase effector domain of this protein. It is not known how this amino acid change may affect functionality of the protein; however, engineered mutations in this domain have been shown to affect its ability to self-assemble (Song *et al.*, 2004). Another interesting feature of *DRP3B* is that alternative splicing can result in three different isoforms. This suggests that this gene may have different regulatory roles in transcription level (Kelemen *et al.*, 2013).

The other necessary gene on Chr2 *AT2G14100* encoded a monooxygenase CYP705A13 involved in coumarin and lignin biosynthesis (www-ibmp.u-strasbg.fr/~CYPedia). In addition, it is expressed exclusively in roots in Col-0 (eFP browser; Figure S 9). Gene expression analysis showed that this gene is expressed exclusively in roots of Kro-0, BG-5 and their hybrid. Nevertheless, no significant differences in the root phenotypes of F₁, F₂ or F₃ hybrids were observed as well as no correlation between root phenotype and HB classes. It has been shown previously that root grafting from F₁ hybrids to their parents did not recapitulate the F₁ phenotype in the parental accession and grafting parental roots to F₁ plants do not rescue the dwarf bushy phenotype (Muralidharan, 2015). Two non-synonymous SNPs were found in exon 1 causing two changes in amino acids, from tyrosine in BG-5 to phenylalanine in Kro-0 (Y129F) and from methionine in BG-5 to leucine in Kro-0 (M274L). It is not known how these changes can affect the functionality of this protein or may lead to an epistatic interaction with the BG-5 allele.

On Chr3, *AT3G60840* encodes a microtubule-associated protein MAP65-4 that plays a crucial role in phragmoplast in microtubules organization during cytokinesis (Li *et al.*, 2017), and has been previously shown to interact with DRP3B proteins (Derbyshire *et al.*, 2015). A single knockout mutant of this gene did not show any phenotype. However, double mutants of *map65-4 map65-3* in *A. thaliana* showed restricted growth and dwarfism associated with defects in cytokinesis that was restored to wild-type by genetic complementation of *MAP65-4* to the double mutant (Li *et al.*, 2017). In addition, *GFP* fused with *MAP65-4* revealed an additional function of this protein in organizing the cortical cell division (Li *et al.*, 2017). Although it is expressed in many plant organs, higher levels of expression of *MAP65-4* in the SAM in Col-0 were found (eFP browser; S 10). Gene expression analysis showed that this gene was expressed similarly in both F₁ hybrids and their parents (Alhajturki *et al.*, 2017). Also, defects in cell division within the root elongation zone and SAM were not observed, which is a known phenotype associated with the *map65-4* mutant (Li *et al.*, 2017). This gene also has only one non-synonymous SNP in its coding sequence causing an amino acid change from lysine in BG-5 to asparagine in Kro-0 (K516N) at the C-terminal end. Although it is unknown how this specific change may affect the functionality of this protein, it has been found that this domain is conserved in MAP65s, and is responsible for interaction with other proteins. It is also responsible for forming the cross-linking antiparallel microtubules of the phragmoplast toward their plus ends (Schuyler *et al.*, 2003; Smertenko *et al.*, 2004; Ho *et al.*, 2012). Mutations in this domain reduce the ability of this protein to bind to other microtubules (Smertenko *et al.*, 2004). In addition, it has been shown that one of the essential proteins of peroxisome proliferation is peroxin 11 (PEX11) that is responsible of making association with microtubule binding proteins (Koch *et al.*, 2010). It is also suggested that to achieve the peroxisome proliferation and fission, PEX11 proteins functions with dynamin-related proteins and microtubules (Koch *et al.*, 2010).

The second gene on Chr 3 was *AT3G61035* and encodes the monooxygenase CYP76C8. The protein produced from this gene has been shown to be an integral component of the plasma membrane and undergoes alternative splicing (<https://www.arabidopsis.org>). It has also been shown to be involved in indole glucosinolate pathway by tryptophan catabolism (<https://www.arabidopsis.org>). Tryptophan is a precursor of different metabolites and is the main precursor to auxin biosynthesis (Woodward and Bartel, 2005). Similarly, indole glucosinolates (GLS) are linked metabolically to tryptophan-dependent auxin biosynthesis through indole-3-acetaldoxime pathway in *A. thaliana*. Mutants that had interruptions in GLS metabolism showed severe growth defects in plants (Boerjan *et al.*, 1995; Mikkelsen *et al.*, 2000, 2004, 2009; Bak and Feyereisen, 2001; Tantikanjana *et al.*, 2004; Skirycz *et al.*, 2006). *CYP76C8* is expressed exclusively in flowering tissues in Col-0 (eFP browser). Gene expression analysis detected the expression of this gene in roots of Kro-0, BG0-5 and their hybrid. One non-synonymous SNP was found in *AT3G61035* in

exon1 that caused an amino acid change from valine in Kro-0 to leucine in BG-5 (V40L). It is not known how this SNP may affect the functionality of this protein or even cause an epistatic interaction with the Kro-0 allele. In rice, knockout mutants of *CYP76* family members exhibited higher accumulation of JA and SA by regulating *WRKY* transcription factors (Liang *et al.*, 2017).

Altogether, four necessary genes were found for the F₁ dwarf bushy phenotype. Two candidate genes were involved in cell division and of the proliferation of cell compartments such as peroxisomes. The two other candidate genes were involved in coumarin, lignin, and indole glucosinolate pathways. Causality of these necessary genes, however, needs to be confirmed. One of the possible ways of confirmation would be to genetically complement parental lines with these genes (Weigel, 2012).

To date, T₂s of BG-5 and Kro-0 transformed with *AT2G14100* and *AT3G61035* were checked and only T₁ lines of BG-5 and Kro-0 transformed with alleles of *AT2G14115_AT2G14120*, *AT2G14120*, *AT3G60840*, and the two extra genes *AT3G60970* and *AT3G61070*. None of these genes was sufficient alone to induce any change of phenotype in BG-5 and Kro-0 T₁. Further experiments are required to investigate the effect of homozygosity of these alleles in T₂ lines and how crosses between these T₂ lines might affect the F₁ dwarf bushy phenotype.

Altogether, these genes provide a suitable explanation for the F₁ dwarf bushy phenotype and its physiological analysis. However, further analysis is needed to elucidate how they are involved in this hybrid case.

4.4 The two-locus interaction is dose-dependent

F₁ hybrids of BG-5 × Kro-0 produced severe phenotypes in the F₂ generation that manifested as a stunted growth at several developmental stages. Unlike the F₁ phenotype, they were less sensitive to temperature. These F₂ phenotypes were classified into five different classes according to the severity of their phenotypes. Genotyping such classes against the identified intervals associated with the F₁ phenotype revealed that these severe phenotypes were linked to the same loci in a dose-dependent manner. Interestingly, the F₁-like individuals of class-II in the F₂ generation showed more severe phenotypes than the F₁ phenotype itself, with such plants displaying fewer branches, a shorter stem and a significant loss of fitness. This severe phenotype suggests a presence of a modifier that is not necessary for the interaction but exacerbates the phenotype. However, silencing of *DRP3B* in F₂ hybrids rescued all plants within the most severe classes while silencing *MAP65-4* showed a partial rescue (Muralidharan, 2015). This suggests that another gene on Chr3 might be necessary for the F₁ dwarf bushy phenotype.

Altogether, F₁ and F₂ phenotypes appear to be linked to the same genetic base. χ^2 analysis showed that not all F₂ hybrid segregation ratios did match the expected frequencies for two interacting genes. It has been shown that the BG-5 interval suffered a translocation causing a lack of recombination in the mapped locus of Chr3 (Muralidharan, 2015). Thus, observing deviations in phenotypic frequencies is plausible in this case. In general, deviation from expected frequencies in terms of recombination or phenotypic segregation in *A. thaliana* is not rare due to innate heterozygosity in natural accessions (Salomé *et al.*, 2012). Thus, a backcross was proposed to further investigate the possible role of a genetic modifier. Backcrosses have been used in classical genetics and modern breeding to identify the further characterize the behaviour of traits of interest (Hospital, 2005).

Analyzing the segregating phenotypes in backcrosses showed the presence of transgressive phenotypes in parent-like class-I plants that were not observed in F₂ or F₃ generations. This indicates an innate heterozygosity in both accessions that is plausible in wildtype accession (Rieseberg *et al.*, 1999) since the parent accessions are natural and not recombinant inbred lines. It has been shown that the outcrossing rate in *A. thaliana* natural accessions vary, thus; finding innate heterozygosity is not rare among and between local and global accession (Bakker *et al.*, 2006; Jorgensen and Emerson, 2008; Bomblies *et al.*, 2010; Platt *et al.*, 2010; Weigel, 2012).

The F₁-like class-II in BC₁F₁^{BG-5} was similar to the F₁ phenotype while the same class found in F₂ and F₃ generations, as well as BC₁-F₁^{Kro-0}, displayed more severe phenotypes. Since the F₁ phenotype was more severe only in BC₁-F₁^{Kro-0} but not in BC₁F₁^{BG-5} this indicated that an additional genetic modifier that originates from Kro-0 may be present in a recessive manner. In addition, class-V which is the most severe phenotype appeared only in BC₁-F₁^{Kro-0} but not in BC₁F₁^{BG-5}. Taken together, these findings suggest that the effect of the BG-5 allele is either dominant over Kro-0 or that there could be other closely linked gene(s) in the BG-5 interval. This is consistent with previous findings of amiRNA F₂s.

Characterizing and genotyping F₂ hybrids as well as backcrossed plants showed that the genetic base of this case of hybrid incompatibility is relatively simple i.e. two interacting loci, that is influenced by other genetic interactions between parental backgrounds.

4.5 F₁ phenotype depends on the parental background

The four necessary genes that were found have non-synonymous SNPs on coding and non-coding regions between Kro-0 and BG-5. To know whether these SNPs can induce the phenotype between different genetic backgrounds, *A. thaliana* accessions that share the same SNPs on these candidate genes were selected and crossed with the parental lines used. Interestingly, out of the 15 combinations, only F₁ progenies of a cross between Rag-1 that is Kro-0 like for *DRP3B* and BG-5 showed the dwarf bushy phenotype. Furthermore, F₂ segregants of this hybrid exhibited similar dose-dependent phenotypic classes. However,

the same SNPs on *DRP3B* in Rag-1 and Kro-0 were also present in other accessions that their F₁ progenies did not show the phenotype. It is unknown whether this shared element between Rag-1 and Kro-0 is somewhere around the interval or somehow linked to it.

Altogether, no special SNPs were linked to the F₁ phenotype and the majority of accessions chosen for test crosses with parental lines did not recapitulate the F₁ phenotype. This suggests that the hybrid phenotype is either affected by other background-specific variants of Kro-0 and BG-5 or that this could depend on other epistatic interactions between Kro-0 and BG.

Hence, another testing cross was suggested using recombinant lines that share only the genetic background between Kro-0 and BG-5. This crossing scheme was performed to test whether recombination events might affect epistatic interactions between the identified loci or not. Crosses of individuals derived either from a backcross or intercross that showed a parental-like phenotype showed that only 3 crossed combinations gave the expected phenotypic ratios, while all other F₁ hybrids showed the parental-like phenotype.

Taken together, the F₁ dwarf bushy phenotype is dependent on Kro-0 and BG genetic backgrounds in their natural genetic context. Recombination events modified this interaction or masked it, even when these two loci were present in F₁ progeny that did not show the bushy dwarf phenotype. Many cases of genetic-background-dependent epistatic interaction have been reported and reviewed (Wang *et al.*, 2013; Sackton and Hartl, 2016; Press and Queitsch, 2017). In this scenario, the genetic complementation of one necessary allele like *DRP3B*^{Kro-0} into BG-5, even when it is homozygous in T₂, may not give the expected result. In this case, crosses between transgenic lines of Kro-0 and BG-5, in a way that increases or decreases the dose of each allele in F₁, might help in understanding how these genes are involved in this interaction. Also testing all possible combinations of protein-protein interaction assays between the necessary alleles at 17 °C and 21 °C would help in unravelling this mechanism.

4.6 Proposed model for the mechanism of BG-5xKro-0 hybrid incompatibility

Taken together, the BG-5xKro-0 hybrid shows a bushy dwarf phenotype associated with flavonoid accumulation, induced JA, SA and ABA and reduced IAA levels. Candidate genes associated with these changes were *DRP3B* and *MAP65-4* involved in peroxisome fission and two cytochromes *CYP76C8* and *CYP705A13* involved in indole glucosinolate and lignin pathways. The interaction between these genes is temperature sensitive in heterozygous individual and becomes intrinsic in homozygous individuals in the F₂ generation. Silencing of *DRP3B* and *MAP65-4* in F₂ hybrids rescued HB classes at different extents, while, silencing cytochromes did not. Thus, a major effect comes from *DRP3B* and *MAP65-4* and a secondary effect comes from *CYP705A13* and *CYP76C8*.

The most plausible scenario that can explain the observed phenotypes and physiological aspects associated with it is a defect in peroxisome proliferation and division. Plant peroxisomes are very plastic for endogenous and exogenous factors and are jointly involved in numerous metabolic processes with mitochondria and chloroplasts (Hayashi and Nishimura, 2006). These metabolic processes include auxin biosynthesis through the indole-3-butyric acid dependent pathway, as well as JA, SA, H₂O₂, indole glucosinolates and other metabolites (Figure 4.1 A) (Korasick *et al.*, 2013; Reumann and Bartel, 2016). Peroxisome multiplication occurs constitutively in the cell, however, the rate of proliferation and division of peroxisomes is sensitive to inducible elements (Yan *et al.*, 2005; Desai and Hu, 2008). It has been found that promoters of the genes involved in peroxisome elongation like *AtPEX11b*, interact with responsive transcription factors to environmental stimuli like light. Overexpression mutants of *AtPEX11* family members show a higher rate of peroxisome elongation (Lingard and Trelease, 2006; Orth *et al.*, 2007). *DRP3B* is functionally featured in mitochondria and peroxisome division by promoting fission after elongation and constriction (Fujimoto *et al.*, 2009; Zhang and Hu, 2010) and has three different copies due to alternative splicing. This suggests that this gene is also under the control of transcription factors. Altogether, three major genes *PEX11*, *DRP3B*, and *MAP65* coordinate for a proper peroxisome elongation, fission and distribution (Figure 4.1 B) (Titorenko and Mullen, 2006; Fagarasanu *et al.*, 2007).

According to this hypothetical model, in heterozygous individuals (F₁), a malfunction in the self-assembly of *DRP3B* and docking with *MAP65-4* is lessened. Such malfunctions can be compensated for by other isoforms like *FISSION1*, *DRP3A* and *MAP65-3* at 21 °C, where the rate of proliferation and fission of peroxisomes is moderate. At 17 °C however, a responsive reaction leads to a higher rate of peroxisome proliferation that requires a full function of *DRP3B* with *MAP65-4* for optimal fission after constriction. When this does not take place, enlarged, deformed peroxisomes occur within the cell leading to the imbalance of metabolic homeostasis and trigger an internal stress response. In F₂ individuals, the harmful allele at one locus is homozygous and the other is heterozygous, which causes a more severe case of protein malfunction between *DRP3B* and *MAP65-4*. This leads to more highly deformed peroxisomes at an earlier developmental stage and produces a dramatic imbalance of hormonal and secondary metabolites leading to early cell death. If one of the imbalanced pathways is repressed, indole glucosinolates, for example, this might mitigate the effect of a heterozygous malfunction in the F₁ but not in homozygous F₂ hybrids.

This model can be investigated by using *GFP::DRP3B^{Kro-0}* and *GFP::MAP65-4^{BG-5}* that were produced in F₁ hybrids or in F₂ HB individuals to monitor the integrity of peroxisomes. Also, protein-protein interaction assays for these genes would enable one to check how they interact whether they are from one parent or from both (F₁ case). The assumption

that cytochromes are only a secondary effect can be checked by silencing JA or SA peroxisomal pathways to see whether this might also rescue the F₁ phenotype.

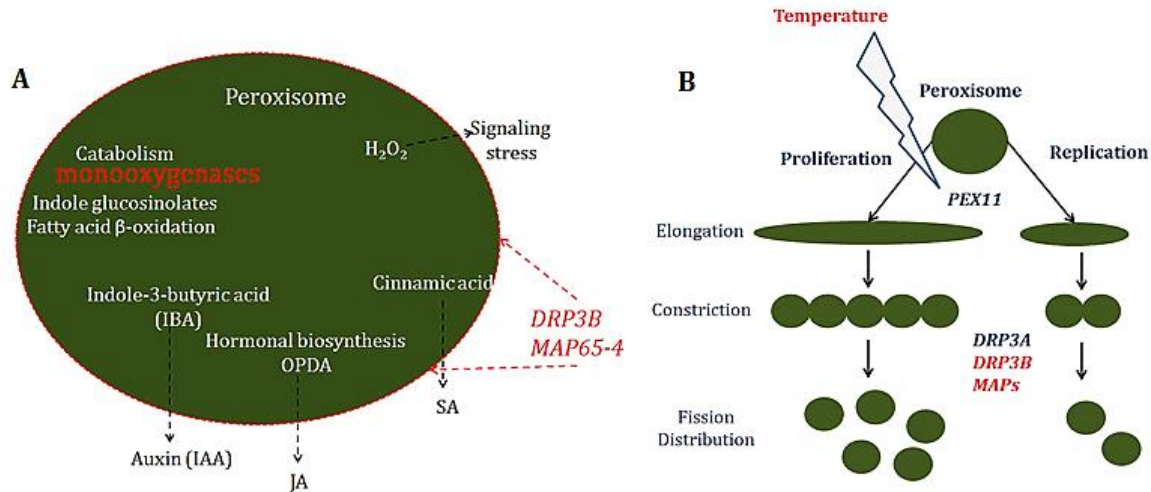


Figure 4.1 Schematic diagrams presenting peroxisome metabolic functions and localization of *DRP3B* and *MAP65-4* on the outer membrane of peroxisome (A) *DRP3B* and *MAP65-4* localize on the membranes of peroxisome in *A. thaliana*. (B) Temperature act as external stimulant affects the rate of peroxisome elongation where *DRP3B* with *MAP65-4* are responsible of fission and distribution of peroxisomes. When a defect prevents *DRP3B* from docking or interacting with *MAP65-4*, some enlarged deformed peroxisomes won't be fissioned properly leading into imbalance of metabolic processes in peroxisome triggering internal stress in plant.

5. Conclusion and future perspectives

In sum, BG-5 x Kro-0 hybrid incompatibilities are an interesting case providing an opportunity to unravel a novel mechanism of post-zygotic reproductive isolation. This incompatibility case in *A. thaliana*, unravelled four candidate genes that were so far not directly linked to shoot branching. The interaction between these genes is environmentally plastic in hybrids and associated with hormonal and secondary metabolite homeostasis. Such interaction seems to provide a robust fitness for F₁ but a loss of fitness in successive generations. Further investigation on this case will definitely illustrate new knowledge about this genetic interaction and how the environment is shaping it. To further investigate the role of hormones and flavonoids in the F₁ generation, silencing strategies targeting peroxisome-specific hormonal pathways and flavonoids should be considered. Spatiotemporal quantification of auxin by e.g. DR5_{v2}, R₂D₂, and auxin transport using *PIN::GFP* or *PGP::GFP* vectors would be informative to have an insight into the auxin status in SAM tissues in different developmental stages in F₁. Although the morphology of SAM and RAM in F₁ hybrids did not show any defects in cell division, it is still worth to use cell division markers to investigate cell division and proliferation. To monitor the integrity of peroxisomal proliferation and fission *GFP::DRP3B^{Kro-0}* and *GFP::MAP65-4^{BG-5}* in F₁ hybrids or in F₂ HB could be used. This would provide an alternative approach as genetic complementation did not show any effects and testcrosses suggested genetic background-dependency. Also, different directions of crosses between genomic lines of Kro-0 and BG-5 should be tested to see how increasing or decreasing the dose of harmful alleles can affect F₁ and F₂ hybrids. Lastly, elucidating the mechanism of this hybrid case is toward a better understanding of reproductive isolation evolution.

6. Acknowledgements

This work was supported by a PhD fellowship from the German Academic Exchange Service (**DAAD**), Max Planck Institute of Molecular Plant Physiology (**MPIMP**) and Potsdam University. Thanks are due to Roosa Laitinen who gave me the opportunity to work on this very interesting project and to all my colleagues in AG Laitinen, Markus, Björn, Andres, Neha, Kate, Christian, Jing and all past and present members for all the fruitful discussions and help.

Thanks to my PhD advisory committee Dr. John Lunn, Dr. Stefan Greiner and Prof. Isabel Bäurle for their supportive guidance. I would like also to thank Dr. John E Lunn, Dr. Franziska Fichtner and Regina Feil for all the help in sugar measurements, molecular biology and fruitful discussion about branching phenotypes. Also I would like to thank Dr. Alisdair Fernie, Dr. Patrick Giavalisco, Dr. Saleh Alseekh and Dr. Mohamed Abd Allah Salem for all the help in hormone and secondary metabolite measurements. Thanks for Dr. Karin Kohl and Green Team of MPIMP for taking an excellent care of plants. Thanks also to Dr. Arun Sampathkumar for the helpful aid and discussions about the SAM and auxin transport and shoot branching.

Special thanks to Sandra Mae-Lin Kerbler for correcting my English pitfalls and polishing my thesis. Katelynn Sageman-Furnas and Neha Vaid are thanked for their critical reading of my thesis and the helpful discussions.

My friends in MPIMP and outside for all the support and help and the happy times we had together, especially, Jan Kubiczek and Laura Demeter for every funky hat day.

My family that was always supporting me and pushing my dreams further, especially, my youngest brother who is always the only source of unique unexpected thriller and suspense. Lastly, to my second family, Edith Wolff, Rudolf Kubiczek and Melitta Kubiczek for all Christmas lovely nights.

7. Bibliography

- "1001genomes.Org." <http://1001genomes.org/>
- "Arabidopsis EFP Browser." <http://bar.utoronto.ca/efp/cgi-bin/efpWeb.cgi/>
- "SWISS-MODEL" <https://swissmodel.expasy.org/>
- "WMD3 - Web MicroRNA Designer" <http://wmd3.weigelworld.org/cgi-bin/webapp.cgi>
- "www-ibmp.u-strasbg.fr/~CYPedia"
- "<https://benchling.com/>"
- "www.ncbi.nlm.nih.gov"
- "<http://plantregmap.cbi.pku.edu.cn/>"
- Adams S, Vinkenoog R, Spielman M, Dickinson HG, Scott RJ. 2000. "Parent-of-origin effects on seed development in *Arabidopsis thaliana* require DNA methylation" *Development* (127) 2493–2502
- Aguilar-Martinez J A, Poza-Carrion C, Cubas P. 2007. "Arabidopsis *BRANCHED1* acts as an integrator of branching signals within axillary buds" *Plant cell* (19) 458–472
- Alcázar R, Ana V G, Parker J E, and Reymond M. 2009. "Incremental steps toward incompatibility revealed by Arabidopsis epistatic interactions modulating salicylic acid pathway activation" *National academy of sciences* (1) 334–39
- Alhajturki D, Muralidharan S, Nurmi M, Rowan M B A, Lunn J E, Boldt H, Salem M A, *et al.* 2018. "Dose-dependent interactions between two loci trigger altered shoot growth in BG-5 × Krotzenburg-0 (Kro-0) hybrids of *Arabidopsis thaliana*" *New Phytologist* 217 (1) 392-406
- Anderson, E. 1953. "Introgressive hybridization" *Biological Reviews* 28 (3) 280–307
- Antoun M, Ouellet F. 2013. "Growth temperature affects inflorescence architecture in *Arabidopsis thaliana*" *Botany* (91) 642-651
- Arnold M L and Martin N H. 2009. "Adaptation by introgression" *Journal of Biology* 8 (9) 82
- Aung K and Hu J. 2012. "Differential roles of Arabidopsis dynamin-related proteins DRP3A, DRP3B, and DRP5B in organelle division" *Journal of Integrative Plant Biology* 54 (11) 921–31
- Bak S, Feyereisen R.2001. "The involvement of two p450 enzymes, CYP83B1 and CYP83A1, in auxin homeostasis and glucosinolate biosynthesis" *Plant Physiol* (127) 108–118
- Bakker E G, Stahl E A, Toomajian C, Nordborg M, Kreitman M, Bergelson J.2006. "Distribution of genetic variation within and among local populations of *Arabidopsis thaliana* over its species range" *Molecular Ecology* (15) 1405–1418
- Bangerth F.1994. "Response of cytokinin concentration in the xylem exudate of bean (*Phaseolus vulgaris* L.) plants to decapitation and auxin treatment, and relationship to apical dominance" *Planta* (194) 439–442
- Barbier F F, Lunn J E, Beveridge C A. 2015. "Ready, Steady, Go! a sugar hit starts the race to shoot branching" *Current Opinion in Plant Biology* (25) 39–45
- Bateson W. 1909. "Mendel's Principles of Heredity" *Cambridge University Press* p.369-385
- Bateson W.1909. "Heredity and variation in modern lights" *Biodiversity Heritage Library* <http://biodiversitylibrary.org/oai>
- Bencivenga S, Serrano-Mislata A, Bush M, Fox F, Sablowski R. 2016. "Control of oriented tissue growth through repression of organ boundary genes promotes stem morphogenesis" *Developmental Cell* (39) 198–208
- Besseau S, Hoffmann L, Geoffroy P, Lapierre C, Pollet B, Legrand M. 2007. "Flavonoid accumulation in arabidopsis repressed in lignin synthesis affects auxin transport and plant growth" *The Plant Cell* 19 (1) 148–62
- Bikard D, Patel D, Metté C L, Giorgi V, Camilleri C, Bennett M J, Loudet O. 2009. "Divergent evolution of duplicate genes leads to genetic incompatibilities within *A.thaliana*" *Science* 323 (5914) 623–26

- Boerjan W, Cervera M T, Delarue M, Beeckman T, Dewitte W, Bellini C, Caboche M, Van Onckelen H, Van Montagu M, Inzé D. 1995. "Superroot, a recessive mutation in Arabidopsis, confers auxin overproduction" *Plant Cell* (7) 1405–1419
- Boldt H. 2009. "Genetic and phenotypic characterization of the BG-5 x Kro-0 F₁ hybrids of *Arabidopsis thaliana*" MSc. thesis
- Bomblies K, Lempe J, Epple P, Warthmann N, Lanz C, Dangl J L, Weigel D. 2007. "Autoimmune response as a mechanism for a dobzhansky-muller-type incompatibility syndrome in plants" *PLoS Biology* 5 (9) e236
- Bomblies K, Weigel D. 2007. "Hybrid necrosis: autoimmunity as a potential gene-flow barrier in plant species" *Nature Reviews Genetics* 8 (5) 382–93
- Bomblies K, Weigel D. 2010. "Arabidopsis and relatives as models for the study of genetic and genomic incompatibilities" *Philosophical Transactions of the Royal Society of London. Series B, Biological Sciences* 365 (1547) 1815–23
- Bomblies K, Yant L, Laitinen RA, Kim ST, Hollister JD, Warthmann N, Fitz J, Weigel D. 2010. "Local-scale patterns of genetic variability, outcrossing, and spatial structure in natural stands of *Arabidopsis thaliana*" *PloS Genet* (6) e1000890
- Bownam J. 1994. "Arabidopsis: an atlas of morphology and development" *Springer Science & Business Media*. Book ISBN 10: 0387940898
- Braam J, Davis R W. 1990. "Rain-, Wind-, and touch-induced expression of calmodulin and calmodulin-related genes in arabidopsis" *Cell* 60 (3) 357–64
- Braam J. 2005 "In touch: plant responses to mechanical stimuli" *New Phytologist* (165) 373-389
- Braun N, De Saint Germain A, Pillot J P, Boutet-Mercey S, Dalmais M, Antoniadis I, Li X, Maia-Grondard A, Le Signor C, Bouteiller N, Luo D, Bendahmane A, Turnbull C, Rameau C. 2012. "The pea TCP transcription factor *PsBRC1* acts downstream of strigolactones to control shoot branching" *Plant Physiology* (158) 225–238
- Bridge L J, Franklin K A, Homer M E. 2013. "Impact of plant shoot architecture on leaf cooling: a coupled heat and mass transfer model" *Journal of the Royal Society, Interface* 10, 20130326
- Brown D E, Rashotte A M, Murphy A S, Normanly J, Tague B W, Peer W A, Taiz L, Muday G K. 2001. "Flavonoids act as negative regulators of auxin transport in vivo in arabidopsis" *Plant Physiology* 126 (2) 524–35
- Burton R S, Pereira R J, Barreto F S. 2013. "Cytonuclear genomic interactions and hybrid breakdown" *Annu. Rev. Ecol. Evol. Syst* (44) 281–302
- Chae E, Bomblies K, Kim S, Karelina D, Zaidem M, Ossowski S, Martín-Pizarro C, et al. 2014. "Species-Wide genetic incompatibility analysis identifies immune genes as hot spots of deleterious epistasis" *Cell* 159 (6) 1341–51
- Challis R J, Hepworth J, Mouchel C, Waites R, Leyser O. 2013. "A Role for *MORE AXILLARY GROWTH1* (*MAX1*) in evolutionary diversity in strigolactone signaling upstream of *MAX2*" *Plant Physiology* 161 (4) 1885–1902
- Chandler J W. 2009. "Local auxin production: a small contribution to a big field" *Bioessays* 31, 60–70
- Chehab E W, Eich E, Braam J. 2008. "Thigmomorphogenesis: a complex plant response to mechanostimulation" *Journal of Experimental Botany* 60 (1) 43–56
- Chen C, Chen H, Lin Y, Shen J, Shan J, Qi P, Shi M, Mei-Zhen Zhu, Xue-Hui Huang, Qi Feng, Bin Han, Liwen Jiang, Ji-Ping Gao, and Hong-Xuan Lin. 2014. "A Two-Locus interaction causes interspecific hybrid weakness in rice" *Nature Communications* (5) 3357
- Chen C, Zhiguo E, Lin H. 2016. "Evolution and molecular control of hybrid incompatibility in plants" *Frontiers in Plant Science* (7) 1208
- Clough S J, Bent A F. 1998. "Floral Dip: a simplified method for agrobacterium-mediated transformation of Arabidopsis Thaliana" *The Plant Journal* 16 (6) 735–43
- Collins T J. 2007. "ImageJ for Microscopy" *BioTechniques* (43) 25–30

- Conti L, Bradley D. 2007. "TERMINAL FLOWER1 is a mobile signal controlling Arabidopsis Architecture" *The Plant Cell* 19 (3) 767-78
- Cosmides L M, Tooby J. 1981. "Cytoplasmic inheritance and intragenomic conflict" *Journal of Theoretical Biology* 89 (1) 83-129
- Coyne J A, Orr A H, Orr H A. 2004. "Speciation" Book 545 pages ISBN: 0878930914
- Coyne J A. 2016. "Theodosius Dobzhansky on hybrid sterility and speciation" *Genetics* 202 (1) *Genetics Society of America*, 5-7
- Darwin C. 1859. "The origin of species" Book, 502 p. publishers: John Murray.
- Davière J M, Wild M, Regnault T, Baumberger N, Eisler H, Genschik P, Achard P .2014. "Class I TCP-DELLA interactions in inflorescence shoot apex determine plant height" *Curr. Biol.* (24) 1923-1928
- Davière J M, Achard P. 2013. "Gibberellin signaling in plants" *Development* (140) 1147-1151
- Derbyshire P, Ménard D, Green P, Saalbach G, Buschmann H, Lloyd C W, Pesquet E. 2015. "Proteomic analysis of microtubule interacting proteins over the course of xylem tracheary element formation in arabidopsis" *The Plant Cell* 27(10) 2709-2726
- Desai M, Hu J .2008. "Light induces peroxisome proliferation in Arabidopsis seedlings through the photoreceptor phytochrome A, the transcription factor *HY5* homolog, and the peroxisomal protein *PEROXIN11b*" *Plant Physiol* (1) 1117-1127
- Djennane S, Hibrand-Saint L O, Kawamura K, Lalanne D, Laffaire M, Thouroude T, Chalain S, Sakr S, Boumaza R, Foucher F, Leduc N. 2014. "Impacts of light and temperature on shoot branching gradient and expression of strigolactone synthesis and signalling genes in rose" *Plant Cell Environ* (37) 742-757
- Dobzhansky T, Beadle G W. 1936. "Studies on hybrid sterility iv. transplanted testes in drosophila pseudoobscura" *Genetics* 21 (6) 832-40
- Dobzhansky, T. 1936. "Studies on hybrid sterility. ii. localization of sterility factors in drosophila pseudoobscura hybrids" *Genetics* 21 (2) 113-35
- Doyle J. 1991. "DNA Protocols for Plants" *In Molecular Techniques in Taxonomy*, 283-93
- Dun E A, De Saint Germain A, Rameau C, Beveridge C A .2012. "Antagonistic action of strigolactone and cytokinin in bud outgrowth control" *Plant Physiol* (158) 487-498
- Durand S, Bouché N, Strand E P, Loudet O, Camilleri C. 2012. "Rapid establishment of genetic incompatibility through natural epigenetic variation" *Current Biology* 22 (4) 326-31
- Fagarasanu A, Fagarasanu M, Rachubinski R A. 2007. "Maintaining peroxisome populations: a story of division and inheritance" *Annu. Rev. Cell Dev. Biol* (1) 321-344
- Ferguson B J, Beveridge C A. 2009. "Roles for auxin, cytokinin, and strigolactone in regulating shoot branching" *Plant Physiol* (149) 1929-1944
- Fichtner F, Barbier F F, Feil R, Watanabe M, Annunziata M G, Chabikwa T G, Höfgen R, Stitt M, Beveridge C A, Lunn J E. 2017. "Trehalose 6-Phosphate is involved in triggering axillary bud outgrowth in garden pea (*Pisum Sativum* L.)" *The Plant Journal* 92 (4) 611-23
- Figueiredo A, Monteiro F, Sebastiana M. 2014. "Subtilisin-like proteases in plant-pathogen recognition and immune priming: a perspective" *Frontiers in Plant Science* (5) 739
- Figuroa C M, Feil R, Ishihara H, Watanabe M, Kölling K, Krause U, Höhne M, Encke B, Plaxton WC, Zeeman SC, Li Z, Schulze WX, Hoefgen R, Stitt M, Lunn JE. 2016. "Trehalose 6-Phosphate coordinates organic and amino acid metabolism with carbon availability" *The Plant Journal* 85 (3) 410-23
- Fishman L, Sweigart A J. 2018. "When two rights make a wrong: the evolutionary genetics of plant hybrid incompatibilities" *Annual Review of Plant Biology* 69 (1) 707-731
- Fu C, Wang F, Sun B, Liu W, Li J, Deng R, Liu D, Liu ZR, Zhu MS, Liao YL . 2013. "Genetic and cytological analysis of a novel type of low temperature-dependent intra-subspecific hybrid weakness in rice" *PloS One* 8 (8) e73886

- Fujimoto M, Arimura S, Mano S, Kondo M, Saito C, Ueda T, Nakazono M, Nakano A, Nishimura M, Tsutsumi N. 2009. "Arabidopsis dynamin-related proteins *DRP3A* and *DRP3B* Are functionally redundant in mitochondrial fission, but have distinct roles in peroxisomal fission" *Plant Journal* 58 (3) 388–400
- Galletti R, Verger S, Hamant O, Ingram G. 2016. "Developing a 'Thick Skin': a paradoxical role for mechanical tension in maintaining epidermal integrity?" *Development* 143 (18) 3249–58
- Gehring M, Satyaki PR. 2017. "Endosperm and imprinting, inextricably linked" *Plant Physiology* 173 (1) 143–154
- Giavalisco P, Köhl K, Hummel J, Seiwert B, Willmitzer L. 2009. "13 C Isotope-Labeled metabolomes allowing for improved compound annotation and relative quantification in liquid chromatography-mass spectrometry-based metabolomic research" *Analytical Chemistry* 81 (15) 6546–51
- Gobron N, Waszczak C, Simon M, Hiard S, Boivin S, Charif D, Ducamp A, Wenes E, Budar F. 2013. "A cryptic cytoplasmic male sterility unveils a possible gynodioecious past for *Arabidopsis thaliana*" *PLoS One* 8 (4) e62450
- Gonzalez-Grandio E, Pajoro A, Franco-Zorrilla JM, Tarancon C, Immink RG, Cubas P. 2017. "Abscisic acid signaling is controlled by a *BRANCHED1/HD-ZIPI* cascade in *Arabidopsis* axillary buds" *PNAS* (114) 245–54
- Gonzalez-Grandio E, Poza-Carrion C, Sorzano C O S, Cubas P. 2013. "*BRANCHED1* promotes axillary bud dormancy in response to shade in *Arabidopsis*" *The Plant Cell* 25 (3) 834–50
- Grace J. 1988. "Plant Response to Wind" 3rd chapter of Book, *Agriculture, Ecosystems & Environment* 71–88
- Grbić V, Bleecker A B. 2000. "Axillary meristem development in *Arabidopsis thaliana*" *The Plant Journal For Cell and Molecular Biology* 21 (2) 215–23
- Greb T, Clarenz O, Schafer E, Muller D, Herrero R, Schmitz G, Theres K. 2003. "Molecular analysis of the lateral suppressor gene in *Arabidopsis* reveals a conserved control mechanism for axillary meristem formation" *Genes & Development* 17 (9) 1175–87
- Grunewald W, Vanholme B, Pauwels L, Plovie E, Inzé D, Gheysen G, Goossens A. 2009. "Expression of the *Arabidopsis* jasmonate signaling repressor *JAZ1/TIFY10A* is stimulated by auxin" *EMBO Reports* (10) 923–928
- Guo D, Qin G. 2016. "*EXB1/WRKY71* Transcription factor regulates both shoot branching and responses to abiotic stresses" *Plant Signaling & Behavior* 11 (3) e1150404
- Gupta A, Hisano H, Hojo Y, Matsuura T, Ikeda Y, Mori I C, Senthil-Kumar M. 2017. "Global Profiling of Phytohormone Dynamics during Combined Drought and Pathogen Stress in *Arabidopsis thaliana* Reveals ABA and JA as Major Regulators" *Scientific Reports* 7 (1)
- Hall H, Ellis B. 2012. "Developmentally equivalent tissue sampling based on growth kinematic profiling of *Arabidopsis* inflorescence stems" *New Phytologist* 194 (1) 287–96
- Harrison C J. 2017. "Auxin transport in the evolution of branching forms" *New Phytologist* 215 (2) 545–51
- Hayashi M, Nishimura M. 2006. "*Arabidopsis thaliana*—A model organism to study plant peroxisomes" *Biochim.Biophys.Acta* 1763 (12) 1382–1391
- Hayward A, Stirnberg P, Beveridge C, Leyser O. 2009. "Interactions between auxin and strigolactone in shoot branching control" *Plant Physiol* (151) 400–412
- Heisler M G, Ohno C, Das P, Sieber P, Reddy G V, Long J A, Meyerowitz E M. 2005. "Patterns of auxin transport and gene expression during primordium development revealed by live imaging of the *Arabidopsis* inflorescence meristem" *Current Biology* 15 (21) 1899–1911
- Hellens R P, Edwards E A, Leyland N R, Bean S, Mullineaux P M. 2000. "PGreen: a versatile and flexible binary Ti vector for *Agrobacterium*-mediated plant transformation" *Plant Molecular Biology* (42) 819–32

- Hentrich M, Böttcher C, Düchting P, Cheng Y, Zhao Y, Berkowitz O, Masle J, Medina J, Pollmann S. 2013. "The jasmonic acid signaling pathway is linked to auxin homeostasis through the modulation of *YUCCA8* and *YUCCA9* gene expression" *The Plant Journal* (74) 626–637
- Ho C-MK, Lee Y-RJ, Kiyama LD, Dinesh-Kumar SP, Liu B. 2012. "Arabidopsis microtubule-associated protein *MAP65-3* cross-links antiparallel microtubules toward their plus ends in the phragmoplast via its distinct C-terminal microtubule binding domain" *Plant Cell* 24 (5) 2071–85
- Hospital F. 2005. "Selection in Backcross Programmes" *Biological Sciences* 360 (1459) 1503–11
- Hunter B, Bomblies K. 2010. "Progress and promise in using arabidopsis to study adaptation, divergence, and speciation" *The Arabidopsis Book* 8. e0138
- Ichitani K, Fukuta Y, Taura S, Sato M. 2001. "Chromosomal location of *Hwc2*, one of the complementary hybrid weakness genes, in rice" *Plant Breed* (120) 523–525
- Ichitani K, Namigoshi K, Sato M, Taura S, Aoki M, Matsumoto Y, Saitou T, Marubashi W, Kuboyama T. 2007. "Fine mapping and allelic dosage effect of *Hwc1*, a complementary hybrid weakness gene in rice" *Theor. Appl. Genet.* (114) 1407–1415
- Ito S, Nozoye T, Sasaki E, Imai M, Shiwa Y, Shibata-Hatta M, Ishige T, Fukui K, Ito K, Nakanishi H, Nishizawa N K, Yajima S, Asami T. 2015. "Strigolactone regulates anthocyanin accumulation, acid phosphatases production and plant growth under low phosphate condition in arabidopsis" *PLoS One* (3) e0119724
- Jackson S D. 2009. "Plant Responses to Photoperiod" *New Phytologist* 181 (3) 517–31
- James G V, Patel V, Nordström K J V, Klasen R J, Salomé P A, Weigel D, Schneeberger K. 2013. "User Guide for Mapping-by-Sequencing in Arabidopsis" *Genome Biology* 14 R61
- Jorgensen T H, Emerson B C. 2008. "Functional variation in a disease resistance gene in populations of *Arabidopsis thaliana*" *Molecular Ecology* (17) 4912–4923
- Kao Y-T, Gonzalez KL, Bartel B. 2018. "Peroxisome function, biogenesis, and dynamics in plants" *Plant Physiol. American Society of Plant Biologists* 176 (1) 162–77
- Karimi M, Inzé D, Depicker A. 2002. "GATEWAY vectors for agrobacterium-mediated plant transformation" *Trends in Plant Science* 7 (5) 193–95
- Kelemen O, Convertini P, Zhang Z, Wen Y, Shen M, Falaleeva M, Stamm S. 2013. "Function of alternative splicing" *Gene* (1) 1-30
- Keller T, Abbott J, Moritz T, Doerner P. 2006. "Arabidopsis *REGULATOR OF AXILLARYMERISTEMS1* controls a leaf axil stem cell niche and modulates vegetative development" *Plant Cell* (18) 598–611
- Koch J, Pranjic k, Huber A, Ellinger A, Hartig A, Kragler F, Brocard C. 2010. "*PEX11* family members are membrane elongation factors that coordinate peroxisome proliferation and maintenance" *Journal of Cell Science* 123 (19) 3389–3400
- Korasick DA, Enders TA, Strader LC. 2013. "Auxin biosynthesis and storage forms" *Journal of Experimental Botany* (64) 2541–2555
- Krzywinski M, Altman N. 2014. "Visualizing samples with box plots" *Nature Methods* 11 (2) 119-120
- Lafon-Placette C, Köhler C. 2016. "Endosperm-based postzygotic hybridization barriers: developmental mechanisms and evolutionary drivers" *Molecular Ecology* (25) 2620–2629
- Leduc N, Roman H, Barbier F, Péron T, Huché-Théliet L, Lothier J, Demotes-Mainard S, Sakr S. 2014. "Light Signaling in Bud Outgrowth and Branching in Plants" *Plants* 3 (2) 223–50
- Li C J, Guevara E, Herrera G J, Bangerth, F. 1995. "Effect of apex excision and replacement by 1-naphthylacetic acid on cytokinin concentration and apical dominance in pea plants" *Physiol. Plant.* (94) 465–469
- Li H, Sun B, Sasabe M, Deng X, Machida Y, Lin H, Lee Julie Y R, Liu B. 2017. "Arabidopsis *MAP65-4* plays a role in phragmoplast microtubule organization and marks the cortical cell division site" *New Phytologist* 215 (1) 187–201

- Li J, Brader G, Palva E T. 2004. "The *WRKY70* Transcription factor: A node of convergence for jasmonate-mediated and salicylate-mediated signals in plant defense" *The Plant Cell* 16 (2) 319-31
- Liang X, Chen X, Li C, Fan J, Guo Z. 2017. "Metabolic and transcriptional alternations for defense by interfering *OsWRKY62* and *OsWRKY76* transcriptions in rice" *Sci.Rep.Nature Publishing Group* 7 (1) 2474
- Lingard M J, Trelease R N. 2006. "Five Arabidopsis peroxin 11 homologs individually promote peroxisome elongation, duplication or aggregation" *J. Cell Sci* (1) 1961-1972
- Ljung K. 2013. "Auxin Metabolism and Homeostasis during Plant Development" *Development* 140 (5) 943-50
- Long J A, Moan E I, Medford J I, Barton M K. 1996. "A member of the *KNOTTED* class of homeodomain proteins encoded by the *STM* gene of arabidopsis" *Nature* (379) 66-69
- Long Y, Zhao L, Niu B, Su J, Wu H, Chen Y, Zhang Q, Guo J, Zhuang C, Mei M, Xia J, Wang L, Wu H, Liu YG. 2008. "Hybrid male sterility in rice controlled by interaction between divergent alleles of two adjacent genes" *PNAS* 105 (48) 18871-76
- López-Ráez J A, Charnikhova T, Gómez-Roldán V, Matusova R, Kohlen W, De Vos R, Verstappen F, Puech-Pages V, Bécard G, Mulder P, Bouwmeester H. 2008. "Tomato strigolactones are derived from carotenoids and their biosynthesis is promoted by phosphate starvation" *New Phytologist* 178 (4) 863-74
- Lunn J E, Feil R, Hendriks J H M, Y Gibon Y, Morcuende R, Osuna D, Scheible W R, Carillo P, Hajirezaei M R, Stitt M. 2006. "Sugar-Induced increases in trehalose 6-phosphate are correlated with redox activation of ADPglucose pyrophosphorylase and higher rates of starch synthesis in *Arabidopsis thaliana*" *The Biochemical Journal* 397 (1) 139-48
- Lunn J E, Rees T. 1990. "Apparent equilibrium constant and mass-action ratio for sucrose-phosphate synthase in seeds of *Pisum sativum*" *Biochemical Journal* 267 (3) 739-43
- Lunn, J E, Delorge I, Figueroa C M, Dijck P V, Mark Stitt M. 2014. "Trehalose metabolism in plants" *The Plant Journal* 79 (4) 544-67
- Maeda S, Gunji S, Hanai K, Hirano T, Kazama Y, Ohbayashi I, Abe T, Sawa S, Tsukaya H, Ferjani A. 2014. "The conflict between cell proliferation and expansion primarily affects stem organogenesis in Arabidopsis" *Plant and Cell Physiology* 55 (11) 1994-2007
- Maheshwari S, Barbash D A. 2011. "The genetics of hybrid incompatibilities" *Annu. Rev. Genet.* (45) 331-355
- Mason M G, Ross J J, Babst BA, Wienclaw B N, Beveridge C A. 2014. "Sugar demand, not auxin, is the initial regulator of apical dominance" *PNAS* 111 (16) 6092-97
- Matsubara K T, Yamamoto E, Mizobuchi R, Yonemaru J I, Yamamoto T, Kato H, Yano M. 2015. "Hybrid breakdown caused by epistasis-based recessive incompatibility in a cross of rice (*Oryza Sativa* L.)" *The Journal of Heredity* 106 (1) 113-22
- McSteen P, Leyser O. 2005. "Shoot branching" *Annu. Rev. Plant Biol* (56) 353-74
- Mikkelsen M D, Fuller V L, Hansen B G, Nafisi M, Olsen C E, Nielsen H B, Halkier B A. 2009. "Controlled indole-3-acetaldoxime production through ethanol-induced expression of *CYP79B2*" *Planta* (229) 1209-1217
- Mikkelsen M D, Hansen C H, Wittstock U, Halkier B A. 2000. "Cytochrome P450 *CYP79B2* from Arabidopsis catalyzes the conversion of tryptophan to indole-3-acetaldoxime, a precursor of indole glucosinolate and indole-3-acetic acid" *Journal of Biological Chemistry* (275) 33712-33717
- Mikkelsen M D, Naur P, Halkier B A. 2004. "Arabidopsis mutants in the C-S lyase of glucosinolate biosynthesis establish a critical role for indole-3-acetaldoxime in auxin homeostasis" *Plant Journal* (37) 770-777

- Mino M, Maekawa K, Ogawa K I, Yamagishi H, Inoue M. 2002. "Cell Death Processes during Expression of Hybrid Lethality in Interspecific F₁ Hybrid between *Nicotiana Glauca* and *Nicotiana Tabacum*" *Plant Physiology* (4) 1776-87
- Mizuta Y, Harushima Y, Kurata N. 2010. "Rice pollen hybrid incompatibility caused by reciprocal gene loss of duplicated genes" *PNAS* 107 (47) 20417-22
- Morris S E, Cox M C H, Ross J J, Krisantini S, Beveridge C A. 2005. "Auxin dynamics after decapitation are not correlated with the initial growth of axillary buds" *Plant Physiology* 138 (3) 1665-72
- Muller H.J. 1942. "Isolating mechanisms, evolution, and temperature" *Biol. Symp* (6) 71-125
- Muller, H.J. 1940. "Bearing of the drosophila work on systematics" *The New Systematics* 185-268
- Muralidharan S. 2015. "Causes and consequences of hybrid incompatibilities in *Arabidopsis thaliana*" PhD thesis
- Murfet I C, Reid J B.1993. "Developmental mutants" *Peas: Genetics, Molecular Biology and Biotechnology* 165-216
- Murfet I C.2003. "Branching in pea: double mutants of *rms7* with *rms1* through *rms5*" *Pisum Genet* (35) 15-18
- Naseem M, Kaldorf M, Dandekar T. 2015. "The nexus between growth and defence signalling: auxin and cytokinin modulate plant immune response pathways" *Journal of Experimental Botany* 66 (16) 4885-4896
- Noh B, Murphy A S, Spalding E P. 2001. "Multidrug resistance-like genes of arabidopsis required for auxin transport and auxin-mediated development" *The Plant Cell* 13 (11)2441-54
- Norman J M V, Benfey N P. 2009. "*Arabidopsis thaliana* as a model organism in systems biology" *Wiley Interdisciplinary Reviews. Systems Biology and Medicine* 1 (3) 372-79
- Normanly J. 2010. "Approaching cellular and molecular resolution of auxin biosynthesis and metabolism" *Cold Spring Harb. Perspect. Biol.* 2:a001594
- Orr H A. 1996. "Dobzhansky, Bateson, and the Genetics of Speciation" *Genetics* 144 (4) 1331-35
- Orth T, Reumann S, Zhang X, Fan J, Wenzel D, Quan S, Hu J. 2007. "The PEROXIN11 protein family controls peroxisome proliferation in Arabidopsis" *Plant Cell* 19 (1) 333-350
- Ossowski S, Schwab R, Weigel D. 2008. "Gene silencing in plants using artificial micrnas and other small RNAs" *The Plant Journal* 53 (4) 674-90
- Pan J, Fair S J, Mao D. 2011. "Quantitative analysis of skeletal symmetric chlorhexidine in rat plasma using doubly charged molecular ions in LC-MS/MS detection" *Bioanalysis* 3 (12) 1357-68
- Peer W A, Murphy A S. 2007. "Flavonoids and auxin transport: modulators or regulators?" *Trends in Plant Science* 12 (12) 556-63
- Petrásek J, Friml J. 2009. "Auxin transport routes in plant development" *Development* 136 (16) 2675-88
- Petrásek J, Mravec J, Bouchard R, Blakeslee J J, Abas M, Seifertova D, Wisniewska J, Tadele Z, Kubes M, Covanová M, Dhonukshe P, Skupa P, Benková E, Perry L, Krecek P, Lee OR, Fink GR, Geisler M, Murphy AS, Luschnig C, Zazimalová E, Friml J. 2006. "PIN proteins perform a rate-limiting function in cellular auxin efflux" *Science* (312) 914-918
- Platt A, Horton M, Huang YS, Li Y, Anastasio AE, Mulyati NW, Agren J, Bossdorf O, Byers D, Donohue K, Dunning M, Holub EB, Hudson A, Le Corre V, Loudet O, Roux F, Warthmann N, Weigel D, Rivero L, Scholl R, Nordborg M, Bergelson J, Borevitz J O .2010. "The scale of population structure in *Arabidopsis thaliana*" *PLoS Genet* 6: e1000843
- Plötner B, Nurmi M, Fischer A, Watanabe M, Schneeberger K, Holm S, Vaid N, Schottler AM, Walther D, Hoefgen R, Weigel D, Laitinen RAE. 2017. "Chlorosis caused by two recessively interacting genes reveals a role of rna helicase in hybrid breakdown in *Arabidopsis thaliana*" *The Plant Journal* 91 (2) 251-62
- Presgraves DC. 2010. "Darwin and the origin of interspecific genetic incompatibilities" *Am. Nat.* (176) S45-60

- Press M O, Queitsch C. 2017. "Variability in a short tandem repeat mediates complex epistatic interactions in *Arabidopsis thaliana*" *Genetics* 205 (1) 455–64
- Qi L, Yan J, Li Y, Jiang H, Sun J, Chen Q, Li H, Chu J, Yan C, Sun X, Yu Y, Li C, Li C. 2012. "*Arabidopsis thaliana* plants differentially modulate auxin biosynthesis and transport during defense responses to the necrotrophic pathogen *Alternaria brassicicola*" *New Phytologist* (195) 872–882
- R Development Core Team. 2012. "R: A language and environment for statistical computing" *R Foundation for Statistical Computing, Vienna, Austria*. [Http://Www.R-Project.Org/](http://www.R-project.org/)
- Raissig MT, Bemmerl M, Baroux C, Grossniklaus U. 2013. "Genomic imprinting in the *Arabidopsis* embryo is partly regulated by *PRC2*" *PLoS Genetics* 9 (12) e1003862
- Rameau C, Bertheloot J, Leduc N, Andrieu B, Foucher F, Sakr S. 2015. "Multiple Pathways Regulate Shoot Branching" *Frontiers in Plant Science* (5) 741
- Reddy V S, Ali G S, Reddy A. 2003. "Characterization of a pathogen-induced calmodulin-binding protein: mapping of four Ca²⁺-dependent calmodulin-binding domains" *Plant Mol Biol* (52) 143–159
- Reumann S, Bartel B. 2016. "Plant peroxisomes: recent discoveries in functional complexity, organelle homeostasis, and morphological dynamics" *Curr Opin Plant Biol* (34) 17–26
- Rieseberg L H, Blackman B K. 2010. "Speciation genes in plants" *Annals of Botany* 106 (3) 439–55
- Rieseberg L H, Archer M A, Wayne R K. 1999. "Transgressive Segregation, Adaptation and Speciation" *Heredity* 83 (4) 363–72
- Rieseberg, L H, Willis J H. 2007. "Plant Speciation" *Science* 317 (5840) 910–14
- Robert-Seilaniantz A, MacLean D, Jikumaru Y, Hill L, Yamaguchi S, Kamiya Y, Jones JDG. 2011. "The microRNA miR393 re-directs secondary metabolite biosynthesis away from camalexin and towards glucosinolates" *Plant Journal* (67) 218–231
- Sachs R M. 1965. "Stem elongation" *Annual Review of Plant Physiology* 16 (1) 73–96
- Sachs T, Thimann V. 1967. "The role of auxins and cytokinins in the release of buds from dominance" *Am. J. Bot.* (54) 136–144
- Sackton T B, Hartl D L. 2016. "Perspective genotypic context and epistasis in individuals and populations" *Cell* (166) 279–87
- Sairanen I, Novák O, Pěňčík A, Ikeda Y, Jones B, Sandberg G, Ljung K. 2012. "Soluble carbohydrates regulate auxin biosynthesis via PIF proteins in *Arabidopsis*" *The Plant Cell* 24 (12) 4907–16
- Saito T, Ichitani K, Suzuki T, Marubashi W, Kuboyama T. 2007. "Developmental observation and high temperature rescue from hybrid weakness in a cross between Japanese rice cultivars and Peruvian rice cultivar Jamaica" *Breeding Science* 57 (4) 281–88
- Salomé P A, Bomblies K, Fitz J, Laitinen R A E, Warthmann N, Yant L, Weigel D. 2012. "The Recombination Landscape in *Arabidopsis thaliana* F₂ Populations" *Heredity* 108 (4) 447–55
- Schoof H, Lenhard M, Haecker A, Mayer K F, Jürgens G, Laux T. 2000. "The stem cell population of *Arabidopsis* shoot meristems is maintained by a regulatory loop between the *CLAVATA* and *WUSCHEL* Genes" *Cell* 100 (6) 635–44
- Schuyler S C, Liu J Y, Pellman D J. 2003. "The molecular function of Ase1p: evidence for a MAP-dependent midzone-specific spindle matrix" *J. Cell Biol.* (160) 517–528
- Schwab R, Ossowski S, Riester M, Warthmann N, Weigel D. 2006. "Highly specific gene silencing by artificial microRNAs in *Arabidopsis*" *The Plant Cell* 18 (5) 1121–33
- Scott R J, Spielman M, Bailey J, Dickinson HG. 1998. "Parent-of-origin effects on seed development in *Arabidopsis thaliana*" *Development* 125 (17) 3329–41
- Seale M, Bennett T, Leyser O. 2017. "*BRC1* expression regulates bud activation potential but is not necessary or sufficient for bud growth inhibition in *Arabidopsis*" *Development* (144) 1661–73
- Seehausen Ole, Butlin R K, Keller I, Wagner C E, Boughman J W, Hohenlohe P A, Peichel C L, et al. 2014. "Genomics and the origin of species" *Nature Reviews. Genetics* 15 (3) 176–92

- Serrano-Mislata A, Bencivenga S, Bush M, Schiessl K, Boden S, Sablowski R .2018. “*DELLA* genes restrict inflorescence meristem function independently of plant height” *Nature Plants* (3) 749–754
- Serrano-Mislata A, Sablowski R. 2018. “The pillars of land plants: new insights into stem development” *Current Opinion in Plant Biology* (45) 11–17
- Shinohara N, Taylor C, Leyser O. 2013. “Strigolactone can promote or inhibit shoot branching by triggering rapid depletion of the auxin efflux protein *pin1* from the plasma membrane” *PLoS Biology* 11 (1) e1001474
- Sicard A, Kappel C, Lee Y W, Woźniak N J, Marona C, Stinchcombe J R, Wright S I, Lenhard M. 2016. “Standing genetic variation in a tissue-specific enhancer underlies selfing-syndrome evolution in *Capsella*” *PNAS* 113 (48) 13911–16
- Sicard A, Thamm A, Marona C, Lee Y W, Wahl V, Stinchcombe J R, Wright S I, Kappel C, Michael Lenhard M. 2014. “Repeated Evolutionary Changes of Leaf Morphology Caused by Mutations to a Homeobox Gene” *Current Biology* 24 (16) 1880–86
- Simon M, Durand S, Pluta N, Gobron N, Botran L, Ricou A, Camilleri C, Budar F. 2016. “Genomic Conflicts That Cause Pollen Mortality and Raise Reproductive Barriers in *Arabidopsis Thaliana*” *Genetics* 203 (3) 1353–67
- Skirycz A, Reichelt M, Burow M, Birkemeyer C, Rolcik J, Kopka J, et al. 2006. “*DOF* transcription factor *AtDof1.1* (*OBP2*) is part of a regulatory network controlling glucosinolate biosynthesis in *Arabidopsis*” *Plant Journal* (47) 10–24
- Smertenko A P, Chang H Y, Wagner V, Kaloriti D, Fenyk S, Sonobe S, Lloyd C, Hauser M T, and Hussey, P J. 2004. “The *Arabidopsis* microtubule-associated protein *AtMAP65-1*: Molecular analysis of its microtubule bundling activity” *Plant Cell* (16) 2035–2047
- Smith L M, Bomblies K, Weigel D. 2011. “Complex evolutionary events at a tandem cluster of *Arabidopsis thaliana* genes resulting in a single-locus genetic incompatibility” *PLoS Genetics* 7 (7) e1002164
- Somssich M, Il Je B, Simon R, Jackson D. 2016. “*CLAVATA-WUSCHEL* Signaling in the Shoot Meristem” *Development* 143 (18) 3238–48
- Song B D, Yarar D, Schmid S L. 2004. “An assembly-incompetent mutant establishes a requirement for dynamin self-assembly in clathrin-mediated endocytosis in vivo” *Mol Biol Cell* 15(5) 2243–52
- Staiger D. 2015. “Shaping the *Arabidopsis* transcriptome through alternative splicing” *Advances in Botany*, 1–13
- Stansfield WD. 2008. “Mendel’s search for true-breeding hybrids” *J Hered. Oxford University Press* 100 (1) 2–6
- Staswick P E, Serban B, Rowe M, Tiryaki I, Maldonado M T, Maldonado M C, Suza W. 2005. “Characterization of an *Arabidopsis* enzyme family that conjugates amino acids to indole-3-acetic acid” *The Plant Cell* (17) 616–627
- Staswick P E, Tiryaki I. 2004. “The oxylipin signal jasmonic acid is activated by an enzyme that conjugates it to isoleucine in *Arabidopsis*” *The Plant Cell* (16) 2117–2127
- Stitt M, McC. Lilley R, Gerhardt R, Heldt H W. 1989. “metabolite levels in specific cells and subcellular compartments of plant leaves” *Methods in Enzymology* (174) 518–552
- Stubbe W, Steiner E. 1999. “Inactivation of Pollen and Other Effects of Genome-Plastome Incompatibility In *Oenothera*” *Plant Systematics and Evolution* 217 (3–4) 259–77
- Sun J, Xu Y, Ye S, Jiang H, Chen Q, Liu F, Zhou W, Chen R, Li X, Tietz O, Wu X, Cohen JD, Palme K, Li C. 2009. “*Arabidopsis ASA1* is important for jasmonate-mediated regulation of auxin biosynthesis and transport during lateral root formation” *The Plant Cell* (21) 1495–1511
- Sun J, Chen Q, Qi L, Jiang H, Li S, Xu Y, Liu F, Zhou W, Pan J, Li X, Palme K, Li C.. 2011. “Jasmonate modulates endocytosis and plasma membrane accumulation of the *Arabidopsis* PIN2 protein” *New Phytologist* (191) 360–375

- Świadek M, Proost S, Sieh D, Yu J, Todesco M, Jorzig C, Cubillos A E, et al. 2017. "Novel allelic variants in ACD6 cause hybrid necrosis in local collection of *Arabidopsis thaliana*" *New Phytologist* 213 (2) 900–915
- Tamaoki D, Seo S, Yamada S, Kano A, Miyamoto A, Shishido H, Miyoshi S, Taniguchi S, Akimitsu K, Gomi K. 2013. "Jasmonic acid and salicylic acid activate a common defense system in rice" *Plant Signaling & Behavior* 8 (6) e24260
- Tanaka M, Takei K, Kojima M, Sakakibara H, Mori H, 2006. "Auxin controls local cytokinin biosynthesis in the nodal stem in apical dominance" *Plant Journal* (45) 1028–1036
- Tantikanjana T, Mikkelsen M D, Hussain M, Halkier B A, Sundaresan V. 2004. "Functional analysis of the Tandem-Duplicated P450 Genes *SPS/BUS/CYP79F1* and *CYP79F2* in glucosinolate biosynthesis and plant development by ds transposition-generated double mutants" *Plant Physiology*, 135 (2) 840-848
- Tantikanjana T, Yong J W, Letham D S, Griffith M, Hussain M, Ljung K, Sandberg G, Sundaresan V. 2001. "Control of axillary bud initiation and shoot architecture in *Arabidopsis* through the SUPERSHOOT Gene" *Genes & Development* 15 (12) 1577–88
- Tateda C, Zhang Z, Greenberg J T. 2015. "Linking pattern recognition and salicylic acid responses in *Arabidopsis* through *ACCELERATED CELL DEATH6* and receptors" *Plant Signaling & Behavior* 10: e1010912
- Tateda C, Zhang Z, Shrestha J, Jelenska J, Chinchilla D, Greenberg JT. 2014. "Salicylic acid regulates *Arabidopsis* microbial pattern receptor kinase levels and signaling" *Plant Cell* 26: 4171–4187
- Terasaka W K, Blakeslee J J, Titapiwatanakun B, Peer W A, Bandyopadhyay A, Makam S N, Lee O R, Richards EL, Murphy AS, Sato F, Yazaki K . 2005. "*PGP4*, an ATP Binding Cassette P-Glycoprotein, Catalyzes Auxin Transport in *Arabidopsis thaliana* Roots" *The Plant Cell* (17) 2922–2939
- Thimann K, Skoog, F. 1933. "Studies on the growth hormone of plants iii: the inhibitory action of the growth substance on bud development" *PNAS* (19) 714–716
- Thorsten P. 2014. "Title Calculate pairwise multiple comparisons of mean rank sums" <https://cran.r-project.org/web/packages/PMCMR/PMCMR.pdf>
- Titorenko V I, Mullen R T. 2006. "Peroxisome biogenesis: the peroxisomal endomembrane system and the role of the ER" *J. Cell Biol.* 1747 (1) 11–17
- Todesco M, Kim S T, Chae E, Bomblies K, Zaidem M, Smith L M, Weigel D. 2014. "Activation of the *Arabidopsis thaliana* Immune System by Combinations of Common *ACD6* Alleles" *PLoS Genetics* 10 (7) e1004459
- Tong H, Jin Y, Liu W, Li F, Fang J, Yin Y, Qian Q, Zhu L, Chu C. 2009. "DWARF AND LOW-TILLERING, a new member of the GRAS family, plays positive roles in Brassinosteroids signaling in rice" *Plant J.* (58) 803–816
- Trost G, Vi S L, Czesnick H, Lange P, Holton N, Giavalisco P, Zipfel C, Kappel C, Lenhard M. 2014. "Arabidopsis Poly (A) Polymerase *PAPS1* limits founder-cell recruitment to organ primordia and suppresses the salicylic acid-independent immune response downstream of *EDS1/PAD4*" *The Plant Journal* 77 (5) 688–99
- Umehara M, Hanada A, Yoshida S, Akiyama K, Arite T, Takeda-Kamiya N, Magome H, Kamiya Y, Shirasu K, Yoneyama K, Kyojuka J, Yamaguchi S. 2008. "inhibition of shoot branching by new terpenoid plant hormones" *Nature* (455) 195–200
- Van der Knaap E, Song W-Y, Ruan D-L, Sauter M, Ronald PC, Kende H. 1999. "Expression of a gibberellin-induced leucine-rich repeat receptor-like protein kinase in deep water rice and its interaction with kinase-associated protein phosphatase" *Plant Physiol* (122) 695-704
- Vernoux T, Besnard F, Traas J. 2010. "Auxin at the shoot apical meristem" *Cold Spring Harbor Perspectives in Biology* 2 (4) a001487
- Wang B, Smith SM, Li J. 2018. "Genetic regulation of shoot architecture" *Annual Review of Plant Biology* 69 (1) 437–68

- Wang L, Ruan Y L. 2013. "Regulation of cell division and expansion by sugar and auxin signaling" *Frontiers in Plant Science* (4) 163
- Wang D, Amornsiripanitch N, Dong X. 2006. "A genomic approach to identify regulatory nodes in the transcriptional network of systemic acquired resistance in plants" *PLoS Pathogens* 2, e123
- Wang D, Pajerowska-Mukhtar K, Culler A H, Dong X. 2007. "Salicylic acid inhibits pathogen growth in plants through repression of the auxin signaling pathway" *Current Biology* (17) 1784–1790
- Wang Q, Kohlen W, Rossmann S, Vernoux T, Theres K. 2014. "Auxin depletion from the leaf axil conditions competence for axillary meristem formation in arabidopsis and tomato" *The Plant Cell* 26 (5) 2068–79
- Wang Y, Arenas C D, Stoebel D M, Cooper T F. 2013. "Genetic background affects epistatic interactions between two beneficial mutations" *Biol. Lett.* (9) 20120328
- Watanabe H, Marubashi W. 2004. "Temperature-Dependent Programmed Cell Death Detected in Hybrids between *Nicotiana Langsdorffii* and *N. Tabacum* Expressing Lethality" *Plant Biotechnology* 21 (2) *Japanese Society for Plant Cell and Molecular Biology*, 151–54
- Wei S, Gruber MY, Yu B, Gao M-J, Khachatourians GG, Hegedus DD, Parkin AP I, Hannoufa A. 2012. "Arabidopsis mutant *sk156* reveals complex regulation of *SPL15* in a *miR156*-controlled gene network" *BMC Plant Biology* 12 (1) 169
- Weigel D. 2012. "Natural variation in arabidopsis: from molecular genetics to ecological genomics" *Plant Physiology* 158 (1) 2–22
- Weigel D, Alvarez J, Smyth D R, Yanofsky M F, Meyerowitz E M. 1992. "LEAFY Controls Floral Meristem Identity in Arabidopsis" *Cell* 69 (5) 843–59
- Wickham H. 2009. ggplot2 "Elegant Graphics for Data Analysis" *Springer-Verlag New York*
- Willige B C, Isono E, Richter R, Zourelidou M, Schwechheimer C. 2011. "Gibberellin regulates PIN-FORMED abundance and is required for auxin transport-dependent growth and development in *Arabidopsis thaliana*" *Plant Cell* (23) 2184–2195
- Woodward A W, Bartel B. 2005. "Auxin: regulation, action, and interaction" *Ann Bot* 95:707–735
- Yadav U P, Ivakov A, Feil R, Duan G Y, Walther D, Giavalisco P, Piques M, Carillo P, Hubberten HM, Stitt M, Lunn JE. 2014. "The sucrose-trehalose 6-phosphate (tre6p) nexus: specificity and mechanisms of sucrose signalling by Tre6P" *Journal of Experimental Botany* 65 (4) 1051–68
- Yan M, Rayapuram N, Subramani S. 2005. "The control of peroxisome number and size during division and proliferation" *Curr. Opin. Cell Biol.* 177(1) 376–383
- Yang Y, Hammes U Z, Taylor C G, Schachtman D P, Nielsen E. 2006. "High-affinity auxin transport by the *AUX1* influx carrier protein" *Curr. Biol.* (16) 1123–1127
- Yao C, Finlayson S A. 2015. "Abscisic acid is a general negative regulator of Arabidopsis axillary bud growth" *Plant Physiol* (169) 611–26
- Yu Y, Zhao Z, Shi Y, Tian H, Liu L, Bian X, Xu Y, Zheng X, Gan L, Shen Y, Wang C, Yu X, Wang C, Zhang X, Guo X, Wang J, Ikehashi H, Jiang L, Wan J. 2016. "Hybrid sterility in rice (*Oryza sativa* L.) involves the tetratricopeptide repeat domain containing protein" *Genetics* 203 (3) 1439–1451
- Zhang X, Hu J. 2010. "The Arabidopsis chloroplast division protein DYNAMIN-RELATED PROTEIN5B also mediates peroxisome division" *Plant Cell* (22) 431–442
- Zhao J, Dixon R A. 2010. "The 'ins' and 'Outs' of Flavonoid Transport" *Trends in Plant Science* 15 (2) 72–80

8. Supplemental data

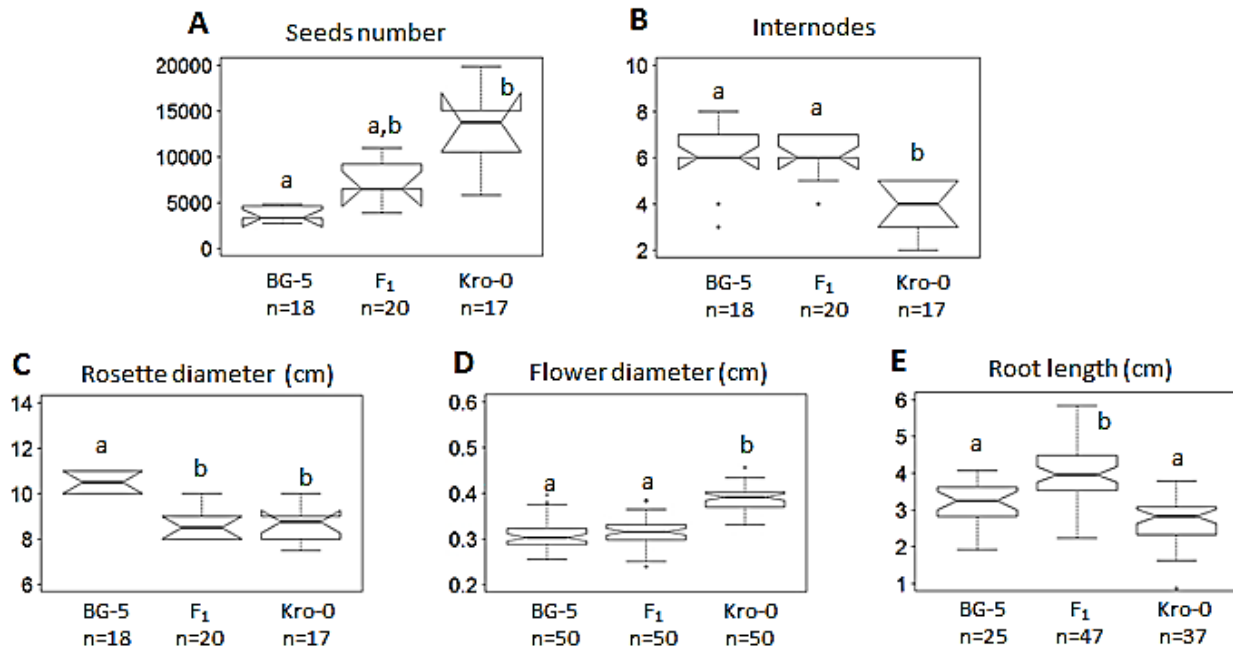


Figure S 1. Phenotypic characterization of F₁ and parents at 17 °C. A: the estimated seeds number of each genotype. B: the number of cauline branches. C: rosette diameter (cm) at bolting stage. D: floral diameter (cm). E: Root length (cm) after two weeks of germination on vertical MS-plates. Different lowercase letters denote significantly different median. Different lowercase letters denote significantly different means. p-values were calculated by Kruskal-Wallis followed by post-hoc kruskal nemenyi test. Numbers in the X-axis denote the number of biological replicates for each phenotypic class. The hinges are versions of the 1st and 3rd quartile while the whiskers are the range × interquartile. Dot above or below whiskers is any data point which lie beyond the extremes of the whiskers. The box is the interquartile range (IQR) and notches are the 95% confidence interval (CI) calculated as $\pm 1.58 \times \text{IQR} / \sqrt{n}$ between two medians. F₁: BG-5 × Kro-0 F₁.

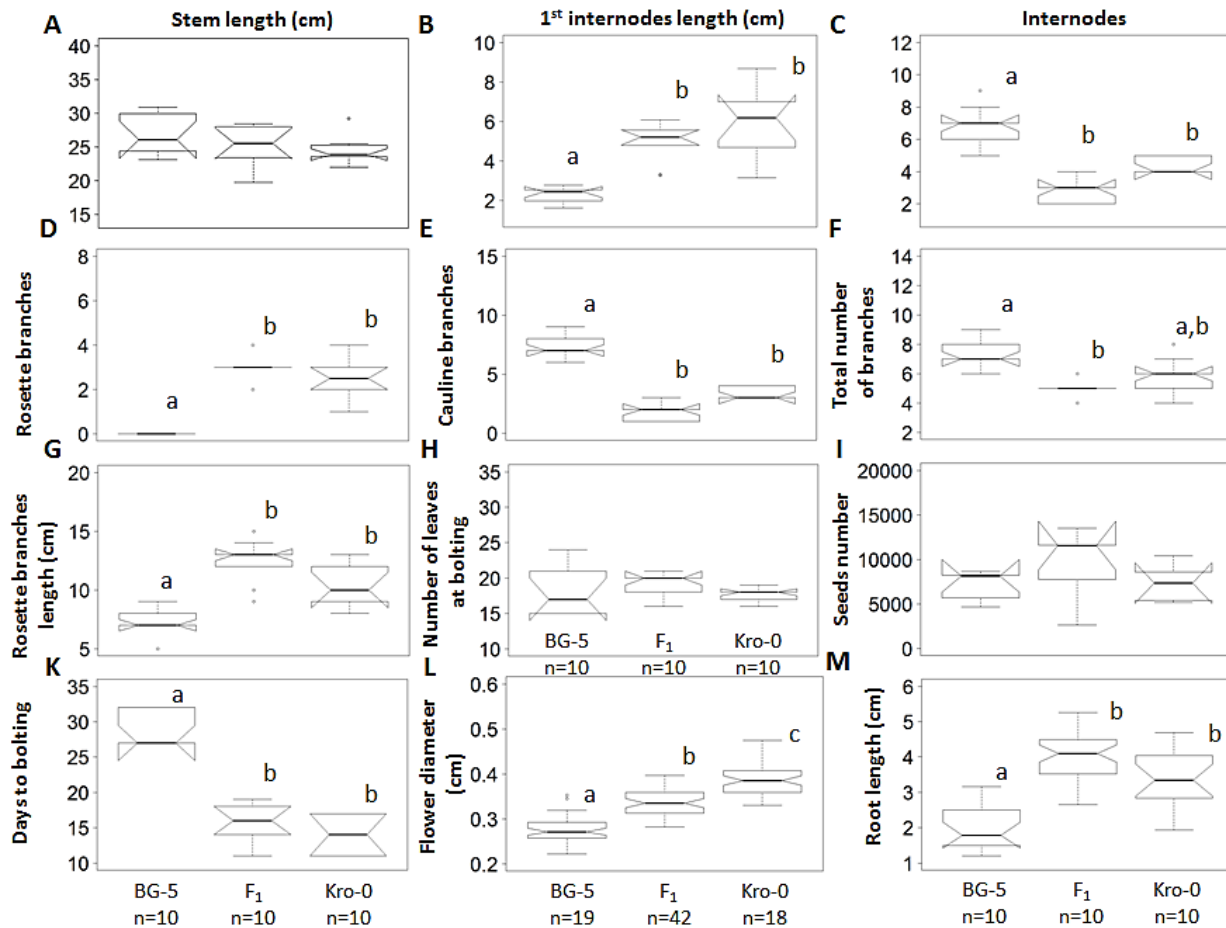


Figure S 2. Phenotypic characterization of F₁ and parents at 21 °C. A: main stem length (cm). B: 1st internode length (cm). C: number of stem segments (segments between nodes). D: number of rosette branches. E: number of cauline branches. F: the total number of cauline and rosette branches. G: The length of rosette branches. H: number of leaves at bolting. I: estimated seeds number for each genotype. K: Days to bolting. L: floral diameter (cm). M: Root length (cm) after two weeks of germination on vertical plates. Different lowercase letters denote significantly different means. p-values were calculated by Kruskal-Wallis followed by post-hoc kruskal nemenyi test. Numbers in the X-axis denote the number of biological replicates for each phenotypic class. The hinges are versions of the 1st and 3rd quartile while the whiskers are the range × interquartile. Dot above or below whiskers is any data point which lie beyond the extremes of the whiskers. The box is the interquartile range (IQR) and notches are the 95% confidence interval (CI) calculated as $\pm 1.58 \times \text{IQR} / \sqrt{n}$ between two medians. F₁: BG-5 × Kro-0 F₁.

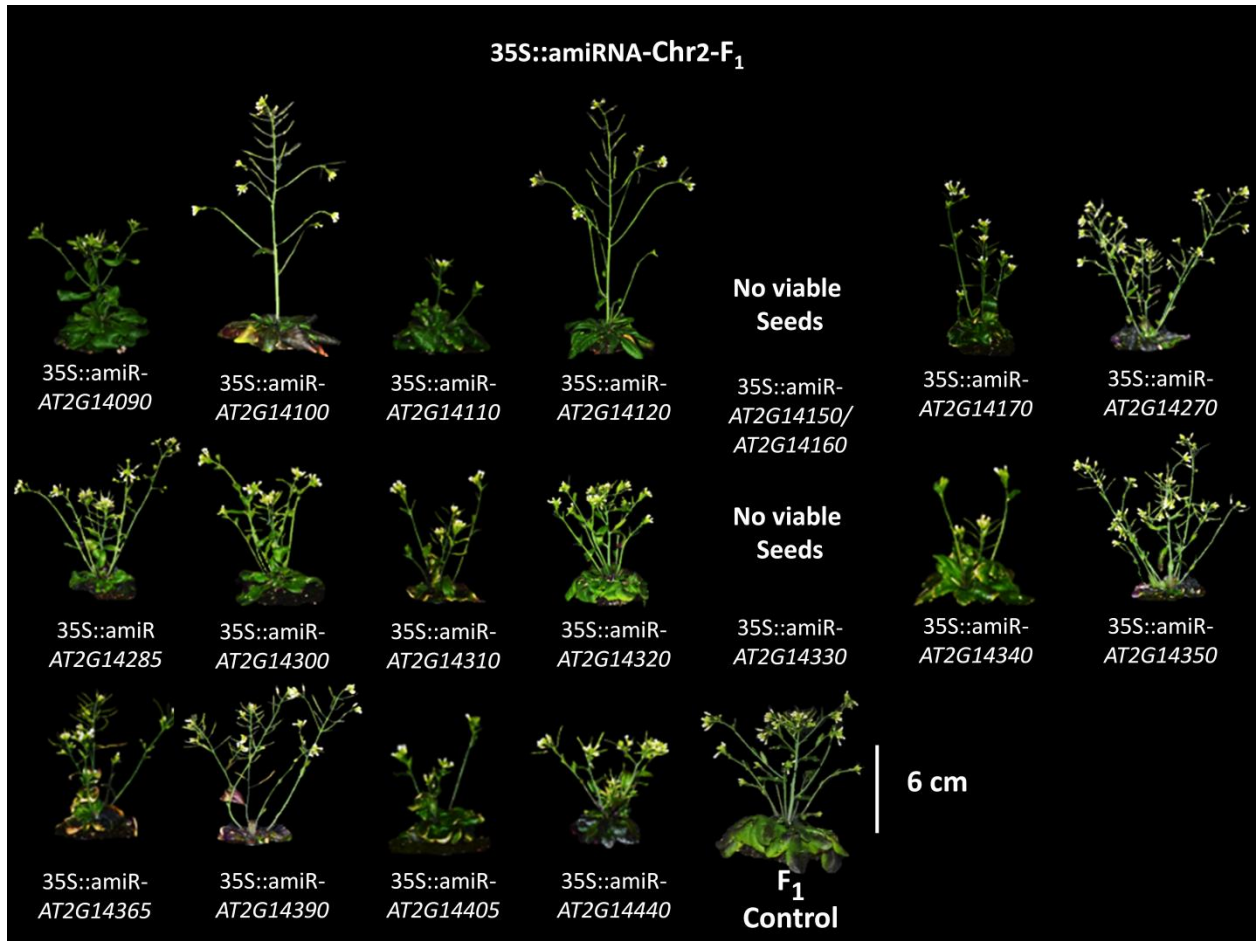


Figure S 3. F₁ hybrids grown at 17 °C targeted with amiRNAs against Chr2 candidate genes.

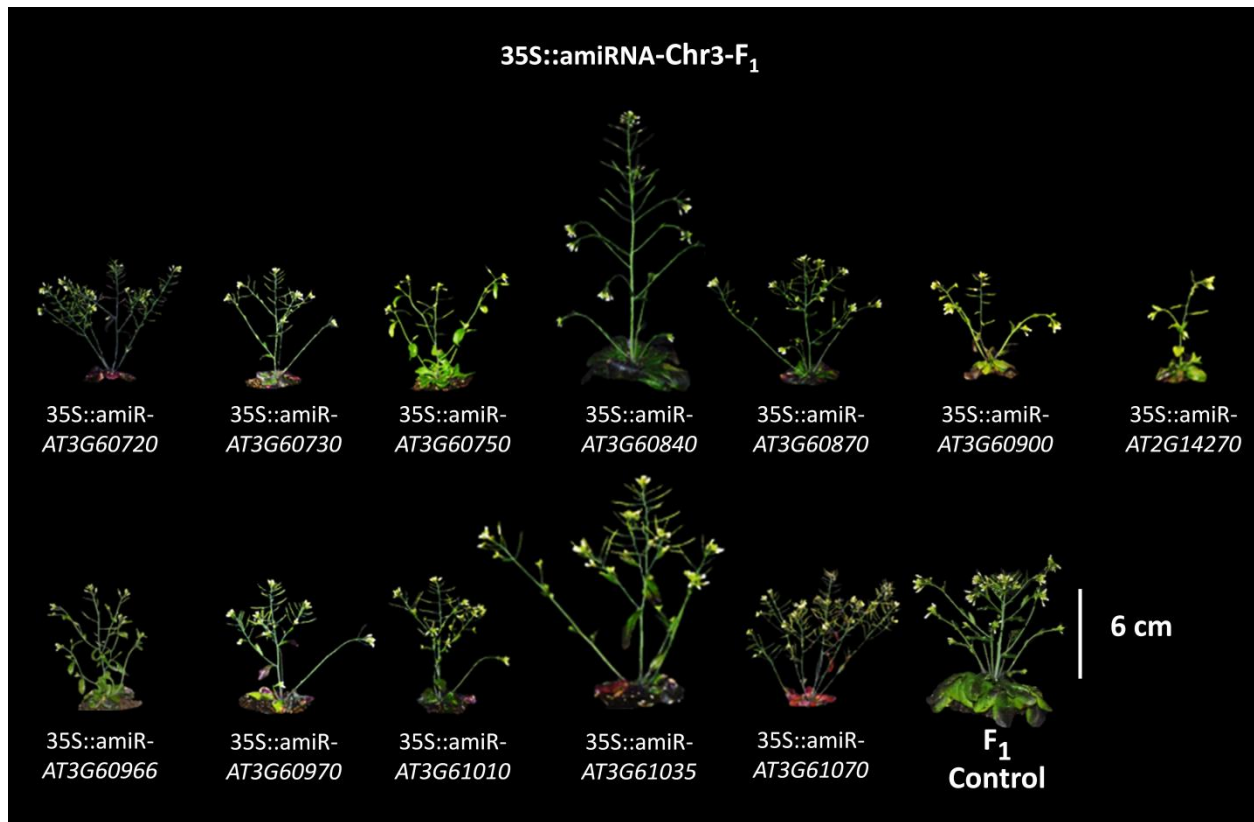


Figure S 4. F₁ hybrids grown at 17 °C targeted with amiRNA against Chr3 candidate genes.

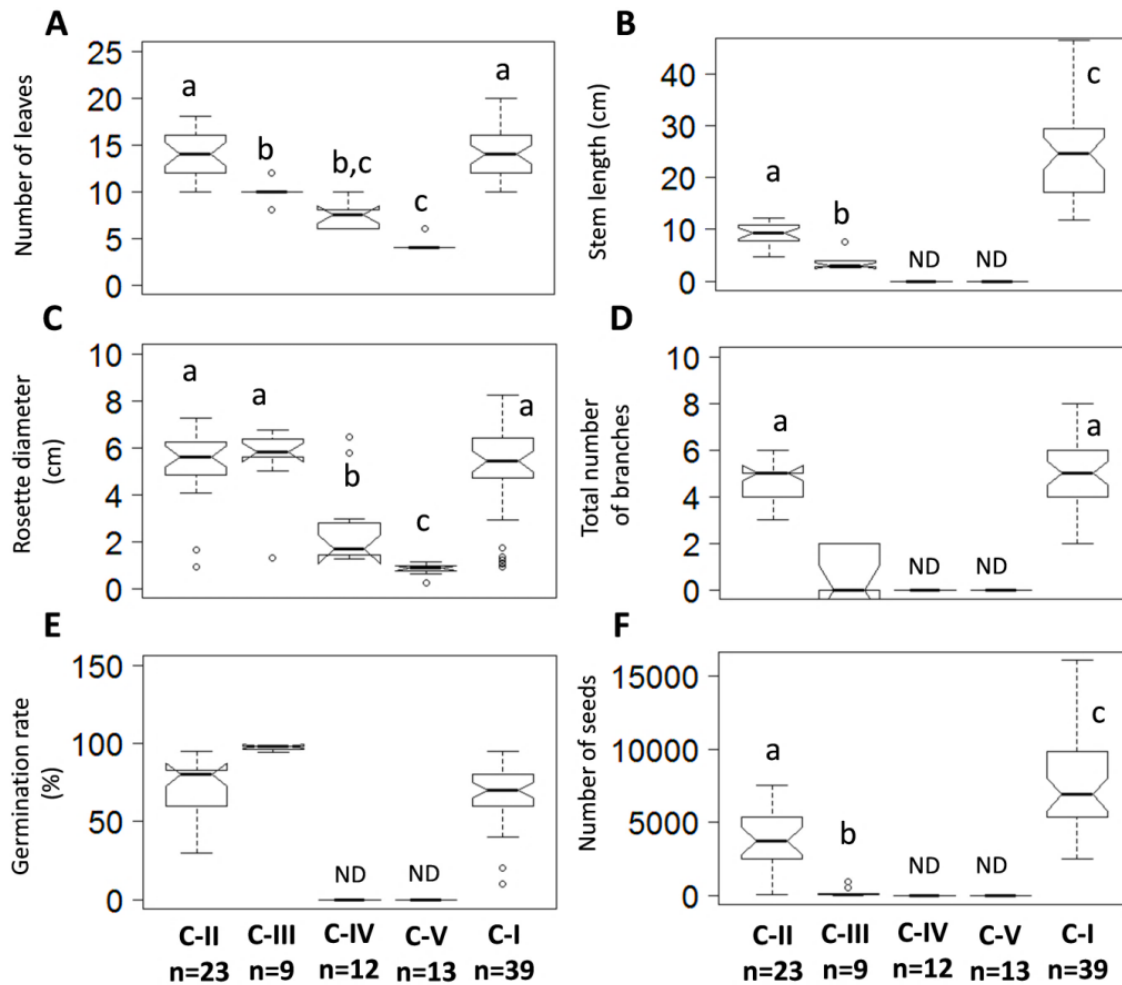


Figure S 5. Phenotypic characterization of F_{2-2} generation grown at 17 °C. A: number of leaves at bolting of different F_{2-2} 5 classes phenotypes. B: stem length (cm) of different F_{2-2} 5 classes phenotypes. C: rosette diameter (cm) of different F_{2-2} 5 classes phenotypes. D: total number of branches of different F_{2-2} 5-classes phenotypes. E: germination rate (%) of different F_{2-2} 5 classes phenotypes. F: the estimated number of seeds of different F_{2-2} 5 classes phenotypes. Different lowercase letters denote significantly different means. p-values were calculated by Kruskal-Wallis followed by post-hoc kruskal nemenyi test. Numbers in the X-axis denote the number of biological replicates for each phenotypic class. Dot above or below whiskers is any data point which lie beyond the extremes of the whiskers. The box is the interquartile range (IQR) and notches are the 95% confidence interval (CI) calculated as $\pm 1.58 \times \text{IQR} / \sqrt{n}$ between two medians.

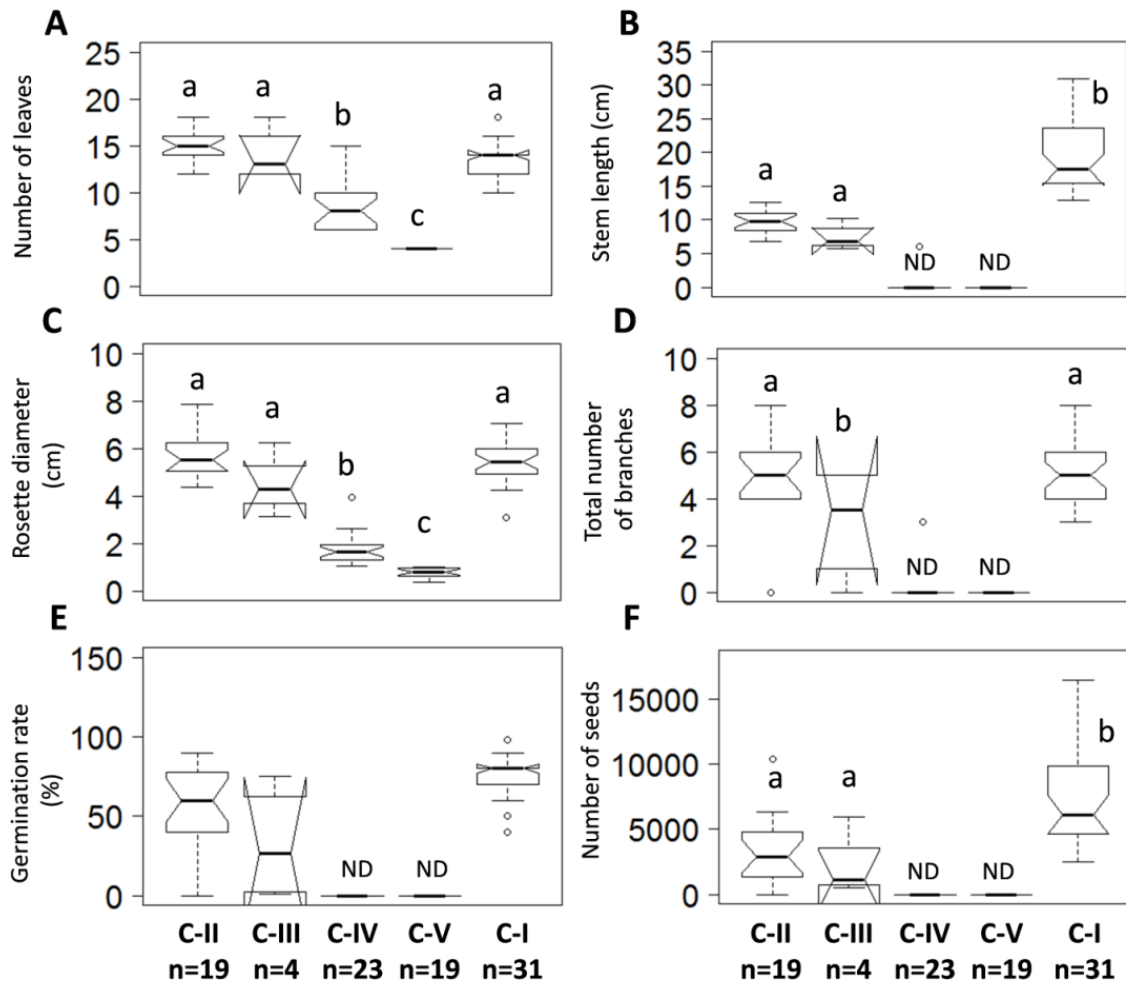


Figure S 6. Phenotypic characterization of F_{2-3} generation grown at 17 °C. A: number of leaves at bolting of different F_{2-3} 5 classes phenotypes. B: stem length (cm) of different F_{2-3} 5 classes phenotypes. C: rosette diameter (cm) of different F_{2-3} 5 classes phenotypes. D: total number of branches of different F_{2-3} 5-classes phenotypes. E: germination rate (%) of different F_{2-3} 5 classes phenotypes. F: the estimated number of seeds of different F_{2-3} 5 classes phenotypes. Different lowercase letters denote significantly different means. p-values were calculated by Kruskal-Wallis followed by post-hoc kruskal nemenyi test. Numbers in the X-axis denote the number of biological replicates for each phenotypic class. The hinges are versions of the 1st and 3rd quartile while the whiskers are the range \times interquartile. Dot above or below whiskers is any data point which lie beyond the extremes of the whiskers. The box is the interquartile range (IQR) and notches are the 95% confidence interval (CI) calculated as $\pm 1.58 \times \text{IQR} / \sqrt{n}$ between two medians.

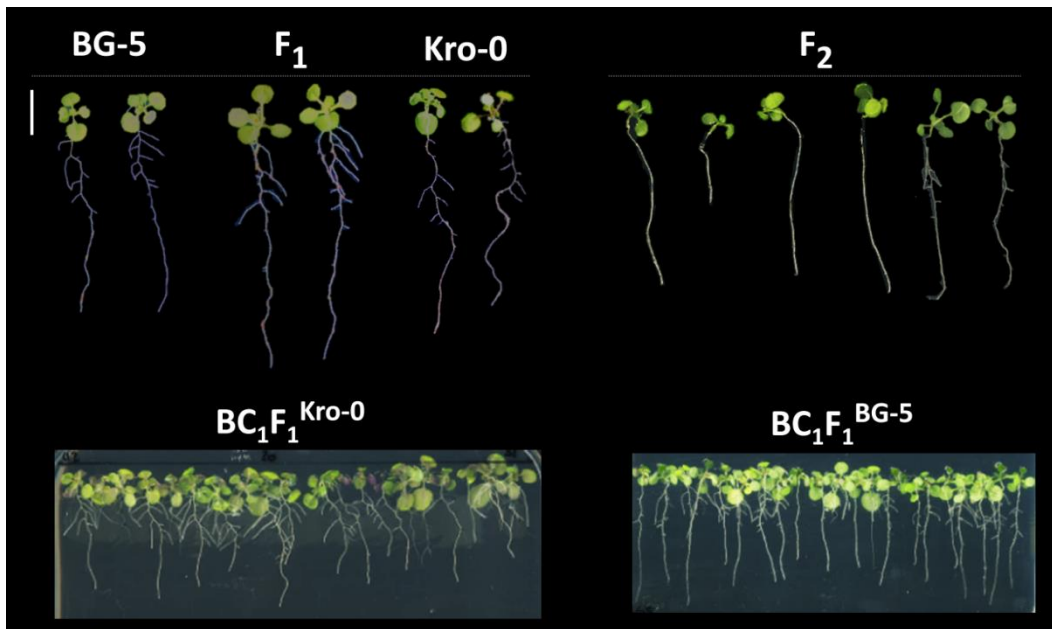
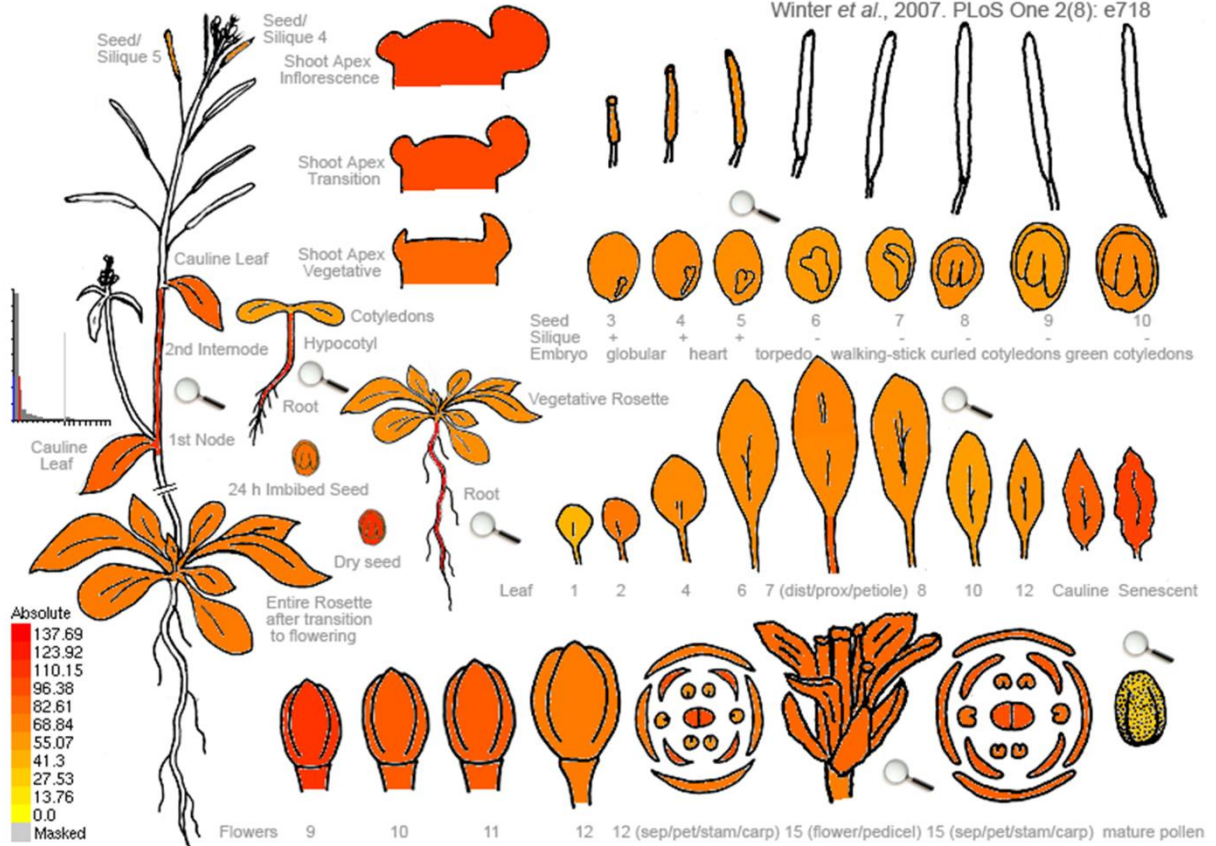


Figure S 7. Root phenotypes in F₁, parents, F₂s and backcross segregants grown at 17 °C. Bar= 1 cm.

At2g14120 263278_at *DRP3B*

Arabidopsis eFP Browser at bar.utoronto.ca
Winter et al., 2007. PLoS One 2(8): e718



eFP Browser by B. Vinegar, drawn by J. Ails and N. Provar. Data from Gene Expression Map of Arabidopsis Development: Schmid et al., 2005, Nat. Gen. 37:501, and the Nambara lab for the imbibed and dry seed stages. Data are normalized by the GCOS method, TGT value of 100. Most tissues were sampled in triplicate.

Figure S 8. Developmental map of the expression of *AT2G14120* (*DRP3B*) indicated by eFPbrowser.

At2g14100 263276_at CYP705A13

Arabidopsis eFP Browser at bar.utoronto.ca
Winter et al., 2007. PLoS One 2(8): e718

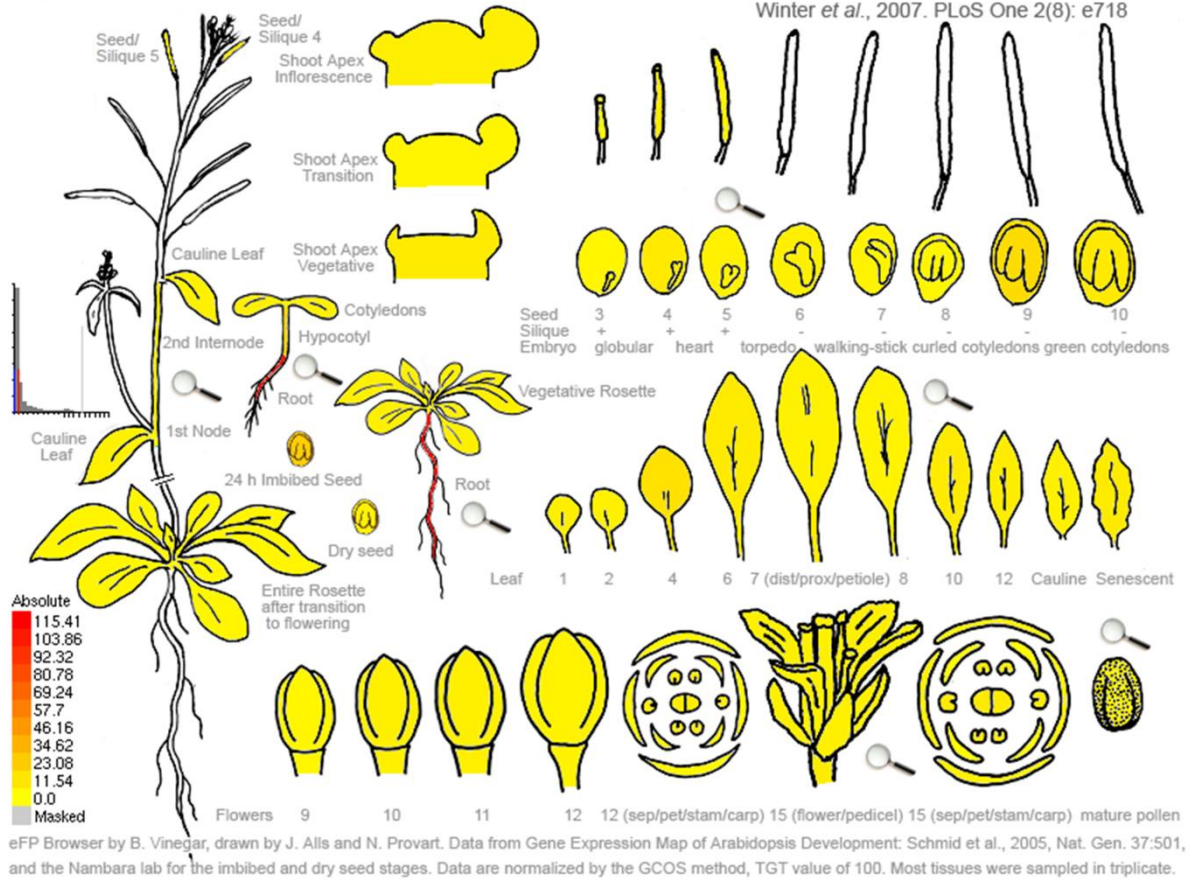


Figure S 9. Developmental map of the expression of *AT2G14100* (*CYP705A13*) indicated by eFPbrowser.

AtGenExpress eFP: AT3G60840 / MA...

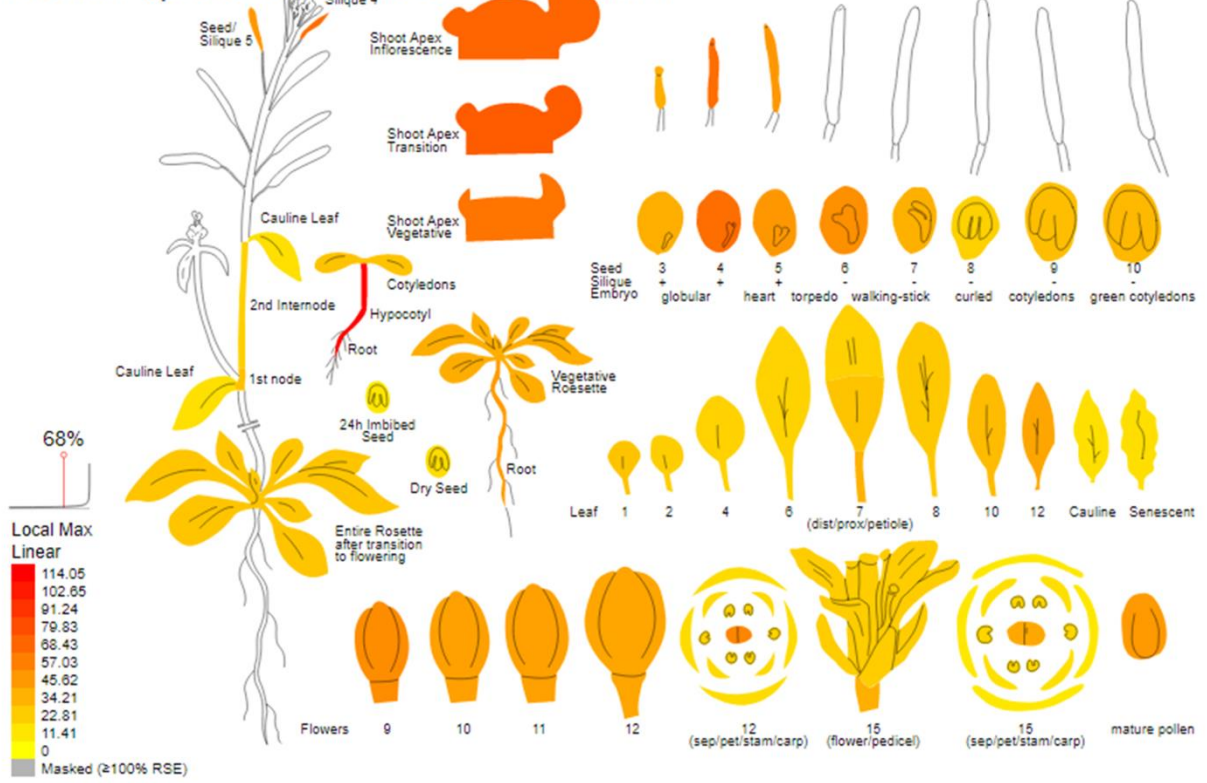


Figure S 10. Developmental map of the expression of *AT3G60840* (*MAP65-4*) indicated by eFPbrowser.

9. Curriculum vitae

Personal Information

Name **DEMA ALHAJTURKI**

Address Charlottenstr.96
14469 Potsdam
Brandenburg
Germany

Mobile +4917647853474

E-mail **Workplace email:** alhajturki@mpimp-golm.mpg.de
Personal email: demah_agro@yahoo.com

Nationality Syrian

Date of birth 10.05.1984

Work Experience **October 2014 – Currently**

Employer AG-Laitinen, Max Planck Institute for Molecular Plant Physiology,
Wissenschaftspark Golm Am Mühlenberg 1 14476 Potsdam Germany.
<http://www.mpimp-golm.mpg.de/2168/en>

Type of business or sector PhD student

Research Group AG-Laitinen “Molecular Mechanisms of Plant Adaptation”

March 2014 – August 2014

Employer International Center for Agricultural Research in the Dry Areas
(ICARDA). Terbol station, Lebanon.

<https://www.icarda.org/>

Type of business or sector Research Placement as Research Assistant

Research project	Regional Bread Wheat program. November 2009 – March 2014
Employer	National Commission for Biotechnology (NCBT) Current Premises in the Campus of the Faculty of Agriculture, P.O.Box: 31902 Damascus Syria Tel: +963 (011) 513 8306 Fax: +963 (011) 513 0104
Type of business or sector	Research Assistant in Plant biotechnology General Lab.
Research project	Research Team member of the Project “Developing of high sugar yielding sweet sorghum hybrids tolerant to drought”

Education

Oct 2014 - Currently	PhD candidate at Max Planck for Molecular Plant Physiology (MPI- MP) Potsdam-Golm Germany in life science and Biology
2008-2012	Master In Agricultural engineering, Field crops Dept., Damascus University, Syria. (Percentage: 86%, GPA: 3.4) With honour degree 96% in master thesis evaluation.
2003-2008	Bachelor degree in Agricultural Engineering. Field crops Dept., Damascus University, Syria. With honour degree 97% in Graduation project.

Training

1-14 September 2012	DAAD/ University of Jordan Amman-Jordan, International Summer School Program “Promoting Conservation Agriculture in the Arab Region”.
19-24 June 2010	Training course on Detection of Genetically Modified Organisms and Bio-safety for Food and Agriculture held at headquarters, Aleppo-Syria.
19-24 June 2010	Training course on Detection of Genetically Modified Organisms and Bio-

safety for Food and Agriculture held at headquarters, Aleppo-Syria.

Teaching

Potsdam University.	2017, Practical teaching/training course “ RE Cloning and transformed plant selection”
At the National Commission for Biotechnology (NCBT)	2013, Practical teaching/training course “ RNA isolation,cDNA synthesis”
Plant biotechnology General Lab	2013, Practical teaching/training course “ DNA isolation and screening”
	2012, Practical teaching/training course “ Introduction into bioinformatics”

Languages

Foreign language	English (Language of communication and study during PhD studies)
Foreign language	German B2
Mother tongue	Arabic Language

Technical Skills

Data management and analysis on R

Hands on Transformation/Cloning/Regeneration (genome editing).

Hands-on multiple mapping techniques and approaches.

General applied genetics in plant biotechnology.

Operations in Field and greenhouse e.g. Plant crossing, stress evaluation.

Hands on tissue culture techniques e.g. double haploid generation.

DRIVING LICENCE (Syrian).

Conferences

Workshops

Presentations/attendance

19 th – 20 th June 2017	Max Planck Symposium on “Organismal Biology meets Epigenetics”
14 th – 16 th September 2016	10th Tri-National Arabidopsis Meeting 2016
6 th – 7 th October 2016	Max Planck Symposium on “COMPLEX TRAIT GENETICS”
28 th -30 th November 2010	Oral presentation in The 50th Science Week International Conference On Agricultural Productivity Increase: Challenges and Means of Development November in Deir-Ezzor Al-Furat University- Syria by a scientific paper titled: (Sweet Sorghum a Water-Saving and Alternative Sugar /Bio-ethanol Crop).
4 th -8 th July 2010	Turkish- Syrian Workshop on a joint project at the National Commission for Biotechnology, Damascus, Syria.
16 th -17 th June 2010	FAO project TCP/RAB/3202 on GMO Detection and Bio-safety, High-level Workshop on Regional Capacity Building for GMO's Detection and Bio-safety for Food and Agriculture 16-17 June, GCSAR-Douma, Damascus, Syria
5 th -7 th January 2010	USA-Syrian Workshop on Sustainable Agriculture in Syria, Identifying Opportunities for the Cooperation University of Damascus in the patronage of ICARDA held at The University presidency headquarters, Damascus, Syria.

Scholarships

Fellowships

Funds

2014	German Academic Exchange Service (DAAD) Scholarship for PhD studies at MPI-MP.
------	--

2014 The CARA UK **Fellowship** for At-Risk Academics for research placement at ICARDA.

2011 **Direct Governmental Fund** from the Higher Commission for Scientific Research (HCSR)- Ministry of Higher Education, Syrian Arab Republic for the project “Developing of high sugar yielding sweet sorghum hybrids tolerant to drought and assessment of gene expression levels of genes responsible for sugar production in stem” at the NCBT.

Publications

2017 **Alhajturki, D.**, Muralidharan, S., Nurmi, M., Rowan, B. A., Lunn, J. E., Boldt, H., Salem, M. A., Alseekh, S., Jorzig, C., Feil, R., Giavalisco, P., Fernie, A. R., Weigel, D. and Laitinen, R. A. E. (2018), Dose-dependent interactions between two loci trigger altered shoot growth in BG-5 × Krotzenburg-0 (Kro-0) hybrids of *Arabidopsis thaliana*. *New Phytol*, 217: 392–406. doi:10.1111/nph.14781

2012 **Alhajturki, D.**, Aljamali, M. Kanbar, and A. Azmah F. (2012). Potential of some Sweet sorghum (*Sorghum bicolor* L.) genotypes under two water regimes for sugar and bio-ethanol production. *Sugar Tech*, (14) 4:376-382.

2011 **Alhajturki, D.**, Aljamali, M. and Kanbar, A.(2011). Genetic Variation of Sorghum (*Sorghum bicolor* L. Moench) Varieties Assessed by ISSR Markers. *Adv. Environ. Biol.*, 5(11): 3504-3510.

2011 **Alhajturki, D.**, Aljamali, M. and Kanbar, A.(2011). 'Relationship between shoot and sugar-related characters of sweet sorghum (*Sorghum bicolor* L.) under contrasting moisture regimes'. *Am.-Eurasian J. Sustain. Agric.*, 5(2): 252-257.

2011 **Alhajturki, D.**, Aljamali, M. Kanbar, A. and Azmah F.(2010) Sweet Sorghum a Water-Saving and Alternative Sugar /Bio-ethanol Crop at The 50th Science Week International Conference On Agricultural Productivity Increase: Challenges and Means of Development November, 28th -30th in Deir-Ezzor Al-Furat University- Syria. (Oral-presentation/printed

publish).

References

Max Planck Institute

Dr Roosa Laitinen

PhD studies supervision

Research Group Leader "Molecular Mechanisms of Adaptation"

Max Planck Institute of Molecular Plant Physiology

Wissenschaftspark Golm

Am Mühlenberg 1

14476 Potsdam

Brandenburg

Laitinen@mpimp-golm.mpg.de

<http://www.mpimp-golm.mpg.de/2168/en>

Max Planck Institute

Dr John E. Lunn

PhD studies Mentorship

Scientist in System Regulation

Max Planck Institute of Molecular Plant Physiology

Wissenschaftspark Golm

Am Mühlenberg 1

14476 Potsdam

Brandenburg

lunn@mpimp-golm.mpg.de

<http://www.mpimp-golm.mpg.de/2168/en>

ICARDA Dr Wuletaw Tadesse Degu

Senior Scientist - Spring Bread Wheat Breeder

Biodiversity and Integrated Gene Management Program

The International Center for Agricultural Research in the Dry Areas
(ICARDA)

w.tadesse@cgiar.org

<https://www.icarda.org/>

**Master degree
supervision**

Dr Adnan Kanbar

Scientist at Plant Stress Subgroup, Molecular Cell Biology, Botanical
Institute

Karlsruhe Institute of Technology

Fritz-Haber-Weg 4, 76131 Karlsruhe

Germany

Adnan.kanbar@kit.edu

<https://www.kit.edu/english/>